

An asymptotic Peskun ordering and its application to lifted samplers

Philippe Gagnon¹, Florian Maire¹

December 21, 2024

¹Department of Mathematics and Statistics, Université de Montréal.

Abstract

A Peskun ordering between two samplers, implying a dominance of one over the other, is known among the Markov chain Monte Carlo community for being a remarkably strong result, but it is also known for being one that is notably difficult to establish. Indeed, one has to prove that the probability to reach a state \mathbf{y} from state \mathbf{x} , using a sampler, is greater than or equal to the probability using the other sampler, and this must hold for all pairs (\mathbf{x}, \mathbf{y}) such that $\mathbf{x} \neq \mathbf{y}$. We provide in this paper a weaker version that does not require an inequality between the probabilities for all these states: the dominance holds asymptotically, as a varying parameter grows without bound, as long as the states for which the probabilities are greater than or equal to belong to a mass-concentrating set. The weak ordering turns out to be useful to compare *lifted* samplers for *partially-ordered* discrete state-spaces with their Metropolis–Hastings counterparts. An analysis yields a qualitative conclusion: they asymptotically perform better in certain situations (and we are able to identify these situations), but not necessarily in others (and the reasons why are made clear). The difference in performance is evaluated quantitatively in important applications such as graphical-model simulation and variable selection. The code to reproduce all numerical experiments is available online.¹

Keywords: Bayesian statistics; binary random variables; Ising model; Markov chain Monte Carlo methods; non-reversible jump algorithms; trans-dimensional samplers; variable selection.

1 Introduction

1.1 Motivation

Establishing a Peskun ordering (Peskun, 1973) is possibly the most sought-after route when one wants to prove that a given Markov chain Monte Carlo (MCMC) algorithm is superior in terms of statistical efficiency to another. This ordering is however known to be rather challenging to establish. The main result of this paper is that a weaker version of this ordering can lead to similar, but weaker, conclusions. This weaker ordering² is particularly well suited for situations where the two Markov chains of

¹See ancillary files on [arXiv:2003.05492](https://arxiv.org/abs/2003.05492).

²For brevity, we will use “weaker ordering” or “weak ordering” to refer to the proposed weaker version of Peskun’s ordering. As will be seen, using such expressions is however an abuse of terminology because the binary relation defined by our “weak ordering” does not establish an order on the set of reversible Markov kernels in the mathematical sense.

interest are well understood, but only on some subsets of the state-space. We believe that this weaker version will allow to compare samplers in situations in which it was not possible before. We begin this manuscript by explaining the motivation behind the introduction of such an ordering.

Let us first present the original ordering. For this purpose, we beforehand introduce notation. Let π be a probability distribution defined on a measurable space $(\mathcal{X}, \mathbf{X})$ where \mathcal{X} is finite and \mathbf{X} is a sigma-algebra on \mathcal{X} . In the following, we assume that \mathcal{X} is also the support of π . Let us consider the problem of sampling from π . In a sampling context, π is called the *target distribution*. We assume that it is not possible to generate independent draws from π . Given the complex dependency structure of modern statistical models such as graphical models and the intractable nature of some distributions that arise, for instance, in Bayesian statistics, this is a realistic assumption. We turn to Markov-chains-based sampling methods which typically rely on an ergodic stochastic process $\{\mathbf{X}_k\} := \{\mathbf{X}_k\}_{k \in \mathbb{N}}$ whose limiting distribution is π . We denote for any function $f : \mathcal{X} \rightarrow \mathbb{R}$ the expectation of $f(\mathbf{X})$ under $\mathbf{X} \sim \pi$ by πf . The expectation, variance and covariance operators denoted by \mathbb{E} , Var and Cov , respectively. For any Markov kernel P acting on $(\mathcal{X}, \mathbf{X})$ and for any f , we denote by $\text{var}(f, P)$ the asymptotic variance in a typical \sqrt{N} -central limit theorem for a MCMC estimator of πf , that is

$$\text{var}(f, P) = \lim_{N \rightarrow \infty} N \mathbb{V}\text{ar} \left[\frac{1}{N} \sum_{k=0}^{N-1} f(\mathbf{X}_k) \right],$$

where $\mathbf{X}_0 \sim \pi$ and $\mathbf{X}_k \mid \mathbf{X}_{k-1} \sim P(\mathbf{X}_{k-1}, \cdot)$ for $k > 0$. In this paper, all considered Markov kernels are assumed to be irreducible and aperiodic, so that the associated samplers are valid.

We are now ready to present the original ordering.

Theorem 1 (Peskun, 1973). *Let P_1 and P_2 be two Markov kernels that are reversible with respect to π . If $P_1(\mathbf{x}, \mathbf{y}) \geq P_2(\mathbf{x}, \mathbf{y})$ for all $(\mathbf{x}, \mathbf{y}) \in \mathcal{X}^2$ with $\mathbf{x} \neq \mathbf{y}$, then $\text{var}(f, P_1) \leq \text{var}(f, P_2)$ for all $f : \mathcal{X} \rightarrow \mathbb{R}$.*

The strength of this result lies in its universality: the order between the asymptotic variances holds for *all* functions f , which explains why we say that a sampler associated with P_1 is superior to a sampler associated with P_2 . However, it is only in specific situations that one can establish that the probability to reach \mathbf{y} from \mathbf{x} with P_1 is greater than or equal to that with P_2 , for all $(\mathbf{x}, \mathbf{y}) \in \mathcal{X}^2$ with $\mathbf{x} \neq \mathbf{y}$.

The result of Peskun (1973) was generalized in several ways. First, Tierney (1998) extended it to general state-spaces. Andrieu *et al.* (2018b) then provided a quantitative form requiring that the order on the Markov kernels holds, but up to a multiplicative factor, i.e. $P_1(\mathbf{x}, \mathbf{y}) \geq \omega P_2(\mathbf{x}, \mathbf{y})$ for some $\omega > 0$, while yielding similar conclusions:

$$\text{var}(f, P_1) \leq \frac{\text{var}(f, P_2)}{\omega} + \frac{1 - \omega}{\omega} \mathbb{V}\text{ar}[f(\mathbf{X}_0)].$$

These results are valid for reversible Markov chains only. Recently, Andrieu and Livingstone (2021) went beyond the reversible scenario. These authors consider a specific type of non-reversibility for which the chains can be seen as being “almost” reversible; they are reversible, up to an involution. This type of non-reversibility nevertheless covers a remarkably large number of known non-reversible MCMC algorithms, including *lifted* algorithms (Horowitz, 1991; Gustafson, 1998; Chen *et al.*, 1999; Diaconis *et al.*, 2000). Empirically, the latter have been seen to often outperform their reversible counterparts. Our motivation to introduce a weaker version of Peskun’s original ordering, which is in our case an asymptotic version as a varying parameter n goes to infinity, is to extend a result in Andrieu and Livingstone (2021) about lifted algorithms. An overview of such algorithms is now provided in order to explain this motivation. Lifted algorithms are described in detail in Section 3.

Lifting the state-space is a generic technique which yields what we call *lifted* samplers. The state-space is *lifted* to incorporate auxiliary variables. The idea is to think of the random variables we want to generate as *position* variables and to associate to them auxiliary variables, which in this case play the role of *direction* variables, to *guide* the Markov chains so as to avoid backtracking, a behaviour often exhibited by reversible schemes that is suspected to increase the autocorrelation of the process. Consider for instance that $\mathcal{X} = \{1, \dots, K\}$, where K is a positive integer. We associate to the variable \mathbf{X} a direction variable $v \in \{-1, +1\}$. A Markov chain is defined on the lifted state-space $\mathcal{X} \times \{-1, +1\}$. The lifted sampler proceeds as a Metropolis–Hastings (MH, (Metropolis *et al.*, 1953; Hastings, 1970)) algorithm in the sense that a proposal is accepted with a given probability, but in this case the proposal is deterministic and given by $\mathbf{y} = \mathbf{x} + v$ when (\mathbf{x}, v) is the current state. The randomness comes from a reversal of direction when the proposal is rejected. The direction variable equips the resulting stochastic process with some memory of its past so as to avoid backtracking by inducing persistent movement, while retaining the Markov property. It can be shown that the resulting Markov chains admit $\pi \otimes \mathcal{U}\{-1, 1\}$ as invariant distribution, where $\mathcal{U}\{-1, 1\}$ denotes the uniform distribution over the set $\{-1, 1\}$ and $\pi \otimes \mathcal{U}\{-1, 1\}$ is the product measure. The sampler is thus valid. Indeed, standard Markov-chain theory allows to establish that a law of large number and a central limit theorem hold, guaranteeing that one is able to approximate expectations under π by considering functions $f : \mathcal{X} \times \{-1, +1\} \rightarrow \mathbb{R}$ of solely the first argument, and that asymptotically the errors around the expectations are normally distributed with variances proportional to the asymptotic variances.

Let P_{lifted} be the Markov kernel associated to this algorithm, and let P_{MH} be the Markov kernel associated to its non-lifted counterpart, which is a MH algorithm proposing $\mathbf{y} = \mathbf{x} + 1$ or $\mathbf{y} = \mathbf{x} - 1$, each with probability 1/2. Theorem 7 in Andrieu and Livingstone (2021) allows to establish that $\text{var}(f, P_{\text{lifted}}) \leq \text{var}(f, P_{\text{MH}})$, for *any* f of solely the first argument and *any* distribution π . As Peskun's, this result is universal. It is however remarkable that it holds, not only for any f , but also for any π . It is also remarkable to obtain such a result given that the lifted sampler is implemented at no additional computational cost over its non-lifted counterpart, and also with no additional implementation difficulty (lifted samplers often possess these qualities). The result on the order between the asymptotic variances is a consequence of the rewriting of P_{MH} as

The superiority of P_{lifted} over P_{MH} for any π at no additional computational cost motivates an investigation of lifted samplers for other types of discrete state-spaces, especially given the limited number (or rather the absence) of real-world models where the state-space is of the form $\mathcal{X} = \{1, \dots, K\}$. This latter set is totally ordered; a natural first step in the investigation is thus to consider *partially-ordered* discrete state-spaces. A definition of partially-ordered sets as well as a generic lifted algorithm to sample from distributions defined on such a set are presented in Section 3. Important applications of such an algorithm include simulation of systems formed from binary variables, such as those simulated using the Ising model, and Bayesian variable selection when the posterior model probabilities can be evaluated, up to a normalizing constant. These examples are studied in Section 5.

In the case of partially-ordered discrete state-spaces, Theorem 7 of Andrieu and Livingstone (2021) still allows to prove the superiority of the lifted algorithm over its non-lifted counterpart, which is a reversible sampler; however in this case, the non-lifted counterpart does not correspond to the MH algorithm over which we wish to establish a superiority. Therefore, to prove that the lifted sampler is superior to this MH algorithm, a possibility is to establish a Peskun-type ordering between the non-lifted counterpart and the MH algorithm. In this paper, we travel that road. As will be seen, a (non-trivial) order between the Markov kernels of these reversible samplers can only be established on a subset of the state-space. Although rather frequent in practice, this situation is, up to our knowledge, yet to be addressed. Recent concepts such as *approximate spectral gaps* introduced in Atchadé (2021)

and *large sets* proposed in [Yang and Rosenthal \(2017\)](#) have shown that bounds on the convergence time of Markov chains can be obtained by exploiting the particular behaviour of the process on some subset of the state-space. When the process is particularly efficient on such a subset, resulting bounds can be tighter than traditional ones that account for the whole state-space. This paper addresses a slightly different problem which is that of comparing two Markov chains by analysing them specifically on some subset of the state-space. More precisely, in our weaker version of Peskun's ordering, it is sufficient to verify an order between two kernels restricted to a subset, as long as the mass concentrates on this subset as a varying parameter n grows unboundedly. The varying parameter n will, for example, play the role of the state-space dimension in our analyses. The price to pay for using the weaker version of Peskun's ordering is that, by contrast with Peskun's, the order on the asymptotic variances holds, but up to an error term that vanishes as $n \rightarrow \infty$, and applies not to all test functions. It will be seen that the assumptions required for this result to hold provide insights into the situations where the lifted samplers for partially-ordered discrete state-spaces are expected to outperform the MH ones, and also the situations where it is expected to be not the case.

1.2 Contributions and organization of the paper

We now summarize our main contributions and describe how the rest of the paper is organized. Our first contribution is a theoretical result: we, as mentioned previously, introduce an asymptotic Peskun ordering; this is done in [Section 2](#). Our second contribution is to use this result to identify situations in which the lifted samplers for partially-ordered discrete state-spaces are expected to outperform (or not) their MH counterparts. Regarding the organization of this part, we first present the lifted samplers in [Section 3](#) and then carry out at [Section 4](#) their analysis using the asymptotic ordering. More precisely, we proceed in [Section 3](#) as follows. We start by providing a definition of partially-ordered state-spaces in [Section 3.1](#). We next present in [Section 3.2](#) a generic lifted MCMC algorithm for sampling from distributions on partially-ordered discrete sets. In that section, we make a third contribution: we make clear that the implementation of lifted samplers for discrete state-spaces is straightforward, as long as a partial order can be established. We put in contrast this contribution with some of other authors by reviewing the literature about sampling on discrete state-spaces in [Section 3.3](#). In [Section 4](#), we proceed by specifying and theoretically analysing two important versions of the generic lifted algorithm: one with uniform proposal distributions ([Section 4.1](#)) and a more efficient version relying on *locally-balanced proposal distributions* recently introduced in [Zanella \(2020\)](#) ([Section 4.2](#)). We next corroborate in [Section 5](#) the theoretical findings on the lifted samplers by contrasting their empirical performance with that of their MH counterparts in two examples: a Ising model ([Section 5.1](#)) and a real variable-selection problem in which the parameters can be integrated out ([Section 5.2](#)). In [Section 6](#), we consider that \mathcal{X} is a model space and propose a lifted trans-dimensional sampler that can be used for, among others, variable selection when it is not possible to integrate out the parameters; this represents our fourth contribution. The paper finishes in [Section 7](#) with retrospective comments and possible directions for future research. All proofs of theoretical results are deferred to [Appendix A](#). While the paper is concerned with efficient sampling of distributions defined on discrete state-spaces, we stress that numerous results and elements of our analyses translate immediately to general state-space contexts, whenever a partial order exists.

2 An asymptotic version of Peskun's ordering

Before presenting the theoretical result, we provide the intuition behind it. This will help justify the assumptions, allow to highlight its relevance, and in fact allow to present a sketch of the proof. Beforehand, we introduce required notation.

In all this section, we consider that the distribution of interest π is parameterized by some $n \in \mathbb{N}$, that is $\pi \equiv \pi_n$. The state-space may also be parameterized by n and is thus denoted by \mathcal{X}_n ; we assume that, for each $n \in \mathbb{N}$, \mathcal{X}_n is finite. We define two collections of Markov kernels, $\{P_{1,n}\}$ and $\{P_{2,n}\}$, for which $P_{1,n}$ and $P_{2,n}$ are π_n -reversible for all n . We define a collection of subsets $\{\tilde{\mathcal{X}}_n \subset \mathcal{X}_n\}$ which we refer to as *control subsets*. We introduce two collections of restricted kernels $\{\tilde{P}_{1,n}\}$ and $\{\tilde{P}_{2,n}\}$ which, for all n , are defined for any $(\mathbf{x}, \mathbf{y}) \in \tilde{\mathcal{X}}_n^2$ by

$$\tilde{P}_{i,n}(\mathbf{x}, \mathbf{y}) := P_{i,n}(\mathbf{x}, \mathbf{y}) + P_{i,n}(\mathbf{x}, \mathcal{X}_n \setminus \tilde{\mathcal{X}}_n) \mathbb{1}_{\mathbf{y}=\mathbf{x}}, \quad i \in \{1, 2\}.$$

The form of states like \mathbf{x} and \mathbf{y} may depend on n , but we make this dependence implicit to simplify. We let $\tilde{\pi}_n$ be the probability measure defined as $\tilde{\pi}_n := \pi_n(\cdot \cap \tilde{\mathcal{X}}_n) / \pi_n(\tilde{\mathcal{X}}_n)$. It can be readily checked that $\tilde{P}_{1,n}$ and $\tilde{P}_{2,n}$ are both $\tilde{\pi}_n$ -reversible, for all n . We define what we call (with some abuse of terminology) the *interior* and the *boundary* of $\tilde{\mathcal{X}}_n$ as $\tilde{\mathcal{X}}_n^\circ := \{\mathbf{x} \in \tilde{\mathcal{X}}_n : P(\mathbf{x}, \tilde{\mathcal{X}}_n^\complement) = 0\}$ and $\partial \tilde{\mathcal{X}}_n := \tilde{\mathcal{X}}_n \setminus \tilde{\mathcal{X}}_n^\circ$, respectively. The functions for which we want to approximate the expectations may also depend on n and are thus denoted by f_n . The π_n -weighted scalar product and p -norm are defined as $\langle f_n, g_n \rangle_{\pi_n} := \sum_{\mathbf{x} \in \mathcal{X}} f_n(\mathbf{x}) g_n(\mathbf{x}) \pi_n(\mathbf{x})$ and $\|f_n\|_{\pi_n, p} := [\sum_{\mathbf{x} \in \mathcal{X}} f_n(\mathbf{x})^p \pi_n(\mathbf{x})]^{1/p}$, respectively, with $\|f_n\|_{\pi_n}$ for the 2-norm. In this section, we consider that the functions are standardized, meaning that $f_n \in \mathcal{L}_{0,1}^2(\pi_n)$, where $\mathcal{L}_{0,1}^2(\pi_n) := \{f_n : \pi_n f_n = 0 \text{ and } \|f_n\|_{\pi_n} = 1\}$. This should not be seen as a restriction given that the magnitude of asymptotic variances, which is proportional to $\|f_n\|_{\pi_n}^2$, is irrelevant when it is of interest to establish an order among them. We note that since for each n , \mathcal{X}_n is finite, $P_{1,n}$ and $P_{2,n}$ admit a non-trivial right spectral gap in $\mathcal{L}_{0,1}^2(\pi_n)$, whose variational expression is given by

$$\lambda_i(n) := \inf_{f_n \in \mathcal{L}_{0,1}^2(\pi_n) : \|f_n\|_{\pi_n} > 0} \frac{\langle f_n, (I_n - P_{i,n}) f_n \rangle_{\pi_n}}{\|f_n\|_{\pi_n}^2}, \quad i \in \{1, 2\}, \quad (1)$$

where I_n is the identity on $\mathcal{L}_{0,1}^2(\pi_n)$. In particular, it can be proved that $\lambda_i(n) \in (0, 2)$. We analogously define the right spectral gaps of $\tilde{P}_{i,n}$ and denote them by $\tilde{\lambda}_i(n)$, $i = 1, 2$, and we define $\underline{\lambda}(n) := \min\{\lambda_1(n), \lambda_2(n), \tilde{\lambda}_1(n), \tilde{\lambda}_2(n)\}$. Finally, we will use o for the little-o notation.

Consider that one wants to establish a Peskun-type ordering between two kernels, but one is only able to establish an order on the kernels on a subset of the state-space, i.e. $P_{1,n}(\mathbf{x}, \mathbf{y}) \geq \omega(n) P_{2,n}(\mathbf{x}, \mathbf{y})$ for all $(\mathbf{x}, \mathbf{y}) \in \tilde{\mathcal{X}}_n^2$ with $\mathbf{x} \neq \mathbf{y}$ where $\omega(n)$ is a positive constant which may depend on n . This ordering implies that $\tilde{P}_{1,n}(\mathbf{x}, \mathbf{y}) \geq \omega(n) \tilde{P}_{2,n}(\mathbf{x}, \mathbf{y})$ for all $(\mathbf{x}, \mathbf{y}) \in \tilde{\mathcal{X}}_n^2$ with $\mathbf{x} \neq \mathbf{y}$, which in turn implies that

$$\text{var}(f_n, \tilde{P}_{1,n}) \leq \frac{1}{\omega(n)} \text{var}(f_n, \tilde{P}_{2,n}) + \frac{1 - \omega(n)}{\omega(n)},$$

by, as mentioned in [Section 1.1, Andrieu *et al.* \(2018b\)](#) (Lemma 33).

Let us consider that π_n concentrates on $\tilde{\mathcal{X}}_n^\circ$. The notion of concentration of π_n naturally implies that we are interested by a certain asymptotic regime, which justifies that we consider a limit $n \rightarrow \infty$. Under this regime, $\pi_n(\tilde{\mathcal{X}}_n^\circ) \rightarrow 1$, implying that $\pi_n(\tilde{\mathcal{X}}_n) \rightarrow 1$. One can imagine that, if the Markov chains associated with $P_{1,n}$ and $P_{2,n}$ do not behave “too badly” outside of $\tilde{\mathcal{X}}_n$, meaning that if they reach the complement $\tilde{\mathcal{X}}_n^\complement$ they do not stay there for “too long”, then $\text{var}(f_n, \tilde{P}_{1,n})$ and $\text{var}(f_n, \tilde{P}_{2,n})$ should be

similar to $\text{var}(f_n, P_{1,n})$ and $\text{var}(f_n, P_{2,n})$. This is what we show in order to prove our theoretical result. In fact, if we think of $P_{1,n}, P_{2,n}, \tilde{P}_{1,n}$ and $\tilde{P}_{2,n}$ as samplers, it is seen in the proof that in order to establish a connection between the asymptotic variances, it simplifies to assume that the performance of the worst of these samplers, measured through $\underline{\lambda}(n)$, is not “too poor”, which is a stronger assumption than a performance assumption on $P_{1,n}$ and $P_{2,n}$ only. Under these assumptions, we are able to establish that $\text{var}(f_n, P_{i,n})$ is equal to $\text{var}(f_n, \tilde{P}_{i,n})$, up to an error term that depends on n and that vanishes in the large n regime, $i \in \{1, 2\}$, which essentially yields our result. The concentration assumption is reasonable given that in practice the mass often concentrates on a manifold of the state-space. This is especially true in high dimensions or when the sample size is large in a Bayesian statistics context (see, e.g., [Van der Vaart \(2000\)](#) and [Kleijn and Van der Vaart \(2012\)](#)).

In light of the above, it is understood that three assumptions are required: the order on the kernels on the control subset, the concentration of π_n and a performance guarantee on the samplers. We now state formally the first two assumptions and then present a simplified version of the theoretical result with a strong performance guarantee. We next present a more general version. To simplify the results, yet keeping the focus on most important cases, we consider in the following that $\omega(n) \leq 1$ and $\lambda_1(n), \lambda_2(n), \tilde{\lambda}_1(n), \tilde{\lambda}_2(n) < 1$ for all n , meaning that we exclude cases where $P_{1,n}$ is overly dominant on $\tilde{\mathcal{X}}_n$ and rare cases where one right spectral gap is greater than or equal to 1, which can be observed with extremely antithetic chains ([Rosenthal, 2003](#)).

Given $\{\pi_n\}$, $\{P_{1,n}\}$ and $\{P_{2,n}\}$, the control subsets $\{\tilde{\mathcal{X}}_n\}$ are chosen so that the following two assumptions are satisfied.

Assumption 1 (Kernel ordering). *For each n ,*

$$P_{1,n}(\mathbf{x}, \mathbf{y}) \geq \omega(n) P_{2,n}(\mathbf{x}, \mathbf{y}),$$

for all $(\mathbf{x}, \mathbf{y}) \in \tilde{\mathcal{X}}_n^2$ with $\mathbf{x} \neq \mathbf{y}$, where $\omega(n)$ admits a limit, i.e.

$$\lim_{n \rightarrow \infty} \omega(n) =: \bar{\omega} > 0.$$

Assumption 2 (Mass concentration). *The mass concentrates on $\tilde{\mathcal{X}}_n^\circ$:*

$$\lim_{n \rightarrow \infty} \pi_n(\tilde{\mathcal{X}}_n^\circ) = 1.$$

Given that together Assumptions 1 and 2 correspond to the assumptions of a classic Peskun ordering as in [Andrieu et al. \(2018b\)](#) in the limit, one can only hope to establish, under Assumptions 1 and 2, a version of this ordering that holds in some limiting sense. We will present two versions that hold under conditions on the rates of convergence of the different functions of n involved. We acknowledge the fact that estimating certain rates appearing in those conditions, especially the rates of spectral quantities, may already constitute a problem in itself. It is the case for instance for the Ising-model and variable-selection examples that are presented in [Section 5](#). We leave the estimation of the rates required for applying our theoretical results in these examples for future work. These examples are used to, among others, support with empirical evidence the theoretical findings of the study of two lifted samplers presented in [Section 4](#). In this study, $P_{1,n}$ and $P_{2,n}$ play the role of the non-lifted counterpart to the lifted sampler and the MH sampler, respectively. This study is conducted in generality. More precisely, the target distribution is not specified; we will thus not be in a position to explicitly estimate the rates appearing in the conditions of our theoretical results. Making assumptions regarding these rates and defining judiciously the control subsets will allow to gain general insights into the situations in which

the lifted samplers are expected to outperform their MH counterparts, and also into those in which it is not the case.

One may be tempted to assume a (non-trivial) relationship between $\tilde{\lambda}_i(n)$ and $\lambda_i(n)$ given that $\tilde{P}_{i,n}$ is a restriction of $P_{i,n}$ on a subset of the state-space \mathcal{X}_n . It turns out that counterexamples show that it is not possible to obtain an interesting result in the general case. In regular sampling contexts, we expect the rates at which $\tilde{\lambda}_i(n)$ and $\lambda_i(n)$ vanish to be in the same regime (i.e. both exponential, both polynomial, etc.). Should that be the case, that would leave only the rates of $\lambda_1(n)$ and $\lambda_2(n)$ or $\tilde{\lambda}_1(n)$ and $\tilde{\lambda}_2(n)$ to estimate. In an example presented in the supplementary material (Appendix B) for which we can numerically estimate all rates, $\lambda_1(n), \lambda_2(n), \tilde{\lambda}_1(n), \tilde{\lambda}_2(n)$ all vanish at the same speed. In this example, $\tilde{P}_{2,n}$ is similar to a random walk on the set $\{1, \dots, n\}$ for which an estimate of the rate exists (see, e.g., [Diaconis et al. \(2000\)](#)). We numerically observe that this rate correspond to the rates of $\lambda_1(n), \lambda_2(n), \tilde{\lambda}_1(n), \tilde{\lambda}_2(n)$, meaning that such literature can be useful to estimate the rates of the spectral gaps (see, e.g., [Boyd et al. \(2005\)](#) for results on graphs).

Theorem 2 (A simple asymptotic Peskun ordering). *Suppose that Assumptions 1 and 2 hold. Assume that the right spectral gaps of $P_{i,n}$ and $\tilde{P}_{i,n}$ are bounded away from zero for all n , $i = 1, 2$. Assume also that the sequence $\{f_n\}$ is such that $f_n \in \mathcal{L}_{0,1}^2(\pi_n)$ for all n and such that there exist $\delta > 0$ and $\delta/(2 + \delta) > \gamma > 0$ with*

$$\|f_n\|_{\pi_n, 2+\delta} = o\left(\frac{1}{(1 - \pi_n(\tilde{\mathcal{X}}_n^\circ))^\gamma}\right). \quad (2)$$

Then, for any $\bar{\omega} > \epsilon > 0$, there exists $n^ \in \mathbb{N}$, which depends on $\{f_n\}$, such that*

$$\text{var}(f_n, P_{1,n}) \leq \frac{1}{\bar{\omega} - \epsilon} \text{var}(f_n, P_{2,n}) + \frac{1 - \bar{\omega}}{\bar{\omega}} + \epsilon,$$

for each $n > n^$.*

We now make a few remarks about [Theorem 2](#). This result will be seen to be a special case of the next one in which the spectral gaps are allowed to decrease with n , which is usually the case when n is the dimension of the state-space. As mentioned, considering that the spectral gaps are bounded away from zero simplifies the assumptions, at the price of requiring a strong performance guarantee.

In addition to the three assumptions mentioned earlier, another one is made in (2). This assumption essentially states that the functions f_n , in the $(2 + \delta)$ -norm, are allowed to grow with n , but not faster (in fact slightly slower) than $1/(1 - \pi_n(\tilde{\mathcal{X}}_n^\circ))$. It is thus not all sequences $\{f_n\}$ that are admissible. It could be tempting to consider a collection of large subsets $\tilde{\mathcal{X}}_n$ to encourage a fast concentration of π_n on these sets, thus allowing for a large class of admissible sequences of functions in [Theorem 2](#); however, the larger are the subsets, the more difficult it becomes to verify the order on the kernels ([Assumption 1](#)).

Different values of the limit of $\omega(n)$, i.e. $\bar{\omega}$, yield different interpretations of the result. The most important case is when $\bar{\omega} = 1$ for which we can state that the sampler associated with $P_{1,n}$ *asymptotically dominates* that associated with $P_{2,n}$, for the functions that are admissible. When $\bar{\omega} < 1$, [Theorem 2](#) allows to state that $P_{1,n}$ is *asymptotically comparable* to $P_{2,n}$, in the sense that we have a guarantee that the sampler associated with $P_{1,n}$ will asymptotically produce estimators with variances that are at worst $1/\bar{\omega}$ larger than the sampler associated with $P_{2,n}$, again for the functions that are admissible.

We now present the general asymptotic Peskun ordering.

Theorem 3 (A general asymptotic Peskun ordering). *Suppose that [Assumption 1](#) holds. Consider a sequence $\{f_n\}$ such that $f_n \in \mathcal{L}_{0,1}^2(\pi_n)$ for all n . Assume that there exist $\delta > 0$ and $\delta/(2 + \delta) > \gamma > 0$ that*

satisfy

$$\|f_n\|_{\pi_n, 2+\delta} = o\left(\frac{1}{(1 - \pi_n(\tilde{\mathcal{X}}_n^\circ))^\gamma}\right), \quad (3)$$

and

$$1 - \pi_n(\tilde{\mathcal{X}}_n^\circ) = o\left(\underline{\lambda}(n)^{3/(\bar{\delta}-\gamma)}\right), \quad (4)$$

where $\bar{\delta} := \delta/(2 + \delta)$. Then, for any $\bar{\omega} > \epsilon > 0$, there exists $n^* \in \mathbb{N}$, which depends on $\{f_n\}$, such that

$$\text{var}(f_n, P_{1,n}) \leq \frac{1}{\bar{\omega} - \epsilon} \text{var}(f_n, P_{2,n}) + \frac{1 - \bar{\omega}}{\bar{\omega}} + \epsilon,$$

holds for each $n > n^*$.

We see that the difference between [Theorem 3](#) and [Theorem 2](#) is that [Assumption 2](#) is replaced by (4), an assumption connecting $\pi_n(\tilde{\mathcal{X}}_n^\circ)$ to $\underline{\lambda}(n)$, where the latter is now allowed to vanish. After having selected a sequence $\{f_n\}$ and then δ and γ that satisfy (3) (which is equivalent to (2) in [Theorem 2](#)), one has to verify that the choice of δ and γ also allows to verify (4). This equation states that the concentration of π_n on $\tilde{\mathcal{X}}_n^\circ$ has to be faster than $\underline{\lambda}(n)^{3/(\bar{\delta}-\gamma)}$. Note that when the right spectral gaps are bounded away from zero, (4) is equivalent to [Assumption 2](#), showing that [Theorem 2](#) is indeed a special case of [Theorem 3](#).

3 Lifted samplers for partially-ordered discrete state-spaces

In this section, in order to match the classical MCMC framework, we consider the target distribution, state-space, and so on, to be fixed, and will thus denote them without a subscript to simplify.

3.1 Partially-ordered state-spaces

In set theory, a partial order on a set \mathcal{X} is a binary relation defined through a set $\mathcal{R} \subset \mathcal{X}^2$ which is reflexive, antisymmetric, and transitive. A set \mathcal{X} on which a partial order can be defined, is called *partially ordered*. For such a set, pairs $(\mathbf{x}, \mathbf{y}) \in \mathcal{X}^2$ with $\mathbf{x} \neq \mathbf{y}$ are *comparable* when either $(\mathbf{x}, \mathbf{y}) \in \mathcal{R}$ or $(\mathbf{y}, \mathbf{x}) \in \mathcal{R}$ and are said *incomparable* otherwise. This represents the difference with a totally-ordered set such as \mathbb{N} or \mathbb{R} in which every pair of different elements is comparable. We denote $\mathbf{x} \prec \mathbf{y}$ whenever $(\mathbf{x}, \mathbf{y}) \in \mathcal{R}$ and $\mathbf{x} \neq \mathbf{y}$, implying that \mathbf{x} and \mathbf{y} are comparable. Of course, this is not the only way to have comparable \mathbf{x} and \mathbf{y} as we could instead have $\mathbf{y} \prec \mathbf{x}$, i.e. $(\mathbf{y}, \mathbf{x}) \in \mathcal{R}$ and $\mathbf{x} \neq \mathbf{y}$.

An important example of such sets is when any $\mathbf{x} \in \mathcal{X}$ can be written as a vector $\mathbf{x} = (x_1, \dots, x_n)$ for which each component x_i can be of two types, say Type A or Type B, denoted by $x_i \in \{A, B\}$. In this case, an inclusion-based partial order on \mathcal{X} can be defined through

$$\mathcal{R} = \{(\mathbf{x}, \mathbf{y}) \in \mathcal{X} \times \mathcal{X} : \{i : x_i = A\} \subset \{i : y_i = A\}\}. \quad (5)$$

It can be readily checked that \mathcal{R} is reflexive, anti-symmetric and transitive. Moreover, defining $n_A(\mathbf{x})$ to be the number of Type A components in \mathbf{x} , i.e. $n_A(\mathbf{x}) = \sum_{i=1}^n \mathbb{1}_{x_i=A}$, we have that a pair $(\mathbf{x}, \mathbf{y}) \in \mathcal{X}^2$ such that $\mathbf{x} \neq \mathbf{y}$ and $n_A(\mathbf{x}) = n_A(\mathbf{y})$ is incomparable.

Partially-ordered sets are encountered in many important areas of statistics including the modelling of binary data using networks or graphs and in variable selection. Indeed, for the former, \mathcal{X} can be parameterized such that $\mathcal{X} = \{-1, +1\}^n$, where for example for an Ising model, $x_i \in \{-1, +1\}$ represents the state of a spin. For variable selection, $\mathcal{X} = \{0, 1\}^n$ and $x_i \in \{0, 1\}$ indicates whether or not the i -th covariate is included in the model employed.

3.2 Generic algorithm

Let us assume that a neighbourhood structure $\{\mathbf{N}(\mathbf{x}) : \mathbf{x} \in \mathcal{X}\}$ and a partial order \mathcal{R} have been specified on \mathcal{X} . The sampler that we present is a MCMC algorithm that relies on the lifting technique. The state-space is thus extended: we add a direction variable $\nu \in \{-1, +1\}$ to which we assign a uniform distribution $\mathcal{U}\{-1, +1\}$. The target distribution becomes $\pi \otimes \mathcal{U}\{-1, +1\}$. The idea is to generate proposals belonging to a specific subset of the neighbourhood $\mathbf{N}(\mathbf{x})$, where the subset is defined through \mathcal{R} and chosen according to the direction ν , when the current state of the chain is (\mathbf{x}, ν) . In particular, the proposal belongs to $\mathbf{N}_{\nu}(\mathbf{x}) := \{\mathbf{y} \in \mathbf{N}(\mathbf{x}) : \mathbf{x} \prec \mathbf{y}\} \subset \mathbf{N}(\mathbf{x})$ when the current state of the momentum variable is $\nu = +1$ and to $\mathbf{N}_{-\nu}(\mathbf{x}) := \{\mathbf{y} \in \mathbf{N}(\mathbf{x}) : \mathbf{y} \prec \mathbf{x}\} \subset \mathbf{N}(\mathbf{x})$ when $\nu = -1$. The partial order is thus used to induce directions to follow in the state-space. We assume that $\mathbf{N}(\mathbf{x})$ is formed only of states that are comparable to \mathbf{x} so that $\mathbf{N}_{-\nu}(\mathbf{x}) \cup \mathbf{N}_{\nu}(\mathbf{x}) = \mathbf{N}(\mathbf{x})$. The underlying assumption $\mathbf{x} \notin \mathbf{N}(\mathbf{x})$ implies that, strictly speaking, \mathbf{N} is not a neighbourhood in a topological sense. We nevertheless carry on with this abuse of terminology.

Recently, successful applications of the lifting technique have been carried out in contexts where the state-space exhibits a one-dimensional discrete parameter which plays a central role in the sampling scheme: the temperature variable in simulated tempering (Sakai and Hukushima, 2016b) and in parallel tempering (Syed *et al.*, 2021), and the model indicator in selection of nested models (Gagnon and Doucet, 2021). When such a one-dimensional feature does not exist, there is no straightforward way of lifting the state-space and inducing directions without facing issues of reducibility or the risk of obtaining inefficient samplers. Leveraging what can be regarded as a directional neighbourhood structure induced by the partial order on \mathcal{X} allows to break free from the requirement of resorting to an existing one-dimensional parameter to guide the chain.

In what follows, for each $(\mathbf{x}, \nu) \in \mathcal{X} \times \{-1, +1\}$, $\mathbf{N}_{\nu}(\mathbf{x})$ shall be referred to as the ν -directional neighbourhood of state \mathbf{x} . The proposal distribution, denoted by $q_{\mathbf{x}, \nu}$, where (\mathbf{x}, ν) represents the current state of the Markov chain, is assumed to have its support restricted to $\mathbf{N}_{\nu}(\mathbf{x})$. It will be noticed that the implementation of the generic algorithm is straightforward provided that a partial ordering has been established. Indeed, the required inputs are:

- (i) a neighbourhood structure $\{\mathbf{N}(\mathbf{x}) : \mathbf{x} \in \mathcal{X}\}$,
- (ii) a partial ordering \mathcal{R} on \mathcal{X} ,
- (iii) proposal distributions $q_{\mathbf{x}, \nu}$,

and there exist natural candidates for the proposal distributions, as will be explained in Section 3.3 and, in most cases, for the neighbourhood structure as well.

The MCMC algorithm, which bares a strong resemblance with the guided walk (Gustafson, 1998), is presented at Algorithm 1. We use $x \wedge y$ to denote $\min\{x, y\}$.

Given that \mathcal{X} is finite, there exists a boundary, in the sense that, for some (\mathbf{x}, ν) , $\mathbf{N}_{\nu}(\mathbf{x})$ is the empty set and there is thus no mass beyond state \mathbf{x} when the direction followed is ν . This is for instance the case in the context of variable selection when $\mathbf{x} = (1, \dots, 1)$, meaning that the current model is the full model, and the direction is $\nu = +1$. Algorithm 1 may thus seem incomplete: it does not explicitly specify how the algorithm behaves on the boundary. We can consider that for any $\mathbf{x} \in \mathcal{X}$ on the boundary, the support of $q_{\mathbf{x}, \nu}$ is not $\mathbf{N}_{\nu}(\mathbf{x})$ (because this is the empty set), but instead given by a fictive state outside \mathcal{X} . Given that the support of π is \mathcal{X} , then any state outside \mathcal{X} has zero mass under π and such a fictive state is automatically rejected at Step 2. As a consequence, when such a state is proposed, the chain remains at \mathbf{x} and the direction is reversed. Note that this is a technical requirement.

Algorithm 1 A lifted sampler for partially-ordered discrete state-spaces

1. Generate $\mathbf{y} \sim q_{\mathbf{x}, \nu}$ and $u \sim \mathcal{U}[0, 1]$.
2. If

$$u \leq \alpha_\nu(\mathbf{x}, \mathbf{y}) := 1 \wedge \frac{\pi(\mathbf{y}) q_{\mathbf{y}, -\nu}(\mathbf{x})}{\pi(\mathbf{x}) q_{\mathbf{x}, \nu}(\mathbf{y})}, \quad (6)$$

set the next state of the chain to (\mathbf{y}, ν) . Otherwise, set it to $(\mathbf{x}, -\nu)$.

3. Go to Step 1.

In practice, one can simply skip Step 1 when \mathbf{x} is on the boundary and directly set the next state to $(\mathbf{x}, -\nu)$.

MH algorithms thus have an advantage on the boundary: they can make the chains go back towards the centre, without having to remain at \mathbf{x} for an iteration. A way to alleviate this issue with lifted samplers is to make an exception to our definition of directional neighbourhoods by defining otherwise those of states on the boundary. We now explain a strategy; we consider the specific case where $\mathcal{X} = \{-1, +1\}^n$ to facilitate the explanation. Originally, the $+1$ -directional neighbourhood of $\mathbf{x} = (+1, \dots, +1)$ is the empty set. A strategy is to set $\mathbf{N}_{+1}(\mathbf{x}) = \{-\mathbf{x}\}$ for $\mathbf{x} = (+1, \dots, +1)$, which violates the general rule that $\mathbf{y} \in \mathbf{N}_{+1}(\mathbf{x})$ if and only if $\mathbf{x} \prec \mathbf{y}$, and $\mathbf{N}_{-1}(\mathbf{x}) = \{-\mathbf{x}\}$ for $\mathbf{x} = (-1, \dots, -1)$; the other neighbourhoods are unchanged. This construction avoids an automatic rejection on the boundary and provides the Markov dynamic with a torus-like feature given that it connects the most extreme states, from a partial-order perspective. Note that in practice, the chance to reach a boundary point during an algorithm run is often low, implying that this disadvantage of lifted samplers can essentially be seen as a theoretical concern.

It is possible to establish that the Markov chain defined by [Algorithm 1](#) is $\pi \otimes \mathcal{U}\{-1, +1\}$ -invariant by casting it into a more general algorithm framework presented in [Andrieu and Livingstone \(2021\)](#). We present below the associated generalization of [Algorithm 1](#) which has interesting theoretical features. Beforehand, we introduce necessary notation. Let $\rho_\nu : \mathcal{X} \rightarrow [0, 1]$, for $\nu \in \{-1, +1\}$, be a user-defined function for which we require that for all $(\mathbf{x}, \nu) \in \mathcal{X} \times \{-1, +1\}$:

$$0 \leq \rho_\nu(\mathbf{x}) \leq 1 - T_\nu(\mathbf{x}, \mathcal{X}), \quad (7)$$

$$\rho_\nu(\mathbf{x}) - \rho_{-\nu}(\mathbf{x}) = T_{-\nu}(\mathbf{x}, \mathcal{X}) - T_\nu(\mathbf{x}, \mathcal{X}), \quad (8)$$

where we have set, for all $(\mathbf{x}, \nu) \in \mathcal{X} \times \{-1, +1\}$,

$$T_\nu(\mathbf{x}, \mathcal{X}) := \sum_{\mathbf{x}' \in \mathcal{X}} q_{\mathbf{x}, \nu}(\mathbf{x}') \alpha_\nu(\mathbf{x}, \mathbf{x}') = \sum_{\mathbf{x}' \in \mathbf{N}_\nu(\mathbf{x})} q_{\mathbf{x}, \nu}(\mathbf{x}') \alpha_\nu(\mathbf{x}, \mathbf{x}').$$

These conditions are considered satisfied in the sequel as they guarantee, as established in [Proposition 1](#) below, that the Markov chain $\{(\mathbf{X}, \nu)_k\}$ is $\pi \otimes \mathcal{U}\{-1, +1\}$ -invariant and thus that the marginal process $\{\mathbf{X}_k\}$ is π -invariant. Let $Q_{\mathbf{x}, \nu}$ be the probability mass function (PMF) defined through $Q_{\mathbf{x}, \nu}(\mathbf{x}') \propto q_{\mathbf{x}, \nu}(\mathbf{x}') \alpha_\nu(\mathbf{x}, \mathbf{x}')$. The generalization of [Algorithm 1](#) is now presented in [Algorithm 2](#).

Proposition 1. *The transition kernel of the Markov chain $\{(\mathbf{X}, \nu)_k\}$ simulated by [Algorithm 2](#) admits $\pi \otimes \mathcal{U}\{-1, +1\}$ as invariant distribution.*

Algorithm 2 A generalization of [Algorithm 1](#)

1. Generate $u \sim \mathcal{U}[0, 1]$.

- (i) If $u \leq T_v(\mathbf{x}, \mathcal{X})$, generate $\mathbf{y} \sim Q_{\mathbf{x}, v}$ and set the next state of the chain to (\mathbf{y}, v) ;
- (ii) if $T_v(\mathbf{x}, \mathcal{X}) < u \leq T_v(\mathbf{x}, \mathcal{X}) + \rho_v(\mathbf{x})$, set the next state of the chain to $(\mathbf{x}, -v)$;
- (iii) if $u > T_v(\mathbf{x}, \mathcal{X}) + \rho_v(\mathbf{x})$, set the next state of the chain to (\mathbf{x}, v) .

2. Go to Step 1.

One may notice that $T_v(\mathbf{x}, \mathcal{X})$ represents the probability to leave the current state (\mathbf{x}, v) . In [Algorithm 2](#), we thus first decide if we move on from \mathbf{x} , in which case, in Step 1.(i), we randomly select the value of \mathbf{y} , the state to move to (using the conditional distribution). It can be readily checked that choices for ρ_v include $\rho_v(\mathbf{x}) = 1 - T_v(\mathbf{x}, \mathcal{X})$ and $\rho_v(\mathbf{x}) = \max\{0, T_{-v}(\mathbf{x}, \mathcal{X}) - T_v(\mathbf{x}, \mathcal{X})\}$. If $\rho_v(\mathbf{x}) = 1 - T_v(\mathbf{x}, \mathcal{X})$, the condition for Case (iii) of Step 1 is never satisfied, and the algorithm either accepts the proposal and keeps the same direction, or the proposal is rejected and the direction is reversed. In this case, one can show that [Algorithm 2](#) corresponds to [Algorithm 1](#), which is why [Proposition 1](#) allows ensuring the correctness of [Algorithm 1](#) as well. Setting $\rho_v(\mathbf{x})$ otherwise than $\rho_v(\mathbf{x}) = 1 - T_v(\mathbf{x}, \mathcal{X})$ allows in Case (iii) of Step 1 to keep following the same direction, even when the proposal is rejected. Intuitively, this is desirable when the rejection is due to “bad luck”, and not because there is low mass in the direction followed. The function $\rho_v(\mathbf{x})$ aims at incorporating this possibility in the sampler.

In a typical MCMC framework with continuous state-spaces, the function $\mathbf{x} \mapsto T_v(\mathbf{x}, \mathcal{X})$ is intractable. In such a case, it is therefore usually not possible to set $\rho_v(\mathbf{x})$ otherwise than $1 - T_v(\mathbf{x}, \mathcal{X})$. This contrasts with our discrete state-space framework in which it is often possible to directly compute $T_v(\mathbf{x}, \mathcal{X})$. Theorem 6 in [Andrieu and Livingstone \(2021\)](#) states that the best choice of function ρ_v in terms of a mathematical object related to the asymptotic variance is

$$\rho_v^*(\mathbf{x}) := \max\{0, T_{-v}(\mathbf{x}, \mathcal{X}) - T_v(\mathbf{x}, \mathcal{X})\}, \quad (9)$$

and that the worst choice is $\rho_v^w(\mathbf{x}) := 1 - T_v(\mathbf{x}, \mathcal{X})$. [Corollary 1](#) below establishes an order on the asymptotic variances in the context of finite state-spaces of this paper. Denote by P_ρ the transition kernel corresponding to [Algorithm 2](#) for a given function $\rho_v : \mathcal{X} \rightarrow [0, 1]$.

Corollary 1. *If \mathcal{X} is finite, then for any function ρ_v satisfying (7)-(8) and for any function $f : \mathcal{X} \times \{-1, +1\} \rightarrow \mathbb{R}$ such that $f(\mathbf{x}, -1) = f(\mathbf{x}, +1)$, we have*

$$\text{var}(f, P_{\rho^*}) \leq \text{var}(f, P_\rho) \leq \text{var}(f, P_{\rho^w}).$$

The price to pay for using ρ_v^* instead of ρ_v^w is that the algorithm is more complicated to implement because it is required to systematically compute $T_v(\mathbf{x}, \mathcal{X})$ at each iteration (it is also sometimes required to compute $T_{-v}(\mathbf{x}, \mathcal{X})$). Using ρ_v^* thus also comes with an additional computation cost. In our numerical experiments, it is seen that, if we account for this increased computational cost, there is no gain in efficiency of using [Algorithm 2](#) with ρ_v^* over [Algorithm 2](#) with ρ_v^w (corresponding to [Algorithm 1](#)). One may thus opt for simplicity and implement [Algorithm 1](#). Note that the latter and its MH counterpart have essentially the same computational cost.

3.3 Related work about sampling on discrete state-spaces

Sampling on discrete state-spaces is typically performed using uniform proposal distributions in reversible samplers. If we consider for instance that $\mathbf{x} = (x_1, \dots, x_n)$ with $x_1, \dots, x_n \in \{A, B\}$, Glauber dynamics for graphical models or the tie-no-tie sampler for network models selects uniformly at random one of the coordinate, say x_i , and proposes to change its value from A to B (B to A) when $x_i = A$ ($x_i = B$). Such moves are often rejected when the mass concentrates on a manifold of the state-space. To address this issue, [Zanella \(2020\)](#) recently proposed a *locally-balanced* generic approach for which the probability to select the i th coordinate depends on the relative mass of the resulting proposal, i.e. $\pi(\mathbf{y})/\pi(\mathbf{x})$, aiming at proposing less “naive” moves. [Zanella \(2020\)](#) proves that the acceptance probabilities converge to 1 in a high-dimensional regime. This property suggests that locally-balanced samplers are efficient, at least in high dimensions. Indeed, samplers for discrete state-spaces typically use the same neighbourhood structure $\{\mathbf{N}(\mathbf{x}) : \mathbf{x} \in \mathcal{X}\}$, implying that the ranges of the proposal distributions are the same and that higher acceptance probabilities often translate into better mixing properties. [Zanella \(2020\)](#) in fact empirically shows that locally-balanced samplers perform better than alternative solutions to sample from PMFs, and that the difference is highly marked in the high-dimensional regime. Yet, the samplers are reversible, implying that the chains may often go back to recently visited states, or in other words, that the chains exhibit a random-walk behaviour.

In the presented generic algorithms in [Section 3.2](#), there is no restriction on the proposal distributions $q_{\mathbf{x}, \mathbf{v}}$. In [Section 4.2](#), we set them to locally-balanced proposal distributions, thus combining the strengths of the lifting and locally-balanced approaches. An illustration showing the benefit of this combination is provided at [Figure 1](#) in which we measure the performance using the effective sample size (ESS) of a statistic, reported per iteration. ESS per iteration is defined as the inverse of the integrated autocorrelation time. When the chains start in stationarity, integrated autocorrelation time corresponds to the asymptotic variance of a standardized version of the statistic. A smaller asymptotic variance thus yields a higher ESS.

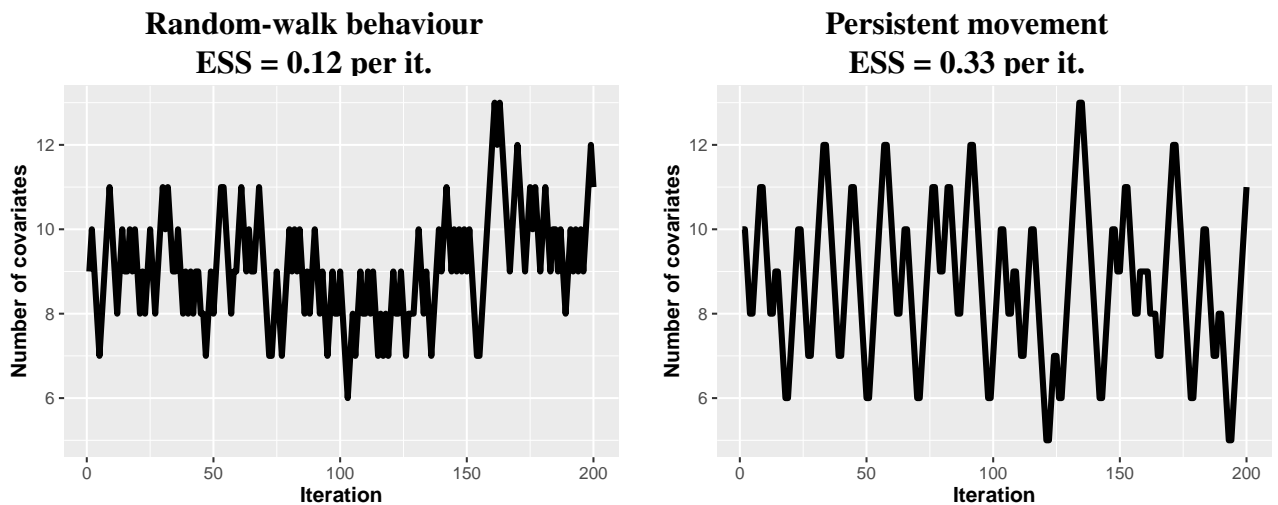


Figure 1. Trace plots for the statistic of number of covariates included in a model for a MH sampler with locally-balanced proposal distributions on the left panel and its lifted counterpart on the right panel, when applied to solve a real variable-selection problem presented in [Section 5.2](#)

Other (somewhat) generic approaches to non-reversible sampling on discrete state-spaces are (to our knowledge) all contemporary to ours: [Bierkens \(2016\)](#), [Sakai and Hukushima \(2016a\)](#), [Power and Goldman \(2019\)](#), [Faizi *et al.* \(2020\)](#) and [Herschlag *et al.* \(2020\)](#). They rely on the lifting technique as

well, except [Bierkens \(2016\)](#). Our work is most closely related to [Power and Goldman \(2019\)](#) in which the approach of [Zanella \(2020\)](#) is also exploited. In fact, when $\mathbf{x} = (x_1, \dots, x_n)$ with $x_1, \dots, x_n \in \{A, B\}$, [Algorithm 1](#) corresponds to the discrete-time version of a specific sampler independently developed in [Power and Goldman \(2019\)](#). [Algorithm 1](#) can also be seen to be a special case of a sampler presented in [Sakai and Hukushima \(2016a\)](#) in which a general extended transition matrix is defined from lifting the MH one. A similar approach, described in [Faizi et al. \(2020\)](#), explicitly incorporates the changes in the function f by moving from a state to another in the transition matrix; this latter approach is closely related to ours when $f(\mathbf{x})$ decreases or increases every time we change \mathbf{x} for \mathbf{y} with $\mathbf{x} < \mathbf{y}$. We consequently do not claim originality for the samplers presented here. In those papers, however, the notion of partial ordering is not identified nor exploited; the focus is rather on improving state-space exploration through the exploitation of *any* symmetric or algebraic structure of \mathcal{X} identified by users. The focus is the same in [Bierkens \(2016\)](#), but the non-reversibility is achieved by directly modifying the acceptance probability in MH, using the notion of vorticity matrix; this approach is valid in general state-space contexts. In [Herschlag et al. \(2020\)](#), the authors generalize non-reversible lifted kernels to *mixed skewed* kernels by means of a series of involutions in a context of undirected graph sampling. In their work, the main application is sampling of districting maps to evaluate the degree of partisan districting. The involutions are created by a series of user-specified vortices that generate non-reversible flows on the state-space. Interestingly, this scheme can be seen as creating directional neighbourhoods.

4 Two specific lifted samplers and their analysis

In this section, we specify two lifted samplers through two different choices of proposal distributions $q_{\mathbf{x}, \nu}$ and provide a theoretical analysis using the asymptotic Peskun ordering. We first present and analyse in [Section 4.1](#) a lifted sampler using uniform proposal distributions. As explained in [Section 3.3](#), this sampler is often inefficient, especially in high dimensions, but it is simple enough to allow an easy understanding of the reasons why lifted samplers *do not* always dominate their MH counterparts. We next turn in [Section 4.2](#) to a more promising choice of proposal distributions, namely the locally-balanced proposal distributions introduced in [Zanella \(2020\)](#), and study the resulting lifted sampler.

For ease of presentation, we consider the setup where $\mathbf{x} = (x_1, \dots, x_n)$ and $x_1, \dots, x_n \in \{A, B\}$ with the partial order on \mathcal{X} defined in [\(5\)](#). We consider, additionally, but without loss of generality, a Ising model context where $A = -1$ and $B = +1$. Finally, we consider that the neighbourhood structure, used by all samplers, is the typical one, i.e. the neighbourhoods are set to $\mathbf{N}(\mathbf{x}) = \{\mathbf{y} \in \mathcal{X}_n : \sum_i |x_i - y_i| = 2\} = \{\mathbf{y} \in \mathcal{X}_n : \text{there exists one and only one } i \text{ such that } y_i = -x_i\}$, so that the algorithms propose to flip a single bit at each iteration. Because of the nature of our analysis, we, as in [Section 2](#), highlight a dependency on n of the target distribution, the state-space, and so on, by denoting them by π_n , \mathcal{X}_n , etc.

4.1 Uniform proposal distributions

In the reversible MH sampler, it is common, as mentioned in [Section 3.3](#), to set the proposal distribution, denoted by $q_{\mathbf{x}}$ for this algorithm, to the uniform distribution over the neighbourhood of the current state $\mathbf{x} \in \mathcal{X}_n$, that is $q_{\mathbf{x}} = \mathcal{U}\{\mathbf{N}(\mathbf{x})\}$. In the framework of Algorithms [1](#) and [2](#), the analogous proposal distribution is naturally defined as $q_{\mathbf{x}, \nu} = \mathcal{U}\{\mathbf{N}_{\nu}(\mathbf{x})\}$. In this case, the acceptance probability [\(6\)](#) of a proposed move becomes

$$\alpha_{\nu}(\mathbf{x}, \mathbf{y}) = 1 \wedge a_{\nu}(\mathbf{x}, \mathbf{y}), \quad a_{\nu}(\mathbf{x}, \mathbf{y}) := \frac{\pi_n(\mathbf{y}) |\mathbf{N}_{\nu}(\mathbf{x})|}{\pi_n(\mathbf{x}) |\mathbf{N}_{-\nu}(\mathbf{y})|},$$

where we call a_ν the *acceptance ratio*. The function $|\cdot|$ when applied to a set is the cardinality.

In the MH sampler, given that the neighbourhoods are set to $\mathbf{N}(\mathbf{x}) = \{\mathbf{y} \in \mathcal{X}_n : \sum_i |x_i - y_i| = 2\}$, the uniform distribution chooses which bit to flip uniformly at random. Therefore, the size of the neighbourhoods in this sampler is constant for any \mathbf{x} and is given by n . This implies that the acceptance probability in this sampler, denoted by $\alpha(\mathbf{x}, \mathbf{y})$, reduces to

$$\alpha(\mathbf{x}, \mathbf{y}) = 1 \wedge a(\mathbf{x}, \mathbf{y}), \quad a(\mathbf{x}, \mathbf{y}) := \frac{\pi_n(\mathbf{y}) q_{\mathbf{y}}(\mathbf{x})}{\pi_n(\mathbf{x}) q_{\mathbf{x}}(\mathbf{y})} = \frac{\pi_n(\mathbf{y})}{\pi_n(\mathbf{x})}.$$

In the lifted case, we have that for any $\nu \in \{-1, +1\}$, $n_\nu(\mathbf{x}) = \sum_{i=1}^n \mathbf{1}_{x_i=\nu}$ and the acceptance probability can thus be rewritten as:

$$\alpha_\nu(\mathbf{x}, \mathbf{y}) = 1 \wedge a_\nu(\mathbf{x}, \mathbf{y}), \quad a_\nu(\mathbf{x}, \mathbf{y}) = a(\mathbf{x}, \mathbf{y}) \frac{n_{-\nu}(\mathbf{x})}{n_\nu(\mathbf{y})}. \quad (10)$$

Indeed, $\mathbf{N}_\nu(\mathbf{x}) = \{\mathbf{y} \in \mathcal{X}_n : \text{there exists one and only one } j \text{ such that } y_j = -x_j = \nu\}$ implies that $|\mathbf{N}_\nu(\mathbf{x})| = n_{-\nu}(\mathbf{x})$. The acceptance probability α_ν thus depends on an additional factor $n_{-\nu}(\mathbf{x})/n_\nu(\mathbf{y})$ compared to α in the MH sampler. While the reversible sampler is allowed to backtrack, which makes the size of the neighbourhoods constant, the size of the neighbourhoods diminishes in the lifted sampler as the chain moves further in a given direction (making the neighbourhoods in the reverse direction bigger and bigger). As a consequence, the longer the acceptance streak, the smaller $n_{-\nu}(\mathbf{x})/n_\nu(\mathbf{y})$. On an acceptance streak, this factor eventually becomes less than one and thus shrinks α_ν , relatively to the MH acceptance ratio, until the lifted chain switches its direction. To summarize, the price to pay when considering a Markov chain with persistent dynamic is a shrinking factor $n_{-\nu}(\mathbf{x})/n_\nu(\mathbf{y})$ in the acceptance ratio.

An *ideal* situation, which is incompatible with most statistical models, is one where

$$|\mathbf{N}_{-1}(\mathbf{x})| = |\mathbf{N}_{+1}(\mathbf{x})| = |\mathbf{N}(\mathbf{x})|/2 = n/2, \quad \text{for } \pi_n\text{-almost all } \mathbf{x} \in \mathcal{X}_n. \quad (11)$$

This implies that if the chain is at state (\mathbf{x}, ν) , $a(\mathbf{x}, \mathbf{y}) = a_\nu(\mathbf{x}, \mathbf{y})$ for all $\mathbf{y} \in \mathbf{N}_\nu(\mathbf{x})$. Qualitatively, the persistent dynamic of the lifted chain is no longer counter-balanced by the shrinking factor and is thus expected to be more efficient than MH. This fact is made rigorous in [Corollary 2](#) below, which follows from Theorem 7 of [Andrieu and Livingstone \(2021\)](#). In the rest of this subsection, the transition kernel corresponding to [Algorithm 2](#) with $q_{\mathbf{x}, \nu} = \mathcal{U}\{\mathbf{N}_\nu(\mathbf{x})\}$ is denoted by $P_{\rho, n}$ and that of the MH sampler with $q_{\mathbf{x}} = \mathcal{U}\{\mathbf{N}(\mathbf{x})\}$ by $P_{\text{MH}, n}$. Recall that [Algorithm 2](#) with ρ_ν^w corresponds to [Algorithm 1](#).

Corollary 2. *Let $n \in \mathbb{N}$. If \mathcal{X}_n is finite and (11) holds, then for any function $f_n : \mathcal{X} \times \{-1, +1\} \rightarrow \mathbb{R}$ such that $f_n(\mathbf{x}, -1) = f_n(\mathbf{x}, +1)$, we have*

$$\text{var}(f_n, P_{\rho, n}) \leq \text{var}(f_n, P_{\text{MH}, n}). \quad (12)$$

The proof of [Corollary 2](#) is postponed to [Appendix A](#) but its main steps are now presented as they highlight what is important to obtain such an ordering. Central to the proof of [Corollary 2](#) is the idea that once a lifted sampler is defined, it is possible to identify a non-lifted counterpart which differs from [Algorithm 2](#) in that the direction is resampled $\nu \sim \mathcal{U}\{-1, +1\}$ at the beginning of each iteration. At each iteration, a choice between $q_{\mathbf{x}, -1}$ and $q_{\mathbf{x}, +1}$ is thus first made uniformly at random, and the proposal is next sampled. Non-lifted refers to the fact that, while operating on the extended state-space, the systematic resampling of ν makes the marginal dynamic $\{\mathbf{X}_k\}$ Markov again, and reversible. This scheme, when looking at functions f_n with $f_n(\mathbf{x}, -1) = f_n(\mathbf{x}, +1)$, makes the extension of state-space

to include the direction variable superfluous, explaining how a comparison between $\text{var}(f_n, P_{\rho,n})$ and $\text{var}(f_n, P_{\text{MH},n})$ is possible. Let $P_{\text{rev},n}$ denote the transition kernel of this non-lifted reversible Markov chain. As noted in [Andrieu and Livingstone \(2021\)](#), $P_{\text{rev},n}$ can indeed be seen as an intermediate kernel through which comparison of the asymptotic variance of $P_{\rho,n}$ and $P_{\text{MH},n}$ is possible if one can establish, perhaps independently, that $\text{var}(f, P_{\rho,n}) \leq \text{var}(f, P_{\text{rev},n})$ and $\text{var}(f, P_{\text{rev},n}) \leq \text{var}(f, P_{\text{MH},n})$. While establishing the former essentially follows from Theorem 7 of [Andrieu and Livingstone \(2021\)](#), the latter may prove more difficult. However, under (11), it turns out that $P_{\text{rev},n} = P_{\text{MH},n}$, trivially establishing that $\text{var}(f, P_{\text{rev},n}) = \text{var}(f, P_{\text{MH},n})$. Indeed, the sub-stochastic part of $P_{\text{rev},n}$ associated with accepted proposals is

$$(1/2)q_{\mathbf{x},+1}(\mathbf{y})\alpha_{+1}(\mathbf{x}, \mathbf{y}) + (1/2)q_{\mathbf{x},-1}(\mathbf{y})\alpha_{-1}(\mathbf{x}, \mathbf{y}), \quad (13)$$

and it can be readily checked that under (11), (13) indeed coincides with the sub-stochastic part of $P_{\text{MH},n}$. These are the same mathematical arguments that allow to prove the dominance mentioned in [Section 1.1](#) of lifted samplers over their MH counterparts when the state-space is totally ordered.

The incompatibility of the condition (11) with most statistical models motivates us to take our analysis one step further, and this is where the asymptotic Peskun ordering presented in [Section 2](#) proves useful. Note that in order to find a model such that (11) is satisfied, one has to be quite creative; an example is provided in the supplementary material ([Appendix B](#)). The next step in our analysis is to establish if the order on the asymptotic variances (12) still holds when (11) is relaxed, and if not, we want to find conditions under which $\text{var}(f_n, P_{\rho,n})$ and $\text{var}(f_n, P_{\text{MH},n})$ can be compared. A modification of our example presented in the supplementary material shows that (12) *does not* necessarily hold when (11) is relaxed. This should not come as a surprise in the light of the aforementioned observations about the potentially shrinking factor in α_v . Comparing the efficiency of $P_{\text{MH},n}$ and $P_{\rho,n}$ beyond the context of [Corollary 2](#) is not an easy task for several reasons:

- $P_{\rho,n}$ is not reversible and most techniques to establish domination results between Markov kernels hold for reversible kernels, [Andrieu and Livingstone \(2021\)](#) being a noteworthy exception;
- the two kernels $P_{\text{MH},n}$ and $P_{\rho,n}$ are not defined on the same state-space.

For these reasons, finding reasonable conditions under which $\text{var}(f_n, P_{\text{rev},n})$ and $\text{var}(f_n, P_{\text{MH},n})$ can be compared appears to be a suitable route to establish a comparison between $P_{\rho,n}$ et $P_{\text{MH},n}$ (given that we already know that $\text{var}(f_n, P_{\rho,n}) \leq \text{var}(f_n, P_{\text{rev},n})$ using similar arguments to those used to prove [Corollary 2](#)). We thus employ Theorems 2 and 3. Note that if one manages to design the distributions $q_{\mathbf{x},v}$ such that $q_{\mathbf{x}}(\mathbf{y}) = (1/2)q_{\mathbf{x},-1}(\mathbf{y}) + (1/2)q_{\mathbf{x},+1}(\mathbf{y})$ for all \mathbf{x}, \mathbf{y} , then one directly has $P_{\text{rev},n} = P_{\text{MH},n}$ and thus a comparison between $P_{\rho,n}$ et $P_{\text{MH},n}$; this is the approach proposed in [Kamatani and Song \(2020\)](#) for general state-spaces, but it is one that cannot in general be applied in the case of discrete state-spaces.

The idea that we now explore is to consider situations where the mass concentrates on an area where we have a control over the factor $n_{-v}(\mathbf{x})/n_v(\mathbf{y})$ in α_v (10), which translates into the existence of a (non-trivial) relationship between the sub-stochastic part of $P_{\text{rev},n}$ and that of $P_{\text{MH},n}$ on this area. To simplify, we consider situations where the mass concentrates on the centre of the domain, i.e. on states where $n_{-1}(\mathbf{x})$ and $n_{+1}(\mathbf{x})$ are not too far from $n/2$, and set

$$\tilde{\mathcal{X}}_n := \{\mathbf{x} \in \mathcal{X}_n : n/2 - \beta(n) \leq n_{-1}(\mathbf{x}), n_{+1}(\mathbf{x}) \leq n/2 + \beta(n)\}, \quad n \in \mathbb{N}, \quad (14)$$

by choosing a specific function $\beta : \mathbb{N} \rightarrow (0, \infty)$. We stress that $\tilde{\mathcal{X}}_n$ is defined through the function β . With this definition of $\tilde{\mathcal{X}}_n$ and that of the neighbourhood structure (mentioned at the beginning of [Section 4](#)), we are able to state that the interior of $\tilde{\mathcal{X}}_n$ is as follows: $\tilde{\mathcal{X}}_n^\circ = \{\mathbf{x} \in \mathcal{X}_n : n/2 - \beta(n) + 1 \leq n_{-1}(\mathbf{x}), n_{+1}(\mathbf{x}) \leq n/2 + \beta(n) - 1\}$

$n_{-1}(\mathbf{x}), n_{+1}(\mathbf{x}) \leq n/2 + \beta(n) - 1\}$. We thus have a clear understanding of what is the difference between $\tilde{\mathcal{X}}_n$ and its interior in this case. Note that the analysis can be done by considering instead that the mass concentrates on states where the minimum between $n_{-1}(\mathbf{x})$ and $n_{+1}(\mathbf{x})$ is not too far from n/κ with $\kappa \geq 2$. The difference is that, with control subsets defined as in (14), $\omega(n)$ will be seen to converge to $\bar{\omega} = 1$, whereas in that general framework $\bar{\omega} \leq 1$ is a function of κ , and the results are more complicated to present. Constructing the control subsets $\{\tilde{\mathcal{X}}_n\}$ as in (14) implies that, remarkably, the analysis is parameterized by the sole function β .

Lemma 1. *Consider the definition of $\tilde{\mathcal{X}}_n$ in (14). Assume that β is such that $\beta(n) = o(n)$. Then for a large enough n , it holds that*

$$\tilde{P}_{\text{rev},n}(\mathbf{x}, \mathbf{y}) \geq \omega(n) \tilde{P}_{\text{MH},n}(\mathbf{x}, \mathbf{y}), \quad \text{for all } (\mathbf{x}, \mathbf{y}) \in \tilde{\mathcal{X}}_n^2 \text{ with } \mathbf{x} \neq \mathbf{y},$$

where

$$\omega(n) = \left(1 - \frac{\beta(n)}{n/2}\right) \left(1 + \frac{\beta(n)}{n/2}\right)^{-2}. \quad (15)$$

Intuitively, if $\beta(n)$ grows like n or faster, then for a large enough n we have $\mathcal{X}_n = \tilde{\mathcal{X}}_n$ which boils down to the initial Peskun's problem so the assumption $\beta(n) = o(n)$ is sensible. If $\beta(n)$ grows *too* slowly then the control subsets $\tilde{\mathcal{X}}_n$ may eventually fail to track the bulk of \mathcal{X}_n , resulting in that the mass of π_n will not concentrate on $\tilde{\mathcal{X}}_n^\circ$ and that the restricted kernels will be too different from the original ones to allow the machinery of Section 2 to work. The condition $\beta(n) = o(n)$, together with (15), means that Assumption 1 holds with $\bar{\omega} = 1$. If we assume that the right spectral gaps are bounded away from zero, which is realistic, for example, when $\beta(n)$ is constant, and that π_n concentrates on $\tilde{\mathcal{X}}_n^\circ$ defined above (implying that Assumption 2 holds), then Theorem 2 can be applied and

$$\text{var}(f_n, P_{\rho,n}) \leq \text{var}(f_n, P_{\text{rev},n}) \leq \frac{1}{1-\epsilon} \text{var}(f_n, P_{\text{MH},n}) + \epsilon,$$

for any $\epsilon > 0$, provided that n is large enough and that we consider functions $f_n \in \mathcal{L}_{0,1}^2(\pi_n)$ satisfying (2) and such that $f_n(\mathbf{x}, -1) = f_n(\mathbf{x}, +1)$. The assumption on the spectral gaps can be relaxed and Theorem 3 can be instead applied if we are able to establish a connection between the rate at which π_n concentrates on $\tilde{\mathcal{X}}_n^\circ$ and that at which $\underline{\lambda}(n)$ vanishes, i.e. if (4) can be verified.

To summarize, our analysis suggests that the lifted sampler with uniform proposal distributions dominates its MH counterpart (at least for n large enough and a specific class of functions) when π_n concentrates on states in the centre of the domain. If it concentrates elsewhere, then the lifted sampler is expected to be comparable to its MH counterpart as long as π_n does not concentrate on areas where the neighbourhoods, and thus the additional factors $n_{-\nu}(\mathbf{x})/n_\nu(\mathbf{y})$ in (10), are very imbalanced.

When n is large, uniform proposal distributions, whether they are used in a lifted or MH sampler, are likely to represent a poor strategy and thus the question to know which sampler dominates the other is not necessarily relevant in practice. We will thus not focus on corroborating the findings on samplers with uniform proposal distributions in our numerical experiments in Section 5. We will rather focus on findings about locally-balanced samplers presented in the next subsection which represent efficient alternatives.

4.2 Locally-balanced proposal distributions

In this section, we discuss and analyse samplers using locally-balanced proposal distributions. For simplicity, we will use the same notation as in Section 4.1: $q_\mathbf{x}$ and $q_{\mathbf{x},\nu}$ are the proposal distributions

in the MH and lifted samplers, respectively, but in this section they are locally-balanced (a definition follows), and $P_{\rho,n}$, $P_{\text{rev.},n}$ and $P_{\text{MH},n}$ are the Markov kernels associated with [Algorithm 2](#), and its non-lifted and MH counterparts, respectively, which are all using locally-balanced proposal distributions. Recall that [Algorithm 1](#) is a special case of [Algorithm 2](#) with $\rho_v(\mathbf{x}) = 1 - T_v(\mathbf{x}, \mathcal{X})$.

As defined in [Zanella \(2020\)](#) in the MH framework, a proposal distribution is locally-balanced if

$$q_{\mathbf{x}}(\mathbf{y}) = g\left(\frac{\pi_n(\mathbf{y})}{\pi_n(\mathbf{x})}\right) / c_n(\mathbf{x}), \quad \mathbf{y} \in \mathbf{N}(\mathbf{x}),$$

where $c_n(\mathbf{x})$ is the normalizing constant, i.e. $c_n(\mathbf{x}) = \sum_{\mathbf{x}' \in \mathbf{N}(\mathbf{x})} g(\pi_n(\mathbf{x}')/\pi_n(\mathbf{x}))$, and g is a positive continuous function such that $g(x)/g(1/x) = x$ for $x > 0$. Such a function g implies that the acceptance probability in the MH algorithm is given by

$$\alpha(\mathbf{x}, \mathbf{y}) = 1 \wedge \frac{\pi_n(\mathbf{y}) q_{\mathbf{y}}(\mathbf{x})}{\pi_n(\mathbf{x}) q_{\mathbf{x}}(\mathbf{y})} = 1 \wedge \frac{c_n(\mathbf{x})}{c_n(\mathbf{y})}. \quad (16)$$

The name *locally-balanced* comes from the fact that, in the limit, when the state-space becomes larger and larger (but the neighbourhoods have a fixed size and proposed moves are thus local), there is no need for an accept-reject step anymore; the proposal distributions leave the distribution π_n invariant. Indeed, as shown in [Zanella \(2020\)](#) in a variety of situations, $\sup_{(\mathbf{x}, \mathbf{y}) \in \mathcal{X}_n : \mathbf{y} \in \mathbf{N}(\mathbf{x})} c_n(\mathbf{x})/c_n(\mathbf{y}) \rightarrow 1$ as $n \rightarrow \infty$ under some assumptions. The author more precisely considers that $\mathbf{x} = (x_1, \dots, x_n)$ and that at any given iteration, only a small fraction of the n components is proposed to change values. The result holds when there exists a uniform bound which does not depend on n on $\pi_n(\mathbf{y})/\pi_n(\mathbf{x})$ for two neighbouring states (\mathbf{x}, \mathbf{y}) and the random variables (X_1, \dots, X_n) exhibit a structure of conditional independence, the latter implying that the normalizing constants $c_n(\mathbf{x})$ and $c_n(\mathbf{y})$ share a lot of terms in common. Note that $c_n(\mathbf{x})$ and $c_n(\mathbf{y})$ are both sums over the same number of terms, which is crucial in showing that $\sup_{(\mathbf{x}, \mathbf{y}) \in \mathcal{X}_n : \mathbf{y} \in \mathbf{N}(\mathbf{x})} c_n(\mathbf{x})/c_n(\mathbf{y}) \rightarrow 1$.

Two valid choices for g are $g(x) = \sqrt{x}$ and $g(x) = x/(1+x)$, the latter being called the *Barker proposal distribution* in reference to [Barker \(1965\)](#)'s acceptance probability choice. The advantage of the latter choice is that it is a bounded function of x , which stabilizes the normalizing constants and thus the acceptance probability, see [Zanella \(2020\)](#), and [Livingstone and Zanella \(2021\)](#) for the continuous-random-variable case. We use this function in our numerical experiments.

A locally-balanced proposal distribution in the lifted sampler framework is naturally defined as

$$q_{\mathbf{x},v}(\mathbf{y}) = g\left(\frac{\pi_n(\mathbf{y})}{\pi_n(\mathbf{x})}\right) / c_{n,v}(\mathbf{x}), \quad \mathbf{y} \in \mathbf{N}_v(\mathbf{x}),$$

where $c_{n,v}(\mathbf{x})$ is the normalizing constant and g is as above. In this case,

$$\alpha_v(\mathbf{x}, \mathbf{y}) = 1 \wedge \frac{\pi_n(\mathbf{y}) q_{\mathbf{y},-v}(\mathbf{x})}{\pi_n(\mathbf{x}) q_{\mathbf{x},v}(\mathbf{y})} = 1 \wedge \frac{c_{n,v}(\mathbf{x})}{c_{n,-v}(\mathbf{y})} = 1 \wedge \frac{c_n(\mathbf{x})}{c_n(\mathbf{y})} \frac{c_{n,v}(\mathbf{x})/c_n(\mathbf{x})}{c_{n,-v}(\mathbf{y})/c_n(\mathbf{y})}. \quad (17)$$

As with the uniform proposal distributions in [Section 4.1](#), we see that the acceptance probability in the lifted sampler (17) differs from that in MH (16). There is thus again a price to pay to use a lifted sampler: there is no guarantee that $c_{n,v}(\mathbf{x})/c_{n,-v}(\mathbf{y}) \rightarrow 1$ for $\mathbf{y} \in \mathbf{N}(\mathbf{x})$, even when $c_n(\mathbf{x})/c_n(\mathbf{y}) \rightarrow 1$. A reason is because the sums $c_{n,v}(\mathbf{x})$ and $c_{n,-v}(\mathbf{y})$ are in this case not over the same number of terms, a consequence of the nature of the lifted sampler.

As previously, the reversible counterpart to the lifted algorithm chooses at each iteration uniformly at random a proposal distribution between $q_{\mathbf{x},-1}$ and $q_{\mathbf{x},+1}$ from which a proposal is sampled. Imagine

that $c_n(\mathbf{x})/c_n(\mathbf{y}) = 1$ for all \mathbf{x}, \mathbf{y} , then one can notice from (17) that the stability of ratios $c_{n,v}(\mathbf{x})/c_{n,-v}(\mathbf{y})$ is crucial to establish a connection between the sub-stochastic parts of $P_{\text{rev.},n}$ and $P_{\text{MH},n}$ (recall (13)). In fact, in an ideal situation, which is again incompatible with most statistical models, one can establish that $P_{\text{rev.},n} = P_{\text{MH},n}$, guaranteeing a dominance of the lifted sampler.

Corollary 3. *Let $n \in \mathbb{N}$. If \mathcal{X}_n is finite and*

$$c_{n,-1}(\mathbf{x}) = c_{n,+1}(\mathbf{x}), \quad \text{for all } \mathbf{x} \in \mathcal{X}_n,$$

then for any function $f_n : \mathcal{X} \times \{-1, +1\} \rightarrow \mathbb{R}$ such that $f_n(\mathbf{x}, -1) = f_n(\mathbf{x}, +1)$, we have $\text{var}(f_n, P_{\rho,n}) \leq \text{var}(f_n, P_{\text{MH},n})$.

Locally-balanced proposal distributions allow to explore the state-space by often proposing points that belong to the manifold on which the mass concentrates. [Corollary 3](#) tells us that, in order to compare $P_{\text{rev.},n}$ to $P_{\text{MH},n}$ (and thus $P_{\rho,n}$ to $P_{\text{MH},n}$), the directional neighbourhoods to which these points belong must have similar mass, implying similar normalizing constants $c_{n,v}(\mathbf{x})$ and $c_{n,-v}(\mathbf{y})$ over the manifold. The analysis can be pushed beyond [Corollary 3](#) by making use of our asymptotic framework. To simplify, we consider, as in [Zanella \(2020\)](#), the situation where $\sup c_n(\mathbf{x})/c_n(\mathbf{y}) \rightarrow 1$ where the supremum is over all neighbouring states \mathbf{x}, \mathbf{y} , and $\bar{\omega} = 1$.

We now turn to the definition of the control subset:

$$\begin{aligned} \tilde{\mathcal{X}}_n &= \{\mathbf{x} \in \mathcal{X}_n : c_n(\mathbf{x})/2 - \beta(n) \leq c_{n,-1}(\mathbf{x}), c_{n,+1}(\mathbf{x}) \leq c_n(\mathbf{x})/2 + \beta(n)\} \\ &= \{\mathbf{x} \in \mathcal{X}_n : 1 - \beta(n)/(c_n(\mathbf{x})/2) \leq c_{n,v}(\mathbf{x})/(c_n(\mathbf{x})/2) \leq 1 + \beta(n)/(c_n(\mathbf{x})/2)\} \\ &= \{\mathbf{x} \in \mathcal{X}_n : |c_{n,-1}(\mathbf{x}) - c_{n,+1}(\mathbf{x})| \leq 2\beta(n)\}, \end{aligned} \tag{18}$$

which again is defined through a function $\beta : \mathbb{N} \rightarrow (0, \infty)$. The equivalence between the sets follows from the fact that $c_n(\mathbf{x}) = c_{n,-1}(\mathbf{x}) + c_{n,+1}(\mathbf{x})$. Under assumptions on the target such as those in [Zanella \(2020\)](#), the normalizing constants $c_n(\mathbf{x})$ scale linearly with n and below we show that lifted and MH samplers can be compared in terms of asymptotic variances when $\beta(n) = o(n)$, because in this case for states in $\tilde{\mathcal{X}}_n$, $\beta(n)/(c_n(\mathbf{x})/2)$ vanishes and the acceptance probabilities in the lifted sampler are close to 1, as those in MH. Notice that in the case of locally-balanced samplers, we cannot state explicitly what the interior of $\tilde{\mathcal{X}}_n$ is without specifying π_n . With the current level of generality, we cannot go beyond the definition presented in [Section 2](#), which in the framework of this section is $\tilde{\mathcal{X}}_n^\circ := \{\mathbf{x} \in \tilde{\mathcal{X}}_n : q_{\mathbf{x}}(\tilde{\mathcal{X}}_n^\circ) = 0\}$.

As in the previous section, the analysis can be done by considering instead that the mass concentrates on states where the minimum between $c_{n,-1}(\mathbf{x})$ and $c_{n,+1}(\mathbf{x})$ is not too far from $c_n(\mathbf{x})/\kappa$ with $\kappa \geq 2$. In this case, $\bar{\omega} \leq 1$ and a function of κ , and the definition of the control subset and results are more complex. From the definition of $\tilde{\mathcal{X}}_n$ in (18), we are able to establish a result analogous to [Lemma 1](#).

Lemma 2. *Consider the definition of $\tilde{\mathcal{X}}_n$ in (18) and let $R_n := \{(\mathbf{x}, \mathbf{y}) \in \tilde{\mathcal{X}}_n^2 : \mathbf{y} \in \mathbf{N}(\mathbf{x})\}$. Assume that*

$$\inf_{(\mathbf{x}, \mathbf{y}) \in R_n} g\left(\frac{\pi_n(\mathbf{y})}{\pi_n(\mathbf{x})}\right) = m, \quad \tau_n := \sup_{(\mathbf{x}, \mathbf{y}) \in R_n} \frac{c_n(\mathbf{x})}{c_n(\mathbf{y})} \rightarrow 1, \quad \beta(n) = o(n).$$

Then, for a large enough n , it holds that

$$\tilde{P}_{\text{rev.},n}(\mathbf{x}, \mathbf{y}) \geq \omega(n) \tilde{P}_{\text{MH},n}(\mathbf{x}, \mathbf{y}), \quad \text{for all } (\mathbf{x}, \mathbf{y}) \in \tilde{\mathcal{X}}_n^2 \text{ with } \mathbf{x} \neq \mathbf{y},$$

with

$$\omega(n) = \left(1 + \frac{\beta(n)}{nm/2}\right)^{-1} \left(\frac{1 - 2\beta(n)/nm}{1 + 2\tau_n\beta(n)/nm} \right).$$

Clearly, under the assumptions of [Lemma 2](#) and that π_n concentrates on $\tilde{\mathcal{X}}_n^\circ$, Assumptions 1 and 2 are satisfied and we can apply [Theorem 2](#) or [Theorem 3](#) with $\bar{\omega} = 1$, depending on whether the spectral gaps are bounded away from 0 or not. This gives an asymptotic ordering between $P_{\text{MH},n}$ and $P_{\text{rev},n}$, and thus between $P_{\text{MH},n}$ and $P_{\rho,n}$. Given that the definition of $\tilde{\mathcal{X}}_n$ and the conditions just mentioned are quite abstract, we provide in the supplementary material ([Appendix B](#)) a synthetic example where they are all detailed and verified. In this example, the mass concentrates on a path along which the lifted sampler explores the state-space. This path is assumed to be longer and longer as n increases. [Theorem 3](#) applies and for a large enough n , it approximatively holds that $\text{var}(P_{\rho,n}, f_n) \leq \text{var}(P_{\text{MH},n}, f_n)$, for suitable $\{f_n\}$. If carried out over the whole state-space, the comparison between $P_{\rho,n}$ and $P_{\text{MH},n}$ is not at all straightforward. Yet, we manage to prove that only a loose comparison between the asymptotic variances of the chains can be achieved; in particular, analysing some pairs of states allows to show that $P_{\text{rev},n}(\mathbf{x}, \mathbf{y}) \geq (1/\alpha)P_{\text{MH},n}(\mathbf{x}, \mathbf{y})$ with $\alpha \geq 2$, implying that at best, one can obtain $\text{var}(P_{\rho,n}, f_n) \leq 2\text{var}(P_{\text{MH},n}, f_n)$.

It is expected that lifted samplers only have an advantage when there is room for persistent movement, meaning that they can explore the state-space by using paths of considerable lengths. It is interesting that this has emerged in our example. The analysis conducted in the current section shows that lifted samplers using locally-balanced proposal distributions are expected to have an advantage when, additionally, the mass does not vary much from a directional neighbourhood to another on the manifold on which π_n concentrates. These samplers are expected to be comparable to their MH counterparts when, on the manifold, the normalizing constants $c_{n,-1}(\mathbf{x})$ and $c_{n,+1}(\mathbf{x})$ are bounded by $c_n(\mathbf{x})/\kappa \pm \beta(n)$ with $\kappa > 2$.

5 Numerical experiments

In this section, we conduct numerical experiments that allow to corroborate the theoretical findings presented in [Section 4](#) about the lifted samplers. As mentioned in that section, we focus on findings about locally-balanced samplers. We first consider in [Section 5.1](#) the simulation of an Ising model and use this as a toy example for which we can control the dimension and the roughness of the target. We show that specific combinations of these parameters are favourable for lifted samplers, in the sense that the mass in directional neighbourhoods varies smoothly over a manifold of considerable size, suggesting the existence of subsets $\tilde{\mathcal{X}}_n$ defined as in (18) and interiors on which the mass concentrates. For these combinations of parameters, lifted samplers outperform MH ones. Other combinations are unfavourable, and the opposite happens. In [Section 5.2](#), a real variable-selection problem yields a target which is favourable for lifted samplers (in the same sense as above), and again lifted samplers outperform MH ones.

5.1 Ising model

Let us consider the two-dimensional Ising model. For this model, the state-space (V_η, E_η) is a $\eta \times \eta$ square lattice regarded here as a square matrix in which each element takes either the value -1 or $+1$. We write each state as a vector as before: $\mathbf{x} = (x_1, \dots, x_n)$, where $n = \eta^2$. The states can be encoded as follows: the values of the components on the first line are x_1, \dots, x_η , those on the second line $x_{\eta+1}, \dots, x_{2\eta}$, and so on. The PMF is given by

$$\pi(\mathbf{x}) = \frac{1}{Z} \exp \left(\sum_i \alpha_i x_i + \lambda \sum_{\langle ij \rangle} x_i x_j \right),$$

where $\alpha_1, \dots, \alpha_n \in \mathbb{R}$ and $\lambda > 0$ are fixed parameters, Z is the normalizing constant and the notation $\langle ij \rangle$ indicates that sites i and j are nearest neighbours. The notion of neighbourhood on (V_η, E_η) should not be confused with that on \mathcal{X}_n on which the samplers rely. The neighbourhood of a site $i \in V_\eta$ comprises, when they exist, its North-South-East-West neighbours on the lattice. Note that we make the dependence of the target on the parameters and n implicit to simplify.

The role of the parameters in this Ising model are worth being explained. The parameter λ is a spatial correlation parameter: the larger it gets, the larger are the chances that two neighbouring nodes share the same spin state. Realizations of such models when λ is large are thus likely to be lattices featuring large patches of identical spin states. The parameter $\alpha := (\alpha_1, \dots, \alpha_n)$ is often referred to as the external field which essentially tends to polarize each spin, regardless its neighbours. In particular, when α_i decreases, x_i has an increasing tendency to align with a negative spin, i.e. $x_i = -1$. If $|\alpha_i| \gg \lambda$ for all i , the dependency structure in the lattice is negligible and thus spins tend to align with the external field. Conversely, if $\lambda \gg |\alpha_i|$ for all i , spins in a vicinity tend to align with one another.

We first consider a base target distribution for which $n = 50^2$, the spatial correlation is moderate and more precisely $\lambda = 0.5$, and which has the external field presented in [Figure 2](#). We generated the

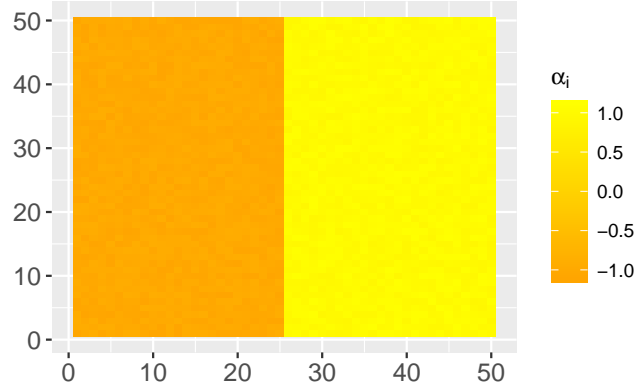


Figure 2. External field of the base target

α_i independently as follows: $\alpha_i = -\mu + \epsilon_i$ if the column index is smaller than or equal to $\ell := \lfloor \eta/2 \rfloor$ and $\alpha_i = \mu + \epsilon_i$ otherwise, where $\mu = 1$, the ϵ_i are independent uniform random variables on the interval $(-0.1, +0.1)$ and $\lfloor \cdot \rfloor$ is the floor function. In this setup, while the mild external field tends to push spins on the left-hand side (LHS) of the lattice to -1 and those on the right-hand side (RHS) to $+1$, the moderate spatial correlation tends to make likely lattices with -1 on the RHS near the centre and $+1$ on the LHS near the centre. This makes the target moderately rough, in the sense that it concentrates on a manifold of the state-space with directional neighbourhoods on the manifold that have a smoothly varying mass. This manifold can be thought of the subset $\tilde{\mathcal{X}}_n$ which is the central ingredient of [Theorems 2](#) and [3](#). The characteristic of the manifold suggests that $\tilde{\mathcal{X}}_n$ satisfies the definition in [\(18\)](#), implying that such a base target represents a favourable scenario for lifted samplers with locally-balanced proposal distributions as described in [Section 4.2](#). We will notice that it is indeed a favourable scenario and observe what happens when modifying target-parameter values.

We now describe the simulation study.

- While keeping the other parameters fixed, we first gradually increase η from 50 to 500 to observe the impact of dealing with larger systems, for targets that are moderately rough. This will thus lead to longer paths along which the state-space can be explored, which is again favourable for lifted samplers. The numerical experiment will allow to measure an increasing difference in

performance between lifted samplers and MH ones, which is not possible with results such as Theorems 2 and 3.

- Next, we gradually increase the value of μ from 1 to 3, while keeping the other parameters fixed (with $\eta = 50$). This increases the contrast in Figure 2. When μ increases, there is less and less chance to observe negative (positive) spins on the RHS (LHS), even near the centre, thus making the target rougher and concentrated on fewer configurations. In the limit, the set of possible lattices shrinks to the one lattice dictated by the external field with -1 's on the LHS and $+1$'s on the RHS. This suggest that in extreme cases, it becomes difficult to define a subset $\tilde{\mathcal{X}}_n$ as in (18) with an interior on which the mass concentrates because such a $\tilde{\mathcal{X}}_n$ is too small implying that its interior is too small as well, in turn suggesting that the assumptions of Theorem 2 or Theorem 3 do not hold. In the experiment, when the value of μ is beyond a threshold, MH samplers become more efficient than lifted ones.

One could vary λ and ℓ as well. Varying λ also makes the target rougher and concentrated on fewer configurations. We thus do not do it to avoid redundancy. Varying ℓ is expected to have a more important impact on the uniform lifted sampler than the other samplers because it modifies the location of the area where the mass concentrates. We do not present the associated results because the graph is uninteresting: the performance is essentially constant for the locally-balanced samplers and that of the uniform ones is so low that we do not see the ESS vary.

We present the simulation results in Figure 3 for Algorithm 1 with uniform and locally-balanced proposal distributions, and their MH counterparts. For such a simulation study, it would be simply too long to obtain the results for Algorithm 2 with ρ_v^* (9). The results are based on 1,000 independent runs of 100,000 iterations for each algorithm and each value of μ and η , with burn-ins of 10,000. For each run, an ESS per iteration is computed for $f(\mathbf{x}, -1) = f(\mathbf{x}, +1) = \sum_i x_i$ and then the results are averaged out. This function is proportional to what is called *magnetisation* in a Ising-model framework. Monitoring such a statistic is relevant as a quicker variation of its value (leading to a higher ESS) indicates that the whole state-space is explored quicker.

For the base target (represented by the starting points on the left of the lines in Figure 3), the mass is, as mentioned, concentrated on a manifold of many configurations with, on the manifold, a mass that does not vary too much from a directional neighbourhood to another. The locally-balanced lifted sampler takes advantage of this and induces persistent movement on the manifold: it is approximately 7 times more efficient than its MH counterpart. The gap widens as η increases (Figure 3 (a)), a consequence of longer paths that the locally-balanced lifted sampler efficiently follows; it is approximately 20 and 70 times more efficient when η is 3.2 and 10 times larger (i.e. when n is 10 and 100 times larger), respectively. We evaluated that the ratio of ESSs increases linearly with η , indicating that the locally-balanced lifted sampler scales better than its MH counterpart. The samplers with uniform proposal distributions perform poorly (the lines are on top of each other).

As μ increases (Figure 3 (b)), the target becomes rougher and concentrated on fewer configurations. When the roughness and concentration level are too severe the performance of the locally-balanced lifted sampler stagnates, whereas that of its MH counterpart continues to improve. There are two reasons for this. Firstly, when these samplers move away from the states with high probability, the acceptance probabilities deteriorate for both samplers, but they do so more rapidly in the lifted one because ratios of mass of directional neighbourhoods are less stable than those of mass of neighbourhoods in MH (recall the explanations provided in Section 4.2). Secondly, when the mass is concentrated on few configurations, it leaves not much room for persistent movement for the lifted sampler. The latter thus loses its advantage. Again, the samplers with uniform proposal distributions perform poorly (the

lines are on top of each other).

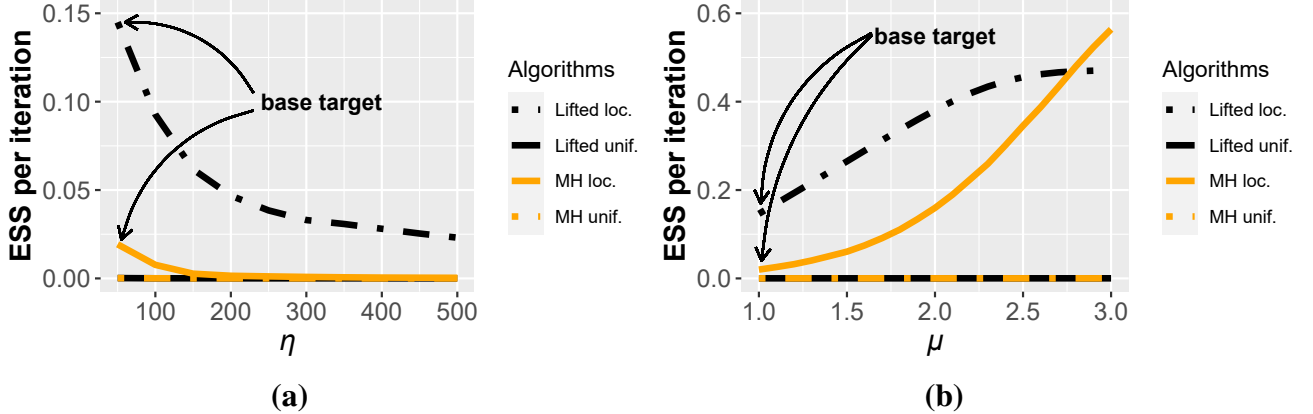


Figure 3. ESS per iteration of $f(\mathbf{x}, -1) = f(\mathbf{x}, +1) = \sum_i x_i$ for [Algorithm 1](#) with uniform and locally-balanced proposal distributions and their MH counterparts when: (a) η increases from 50 to 500 and the other parameters are kept fixed ($\mu = 1$, $\lambda = 0.5$ and $\ell = 25$); (b) μ increases from 1 to 3 and the other parameters are kept fixed ($\eta = 50$, $\lambda = 0.5$ and $\ell = 25$)

5.2 Variable selection: US crime data

In this section, we contrast the performance of the lifted samplers with that of their MH counterparts when applied to solve a real Bayesian variable-selection problem. The data are for a study of crime rate in the United States in 1960. They were aggregated by state and were from 47 states. They were first presented in [Erhlich \(1973\)](#) and then expended and corrected in [Vandaele \(1978\)](#). These authors were in particular interested in studying the connection between crime rate and 15 covariates (some were added by [Vandaele \(1978\)](#)) such as percentage of males of age between 14 and 23 and mean years of schooling in a given state. They were analysed in several statistics papers, for instance in [Raftery *et al.* \(1997\)](#) in a context of model averaging, and are available in the R package MASS.

The data are modelled using a linear regression with normal errors. Here we set the prior distribution of the regression coefficients and scaling of the errors to be, conditionally on a model, the non-informative Jeffreys prior. It can be shown (analogously to in [Gagnon *et al.* \(2021\)](#) in a context of principal component regression) that a simple modification to the uniform prior on the model indicator, represented here by \mathbf{X} , yields a consistent model selection procedure, thus effectively preventing the Jeffreys–Lindley ([Lindley, 1957](#); [Jeffreys, 1967](#)) paradox from arising. The likelihood function and prior density on the parameters allows for the latter to be integrated out. It is thus possible to evaluate the exact marginal posterior probability of any of the $2^{15} = 32,768$ models, up to a normalizing constant. We are consequently able to implement the MH sampler with the Barker locally-balanced proposal distribution of [Zanella \(2020\)](#) and its lifted counterparts, namely [Algorithm 1](#) and [Algorithm 2](#) with ρ_v^* (9), to sample from π , which is, in this context, a posterior model distribution. In the previous statistical studies (such as in [Raftery *et al.* \(1997\)](#)), it was noticed that for many models, the mass varies smoothly; the mass in fact concentrates on the resulting manifold of the state-space and does not vary too much from a directional neighbourhood to another on the manifold. As with the Ising-model example, this suggests the existence of a subset $\tilde{\mathcal{X}}_n$ defined as in (18) with a significant size and an order on the asymptotic variances of some functions between lifted samplers and MH ones. Lifted samplers indeed outperform MH ones in this example. In particular, the locally-balanced lifted chains exhibit

persistent movement, as seen in [Figure 1](#). We do not show the performance of the uniform samplers because, as in the previous section, it is very poor.

The performances of the algorithms are summarized in [Figure 4](#). The results are based on 1,000 independent runs of 10,000 iterations for each algorithm, with burn-ins of 1,000. Each run is started from a distribution which approximates the target. On average, [Algorithm 1](#) and [Algorithm 2](#) with ρ_v^* are 2.7 and 3.3 times more efficient than their MH counterpart, respectively. The benefits of persistent movement thus compensate for a decrease in acceptance rates; the rate indeed decreases from 0.92 for the MH sampler to 0.71 for [Algorithm 1](#) and [Algorithm 2](#) with ρ_v^* ([9](#)). This highlights again the difference in stability of neighbourhood mass versus *directional* neighbourhood mass (recall the difference in the acceptance ratios, ([16](#)) and ([17](#))).

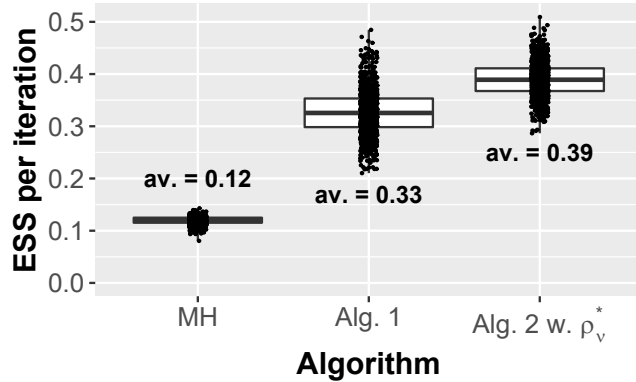


Figure 4. ESS per iteration for $f(\mathbf{x}, -1) = f(\mathbf{x}, +1) = \sum_i x_i$ of 1,000 independent runs for the MH sampler with the Barker locally-balanced proposal distribution and its lifted counterparts ([Algorithm 1](#) and [Algorithm 2](#) with ρ_v^*)

6 Lifted trans-dimensional sampler

In this section, we introduce a generic sampler that can be used for model selection/averaging in situations where it is not possible to integrate out the parameters, contrarily to the linear regression with normal errors and suitable priors (like in [Section 5.2](#)). Examples of such situations include analyses based on linear regression with super heavy-tailed errors ensuring *whole robustness* ([Gagnon et al., 2020, 2021](#)) and generalized linear models and generalized linear mixed models ([Forster et al., 2012](#)).

More precisely, in this section, we introduce a trans-dimensional version of [Algorithm 1](#) which thus represents a non-reversible counterpart to the popular reversible jump (RJ) algorithm introduced by [Green \(1995\)](#). In the same way that [Algorithm 1](#) can be seen as a modification of a MH algorithm, the non-reversible jump (NRJ) algorithm is constructed from the RJ algorithm. To present our lifted trans-dimensional sampler, it is thus convenient to first provide an overview of the RJ one. A lifted trans-dimensional sampler has been recently introduced in [Gagnon and Doucet \(2021\)](#), but it can only be applied when the models can be rearranged in a sequence of nested models, i.e. model 1 is nested in model 2 which is nested in model 3, and so on; in other words, when a total order exists. Only a partial order is sufficient to apply the NRJ proposed here.

In a trans-dimensional framework, we consider that \mathcal{X} is a model space and \mathbf{X} a model indicator. The latter indicates, for instance, through a vector of 0's and 1's which covariates are included in the model employed in variable-selection contexts as in [Section 5.2](#). In the following, we consider that a

neighbourhood structure $\{\mathbf{N}(\mathbf{x}) : \mathbf{x} \in \mathcal{X}\}$ is given. The parameters of a given model \mathbf{x} are denoted by $\boldsymbol{\theta}_{\mathbf{x}} \in \boldsymbol{\Theta}_{\mathbf{x}}$. Trans-dimensional algorithms sample from a target distribution π defined on a union of sets $\cup_{\mathbf{x} \in \mathcal{X}} \{\mathbf{x}\} \times \boldsymbol{\Theta}_{\mathbf{x}}$, which corresponds in Bayesian statistics to the joint posterior distribution of the model indicator \mathbf{X} and the parameters of model \mathbf{X} , i.e. $\boldsymbol{\theta}_{\mathbf{X}}$. Such a posterior distribution allows to jointly infer about $(\mathbf{X}, \boldsymbol{\theta}_{\mathbf{X}})$, or in other words, simultaneously achieve model selection/averaging and parameter estimation. In this section, we assume for simplicity that the parameters of all models are continuous random variables.

We now outline an iteration of a RJ algorithm. Consider that the current state of the Markov chain is given by $(\mathbf{x}, \boldsymbol{\theta}_{\mathbf{x}})$.

1. Sample $u_c \sim \mathcal{U}[0, 1]$.
- 2.(a) If $u_c \leq \tau$, where $0 \leq \tau \leq 1$, attempt a *parameter update*, meaning an update of the parameters of the current model, using a MCMC kernel of invariant distribution $\pi(\cdot | \mathbf{x})$ while keeping the current value of the model indicator \mathbf{x} fixed.
- 2.(b) If $u_c > \tau$, attempt a *model switch*. Sample $\mathbf{y} \sim q_{\mathbf{x}}$ and $u_a \sim \mathcal{U}[0, 1]$, where $q_{\mathbf{x}}$ is a PMF with support $\mathbf{N}(\mathbf{x})$. Next, sample $\mathbf{u}_{\mathbf{x} \rightarrow \mathbf{y}} \sim q_{\mathbf{x} \rightarrow \mathbf{y}}$ and compute $\mathcal{D}_{\mathbf{x} \rightarrow \mathbf{y}}(\boldsymbol{\theta}_{\mathbf{x}}, \mathbf{u}_{\mathbf{x} \rightarrow \mathbf{y}}) =: (\boldsymbol{\theta}'_{\mathbf{y}}, \mathbf{u}_{\mathbf{y} \rightarrow \mathbf{x}})$, where $q_{\mathbf{x} \rightarrow \mathbf{y}}$ is used to denote both the distribution and the probability density function, $\mathcal{D}_{\mathbf{x} \rightarrow \mathbf{y}}$ is a diffeomorphism and $\boldsymbol{\theta}'_{\mathbf{y}}$ is the proposal for the parameter values of model \mathbf{y} . Set the next state of the chain to $(\mathbf{y}, \boldsymbol{\theta}'_{\mathbf{y}})$ if

$$u_a \leq \alpha_{\text{RJ}}((\mathbf{x}, \boldsymbol{\theta}_{\mathbf{x}}), (\mathbf{y}, \boldsymbol{\theta}'_{\mathbf{y}})) := 1 \wedge \frac{q_{\mathbf{y}}(\mathbf{x})}{q_{\mathbf{x}}(\mathbf{y})} r((\mathbf{x}, \boldsymbol{\theta}_{\mathbf{x}}), (\mathbf{y}, \boldsymbol{\theta}'_{\mathbf{y}})),$$

where

$$r((\mathbf{x}, \boldsymbol{\theta}_{\mathbf{x}}), (\mathbf{y}, \boldsymbol{\theta}'_{\mathbf{y}})) := \frac{\pi(\mathbf{y}, \boldsymbol{\theta}'_{\mathbf{y}}) q_{\mathbf{y} \rightarrow \mathbf{x}}(\mathbf{u}_{\mathbf{y} \rightarrow \mathbf{x}})}{\pi(\mathbf{x}, \boldsymbol{\theta}_{\mathbf{x}}) q_{\mathbf{x} \rightarrow \mathbf{y}}(\mathbf{u}_{\mathbf{x} \rightarrow \mathbf{y}}) |J_{\mathcal{D}_{\mathbf{x} \rightarrow \mathbf{y}}}(\boldsymbol{\theta}_{\mathbf{x}}, \mathbf{u}_{\mathbf{x} \rightarrow \mathbf{y}})|^{-1}},$$

and $|J_{\mathcal{D}_{\mathbf{x} \rightarrow \mathbf{y}}}(\boldsymbol{\theta}_{\mathbf{x}}, \mathbf{u}_{\mathbf{x} \rightarrow \mathbf{y}})|$ is the absolute value of the determinant of the Jacobian matrix of the function $\mathcal{D}_{\mathbf{x} \rightarrow \mathbf{y}}$; the dependence of the functions α_{RJ} and r on $\mathbf{u}_{\mathbf{x} \rightarrow \mathbf{y}}$ and $\mathbf{u}_{\mathbf{y} \rightarrow \mathbf{x}}$ is made implicit to simplify. If $u_a > \alpha_{\text{RJ}}((\mathbf{x}, \boldsymbol{\theta}_{\mathbf{x}}), (\mathbf{y}, \boldsymbol{\theta}'_{\mathbf{y}}))$, set the next state of the chain to $(\mathbf{x}, \boldsymbol{\theta}_{\mathbf{x}})$.

3. Go to Step 1.

The notation $\mathbf{x} \mapsto \mathbf{y}$ in subscript is used to highlight a dependence on the model transition that is proposed, which is from model \mathbf{x} to model \mathbf{y} . Recall that a diffeomorphism is a differentiable map having a differentiable inverse. A simple example of a mapping $\mathcal{D}_{\mathbf{x} \rightarrow \mathbf{y}}$ is one where the current parameter value $\boldsymbol{\theta}_{\mathbf{x}}$ is not involved in the parameter-proposal scheme: $\boldsymbol{\theta}'_{\mathbf{y}} = \mathbf{u}_{\mathbf{x} \rightarrow \mathbf{y}}$ and $\mathbf{u}_{\mathbf{y} \rightarrow \mathbf{x}} = \boldsymbol{\theta}_{\mathbf{x}}$, implying that $|J_{\mathcal{D}_{\mathbf{x} \rightarrow \mathbf{y}}}(\boldsymbol{\theta}_{\mathbf{x}}, \mathbf{u}_{\mathbf{x} \rightarrow \mathbf{y}})| = 1$.

In the trans-dimensional framework presented above, $\mathbf{x} \notin \mathbf{N}(\mathbf{x})$, as before, and $q_{\mathbf{x}}$ is used conditionally on the fact that a model switch is proposed. The probability of proposing a model switch is $1 - \tau$, τ representing the probability of proposing a parameter update. In trans-dimensional samplers, the probability of proposing a parameter update is typically allowed to depend on the current state and is incorporated in $q_{\mathbf{x}}$. By contrast, it is considered constant and not incorporated in $q_{\mathbf{x}}$ in this framework so as to guarantee the correctness of the non-reversible counterpart of the RJ sampler.

We now consider that a partial order \mathcal{R} has been specified on \mathcal{X} . In the lifted framework, the state-space is extended to include a direction variable $\nu \in \{-1, +1\}$ to guide the model indicator \mathbf{X} . The state-space and target become $\cup_{\mathbf{x} \in \mathcal{X}} \{\mathbf{x}\} \times \boldsymbol{\Theta}_{\mathbf{x}} \times \{-1, +1\}$ and $\pi \otimes \mathcal{U}\{-1, +1\}$, respectively. Apart from the inclusion of ν in the algorithm process, there is only one major change made to RJ to yield NRJ: given a

current state of $(\mathbf{x}, \boldsymbol{\theta}_{\mathbf{x}}, \nu)$ and that a model switch has been proposed, a model \mathbf{y} is proposed using a PMF $q_{\mathbf{x}, \nu}$ with support $\mathbf{N}_{\nu}(\mathbf{x})$, instead of $q_{\mathbf{x}}$ with support $\mathbf{N}(\mathbf{x})$. The directional neighbourhoods are defined as before: $\mathbf{N}_{+1}(\mathbf{x}) := \{\mathbf{y} \in \mathbf{N}(\mathbf{x}) : \mathbf{x} < \mathbf{y}\} \subset \mathbf{N}(\mathbf{x})$ and $\mathbf{N}_{-1}(\mathbf{x}) := \{\mathbf{y} \in \mathbf{N}(\mathbf{x}) : \mathbf{y} < \mathbf{x}\} \subset \mathbf{N}(\mathbf{x})$. The rest of NRJ is essentially the same as RJ. Given that $q_{\mathbf{x}, \nu}$ is often defined analogously to $q_{\mathbf{x}}$, the implementation is thus straightforward for a RJ user that already specified the functions $q_{\mathbf{x}}$, $\mathcal{D}_{\mathbf{x} \rightarrow \mathbf{y}}$ and $q_{\mathbf{x} \rightarrow \mathbf{y}}$, provided that a partial order can be established on \mathcal{X} . We refer users that have difficulties with the specification of these functions to [Gagnon \(2021\)](#), in which a generic procedure yielding fully informed and efficient RJ is presented.

The NRJ algorithm is now presented in [Algorithm 3](#) and [Proposition 2](#) below establishes its correctness. The proof of [Proposition 2](#) establishes that any valid scheme used for parameter proposals during model switches in the RJ framework, such as those of [Karagiannis and Andrieu \(2013\)](#) and [Andrieu et al. \(2018a\)](#), are also valid in the non-reversible framework.

Algorithm 3 A lifted trans-dimensional sampler for partially-ordered model spaces

1. Sample $u_c \sim \mathcal{U}[0, 1]$.
- 2.(a) If $u_c \leq \tau$, attempt a parameter update using a MCMC kernel of invariant distribution $\pi(\cdot | \mathbf{x})$ while keeping the current value of the model indicator \mathbf{x} and direction ν fixed.
- 2.(b) If $u_c > \tau$, attempt a model switch. Sample $\mathbf{y} \sim q_{\mathbf{x}, \nu}$, $\mathbf{u}_{\mathbf{x} \rightarrow \mathbf{y}} \sim q_{\mathbf{x} \rightarrow \mathbf{y}}$ and $u_a \sim \mathcal{U}[0, 1]$. Next, compute $\mathcal{D}_{\mathbf{x} \rightarrow \mathbf{y}}(\boldsymbol{\theta}_{\mathbf{x}}, \mathbf{u}_{\mathbf{x} \rightarrow \mathbf{y}}) = (\boldsymbol{\theta}'_{\mathbf{y}}, \mathbf{u}_{\mathbf{y} \rightarrow \mathbf{x}})$. If

$$u_a \leq \alpha_{\text{NRJ}}((\mathbf{x}, \boldsymbol{\theta}_{\mathbf{x}}), (\mathbf{y}, \boldsymbol{\theta}'_{\mathbf{y}})) := 1 \wedge \frac{q_{\mathbf{y}, -\nu}(\mathbf{x})}{q_{\mathbf{x}, \nu}(\mathbf{y})} r((\mathbf{x}, \boldsymbol{\theta}_{\mathbf{x}}), (\mathbf{y}, \boldsymbol{\theta}'_{\mathbf{y}})),$$

set the next state of the chain to $(\mathbf{y}, \boldsymbol{\theta}'_{\mathbf{y}}, \nu)$. Otherwise, set it to $(\mathbf{x}, \boldsymbol{\theta}_{\mathbf{x}}, -\nu)$.

3. Go to Step 1.

Proposition 2. *The transition kernel of the Markov chain $\{(\mathbf{X}, \boldsymbol{\theta}_{\mathbf{X}}, \nu)_k\}$ simulated by [Algorithm 3](#) admits $\pi \otimes \mathcal{U}\{-1, 1\}$ as invariant distribution.*

In [Gagnon \(2021\)](#), the proposed procedure to specify the functions $q_{\mathbf{x}}$, $\mathcal{D}_{\mathbf{x} \rightarrow \mathbf{y}}$ and $q_{\mathbf{x} \rightarrow \mathbf{y}}$ is proved to produce a RJ which asymptotically approaches an ideal one which is able to sample $\boldsymbol{\theta}'_{\mathbf{y}}$ from $\pi(\cdot | \mathbf{y})$ (the correct conditional distribution) and which sets $q_{\mathbf{x}}$ to locally-balanced distributions (because it has access to the exact ratios of marginal probabilities $\pi(\mathbf{y})/\pi(\mathbf{x})$), as the sample size goes to infinity in a Bayesian statistics context. The analogous conclusions hold for NRJ, and thus $q_{\mathbf{x}, \nu}$ can be set to be asymptotically locally-balanced following the analogous procedure to that in [Gagnon \(2021\)](#). In the limit, the marginal process $\{(\mathbf{X}, \nu)_k\}$ is the same (if we consider only iterations for which model switches are proposed) as that simulated by [Algorithm 1](#). All conclusions previously drawn about the state-space exploration efficiency of [Algorithm 1](#) compared to its MH counterpart thus hold (at least approximatively) for [Algorithm 3](#), but when compared with its RJ counterpart. In particular, if we were to analyse the same data as in [Section 5.2](#), but using the super heavy-tailed regression of [Gagnon et al. \(2020\)](#) for robust inference and outlier detection, it is likely that the algorithm performance results would be the similar. Indeed, [Raftery et al. \(1997\)](#) verified that nothing points towards a gross violation of the assumptions underlying normal linear regression and the robust method is designed for leading to similar results in the absence of outliers. We thus omit further analysis of [Algorithm 3](#).

and we do not illustrate how it performs for brevity. We nevertheless mention that, within the trans-dimensional framework, $r((\mathbf{x}, \theta_{\mathbf{x}}), (\mathbf{y}, \theta'_{\mathbf{y}}))$ can be seen as an estimator of $\pi(\mathbf{y})/\pi(\mathbf{x})$ and it is important that this estimator has a low variance in the lifted framework as persistent movement may be interrupted otherwise because significant noise fluctuations may lead to high rejection rates, as shown in [Gagnon and Doucet \(2021\)](#). The methods of [Karagiannis and Andrieu \(2013\)](#) and [Andrieu *et al.* \(2018a\)](#) can be used to produce an estimator involved in the acceptance probability like $r((\mathbf{x}, \theta_{\mathbf{x}}), (\mathbf{y}, \theta'_{\mathbf{y}}))$, but with a reduced variability.

7 Discussion

In this paper, we have introduced a weaker version of the celebrated Peskun ordering ([Peskun, 1973](#)) and have used it to analyse a class of lifted samplers designed to sample from distributions whose supports are partially-ordered discrete state-spaces. The weaker ordering does not require to establish a relationship between the Markov kernels on the whole state-space; it is only required to establish a relationship on a subset of the state-space, but the order between the asymptotic variances holds asymptotically, as a varying parameter grows without bound, as long as the mass concentrates on the subset. This weaker requirement turned out to be useful to analyse some aspects of the lifted samplers and in particular how they compare to their MH counterparts. We have also shown that these lifted samplers can be straightforwardly implemented, at no additional computational cost and complexity, whenever a partial ordering on \mathcal{X} can be established, and we have introduced a trans-dimensional version of them.

The main contribution of our analysis of the lifted samplers is to provide insights into the situations in which they are expected to outperform their MH counterparts, and also into those in which it is not the case. In particular, our theoretical analysis shows that, in order for locally-balanced lifted samplers to experience constant-momentum excursions, it is crucial that the mass concentrates on regions of the state-space where the individual mass of what we call directional neighbourhoods does not vary too much. It is when they experience constant-momentum excursions of considerable lengths that the lifted samplers shine. While this point was reasonably well understood by the MCMC community, the merit of that part of our research presented in [Section 4](#) has been to provide a rigorous analysis framework, which, *de facto*, can be used to study similar problems, perhaps some for which one does not have a clear intuition. Our analysis was conducted under a general framework, without focussing on specific statistical models or systems, explaining why we were not in a position to explicitly verify the assumptions of [Theorems 2](#) and [3](#). It would be thus interesting to dig deeper and analyse real practical examples in which, for instance, the normalizing constants $c_v(\mathbf{x})$ have simple expressions or can be estimated to take the analysis of lifted samplers one step further.

One of the shortcomings of the application of our theoretical results to lifted samplers is that it does not give any quantitative measurement of the improvement offered by a lifted sampler over its MH counterpart when estimating $\pi_n f_n$, i.e. they are not such that $\text{var}(f_n, P_{\rho,n}) \leq \omega_n \text{var}(f_n, P_{\text{MH},n}) + \text{error}$ for some $\omega_n \in (0, 1)$. Indeed, our analysis only allows to establish an inequality, but in the case where (essentially) $\omega_n \geq 1$. This a consequence of the route we followed to compare the asymptotic variances of the lifted and MH samplers:

$$\text{var}(f_n, P_{\rho,n}) \leq \text{var}(f_n, P_{\text{rev.},n}) \leq \omega_n \text{var}(f_n, P_{\text{MH},n}) + \text{error}.$$

In particular, no quantitative reduction factor is provided in the first inequality, which is expected given that this inequality holds in great generality (for any f_n and any π_n). This leaves one to find an

estimate of ω_n in the second inequality, with the need that $\omega_n < 1$ if one would like to measure the improvement. Given that $P_{\text{rev},n}$ and $P_{\text{MH},n}$ are, at best, similar and in fact, as mentioned in [Section 2](#), ω_n is usually larger than one, a way to have a quantitative variance improvement factor is to obtain a different inequality between $\text{var}(f_n, P_{\rho,n})$ and $\text{var}(f_n, P_{\text{rev},n})$ by leveraging a beneficial structure of the target distribution when it exists. We believe that this is possible, yet difficult, as the analysis needs to take into account the time duration of constant-momentum excursions conducted by the lifted sampler. This typically involves an analysis of k -step transition kernels with $k > 1$ because it is only after k transitions starting from a state \mathbf{x} that we start to see a significant difference between lifted samplers and their non-lifted and MH counterparts.

Our work can also be extended in another direction: the theoretical result can be generalized to general state-spaces and the lifted samplers can be applied in cases where there exist partial orders on these general state-spaces. However, our proof implicitly assumes that the Markov kernels are uniformly ergodic and it would be interesting to see how this assumption can be relaxed.

A methodological question which has been unaddressed in the paper is that of the choice of the partial order. If a specific state-space admits a partial order, it needs not be unique and its choice may significantly impacts the sampler. Indeed, some choices may guarantee more than others those aforementioned constant-momentum excursions. If specifically interested in the estimation of $\pi_n f_n$ for a particular f_n , one could also design the partial order based on f_n , in the spirit of [Faizi et al. \(2020\)](#).

Finally, in terms of applications of the theoretical work on the weak Peskun ordering, it would be interesting to consider the particular case of Bayesian models where a Bernstein von-Mises theorem holds. Comparing two Markov chains sampling from the corresponding posterior distribution, our result suggests that one only needs to compare those samplers locally around a realization of a consistent parameter estimator. A question that naturally arises in this context is: is it possible to have a precise estimate of the sample size beyond which the approximate asymptotic-variance ordering holds? From a methodological standpoint this would motivate the design of samplers that are particularly efficient near the parameter estimate, perhaps at the expense of their behaviour in the tails of the distribution.

References

Andrieu, C., Doucet, A., Yıldırım, S. and Chopin, N. (2018a) On the utility of Metropolis–Hastings with asymmetric acceptance ratio. *arXiv:1803.09527*.

Andrieu, C., Lee, A. and Vihola, M. (2018b) Uniform ergodicity of the iterated conditional SMC and geometric ergodicity of particle Gibbs samplers (supplemental content). *Bernoulli*, **24**, 842–872.

Andrieu, C. and Livingstone, S. (2021) Peskun-Tierney ordering for Markov chain and process Monte Carlo: beyond the reversible scenario. *Ann. Statist.*, **49**, 1958 – 1981.

Atchadé, Y. F. (2021) Approximate spectral gaps for Markov chain mixing times in high dimensions. *SIAM J. Math. Data Sci.*, **3**, 854–872.

Barker, A. A. (1965) Monte Carlo calculations of the radial distribution functions for a proton-electron plasma. *Austral. J. Phys.*, **18**, 119–134.

Bierkens, J. (2016) Non-reversible Metropolis–Hastings. *Stat. Comput.*, **26**, 1213–1228.

Boyd, S. P., Ghosh, A., Prabhakar, B. and Shah, D. (2005) Mixing times for random walks on geometric random graphs. In *ALENEX/ANALCO*, 240–249.

Chen, F., Lovász, L. and Pak, I. (1999) Lifting Markov chains to speed up mixing. In *Proceedings of the thirty-first annual ACM symposium on Theory of computing*, 275–281.

Diaconis, P. (2013) Some things we've learned (about Markov chain Monte Carlo). *Bernoulli*, **19**, 1294–1305.

Diaconis, P., Holmes, S. and Neal, R. M. (2000) Analysis of a nonreversible Markov chain sampler. *Ann. Appl. Probab.*, 726–752.

Erhlich, I. (1973) Participation in illegitimate activities: a theoretical and empirical analysis. *J. Polit. Econ.*, **81**, 521–567.

Faizi, F., Deligiannidis, G. and Rosta, E. (2020) Efficient irreversible Monte Carlo samplers. *J. Chem. Theory Comput.*, **16**, 2124–2138.

Forster, J. J., Gill, R. C. and Overstall, A. M. (2012) Reversible jump methods for generalised linear models and generalised linear mixed models. *Stat. Comput.*, **22**, 107–120.

Gagnon, P. (2021) Informed reversible jump algorithms. *Electron. J. Stat.*, **15**, 3951–3995.

Gagnon, P., Bédard, M. and Desgagné, A. (2021) An automatic robust Bayesian approach to principal component regression. *J. Appl. Stat.*, **48**, 84–104. ArXiv:1711.06341.

Gagnon, P., Desgagné, A. and Bédard, M. (2020) A new Bayesian approach to robustness against outliers in linear regression. *Bayesian Anal.*, **15**, 389–414.

Gagnon, P. and Doucet, A. (2021) Nonreversible jump algorithms for Bayesian nested model selection. *J. Comput. Graph. Statist.*, **30**, 312–323. ArXiv:1911.01340.

Green, P. J. (1995) Reversible jump Markov chain Monte Carlo computation and Bayesian model determination. *Biometrika*, **82**, 711–732.

Gustafson, P. (1998) A guided walk Metropolis algorithm. *Stat. Comput.*, **8**, 357–364.

Hastings, W. K. (1970) Monte Carlo sampling methods using Markov chains and their applications. *Biometrika*, **57**, 97–109.

Herschlag, G., Mattingly, J. C., Sachs, M. and Wyse, E. (2020) Non-reversible Markov chain Monte Carlo for sampling of districting maps. *arXiv:2008.07843*.

Horowitz, A. M. (1991) A generalized guided Monte Carlo algorithm. *Phys. Lett. B*, **268**, 247–252.

Jeffreys, H. (1967) *Theory of Probability*. Oxford Univ. Press, London.

Kamatani, K. and Song, X. (2020) Non-reversible guided Metropolis-Hastings kernel. *arXiv:2005.05584*.

Karagiannis, G. and Andrieu, C. (2013) Annealed importance sampling reversible jump MCMC algorithms. *J. Comp. Graph. Stat.*, **22**, 623–648.

Kleijn, B. J. K. and Van der Vaart, A. W. (2012) The Bernstein-Von-Mises theorem under misspecification. *Electron. J. Statist.*, **6**, 354–381.

Lindley, D. V. (1957) A statistical paradox. *Biometrika*, **44**, 187–192.

Livingstone, S. and Zanella, G. (2021) The Barker proposal: combining robustness and efficiency in gradient-based MCMC. *To appear in J. R. Stat. Soc. Ser. B. Stat. Methodol.*

Metropolis, N., Rosenbluth, A. W., Rosenbluth, M. N., Teller, A. H. and Teller, E. (1953) Equation of state calculations by fast computing machines. *J. Chem. Phys.*, **21**, 1087.

Peskun, P. (1973) Optimum Monte-Carlo sampling using Markov chains. *Biometrika*, **60**, 607–612.

Power, S. and Goldman, J. V. (2019) Accelerated sampling on discrete spaces with non-reversible Markov processes. *arXiv:1912.04681*.

Raftery, A. E., Madigan, D. and Hoeting, J. A. (1997) Bayesian model averaging for linear regression models. *J. Amer. Statist. Assoc.*, **92**, 179–191.

Roberts, G. O. and Rosenthal, J. S. (2004) General state space Markov chains and MCMC algorithms. *Probab. Surv.*, **1**, 20–71.

Rosenthal, J. S. (2003) Asymptotic variance and convergence rates of nearly-periodic Markov chain Monte Carlo algorithms. *J. Amer. Statist. Assoc.*, **98**, 169–177.

Sakai, Y. and Hukushima, K. (2016a) Eigenvalue analysis of an irreversible random walk with skew detailed balance conditions. *Phys. Rev. E*, **93**, 043318.

— (2016b) Irreversible simulated tempering. *J. Phys. Soc. Jpn.*, **85**, 104002.

Syed, S., Bouchard-Côté, A., Deligiannidis, G. and Doucet, A. (2021) Non-reversible parallel tempering: A scalable highly parallel MCMC scheme. *To appear in J. R. Stat. Soc. Ser. B. Stat. Methodol.*

Tierney, L. (1998) A note on Metropolis-Hastings kernels for general state spaces. *Ann. Appl. Probab.*, **8**, 1–9.

Van der Vaart, A. W. (2000) *Asymptotic Statistics*. Cambridge University Press.

Vandaele, W. (1978) Participation in illegitimate activities; Ehrlich revisited. In *Deterrence and incapacitation*, 270–335. Washington, D.C.: National Academy of Sciences Press.

Yang, J. and Rosenthal, J. S. (2017) Complexity results for MCMC derived from quantitative bounds. *arXiv preprint arXiv:1708.00829*.

Zanella, G. (2020) Informed proposals for local MCMC in discrete spaces. *J. Amer. Statist. Assoc.*, **115**, 852–865.

A Proofs of theoretical results and useful lemmas

We now present the proofs of all theoretical results in the same order as the results appeared in the paper. We beforehand present and prove three lemmas which are central to the proofs of Theorems 2 and 3. In the proofs, we will sometimes use a subscript in \mathbb{E} to make clear with respect to which distribution the expectation is computed. We will do the same with \mathbb{P} .

The three lemmas that we now present and prove hold for any fixed n . To simplify the presentation, we thus make implicit the dependence on this parameter of the target distribution, state-space, and so on. In particular, we write p for $p(n) := \pi_n(\tilde{\mathcal{X}}_n)$. We introduce some notation that are required for the presentation of the lemmas. We define four Markov chains $\{\mathbf{X}_k\}$, $\{\tilde{\mathbf{X}}_k\}$, $\{\mathbf{Y}_k\}$ and $\{\tilde{\mathbf{Y}}_k\}$ with Markov kernels P_1 , \tilde{P}_1 , P_2 and \tilde{P}_2 , respectively, started in stationarity. Let $\varrho \in \mathbb{N}$. We define

$$A_\varrho := \bigcap_{k < \varrho} \{\mathbf{X}_k \in \tilde{\mathcal{X}}^\circ\},$$

$$\tilde{A}_\varrho := \bigcap_{k < \varrho} \{\tilde{\mathbf{X}}_k \in \tilde{\mathcal{X}}^\circ\},$$

$$B_\varrho := \bigcap_{k < \varrho} \{\mathbf{Y}_k \in \tilde{\mathcal{X}}^\circ\},$$

and

$$\tilde{B}_\varrho := \bigcap_{k < \varrho} \{\tilde{\mathbf{Y}}_k \in \tilde{\mathcal{X}}^\circ\}.$$

Note that the asymptotic variance can be rewritten for a test-function f as

$$\text{var}(f, P_1) = \mathbb{V}\text{ar}[f(\mathbf{X}_0)] + 2 \sum_{k=1}^{\infty} \mathbb{C}\text{ov}[f(\mathbf{X}_0), f(\mathbf{X}_k)].$$

Lemma 3. *For any $f \in \mathcal{L}_{0,1}^2(\pi)$ and any $\varrho \in \mathbb{N}$,*

$$\begin{aligned} \text{var}(f, P_1) &= p \text{var}(f, \tilde{P}_1) + \pi(f^2 \mathbb{1}_{\tilde{\mathcal{X}}^c}) + p(2\varrho - 1)(\tilde{\pi}f)^2 \\ &\quad + 2 \sum_{k=1}^{\varrho-1} \left\{ \mathbb{E}[f(\mathbf{X}_0)f(\mathbf{X}_k)\mathbb{1}_{A_\varrho^c}] - p\mathbb{E}[f(\tilde{\mathbf{X}}_0)f(\tilde{\mathbf{X}}_k)\mathbb{1}_{\tilde{A}_\varrho^c}] \right\} \\ &\quad + 2 \sum_{k \geq \varrho} \left\{ \mathbb{E}[f(\mathbf{X}_0)f(\mathbf{X}_k)] - p\mathbb{C}\text{ov}[f(\tilde{\mathbf{X}}_0), f(\tilde{\mathbf{X}}_k)] \right\} \end{aligned}$$

Note that the result holds if we replace P_1 and \tilde{P}_1 by P_2 and \tilde{P}_2 , $\{\mathbf{X}_k\}$ and $\{\tilde{\mathbf{X}}_k\}$ by $\{\mathbf{Y}_k\}$ and $\{\tilde{\mathbf{Y}}_k\}$, and A_ϱ and \tilde{A}_ϱ by B_ϱ and \tilde{B}_ϱ .

Proof. First, the relationship between the marginal variances is given by

$$1 = \mathbb{V}\text{ar}[f(\mathbf{X}_0)] = p\mathbb{V}\text{ar}[f(\tilde{\mathbf{X}}_0)] + p(\tilde{\pi}f)^2 + \pi(f^2 \mathbb{1}_{\tilde{\mathcal{X}}^c}).$$

Second, given that $f \in \mathcal{L}_{0,1}^2(\pi)$, $\mathbb{C}\text{ov}[f(\mathbf{X}_0), f(\mathbf{X}_k)] = \mathbb{E}[f(\mathbf{X}_0)f(\mathbf{X}_k)]$. For $k < \rho$,

$$\mathbb{E}[f(\mathbf{X}_0)f(\mathbf{X}_k)\mathbb{1}_{A_\varrho}] = \int \pi(d\mathbf{x}_0) P_1(\mathbf{x}_0, d\mathbf{x}_1) \cdots P(\mathbf{x}_{k-1}, d\mathbf{x}_k) f(\mathbf{x}_0)f(\mathbf{x}_k)\mathbb{1}_{A_\varrho} = p\mathbb{E}[f(\tilde{\mathbf{X}}_0)f(\tilde{\mathbf{X}}_k)\mathbb{1}_{\tilde{A}_\varrho}]$$

because for all $\mathbf{x} \in \tilde{\mathcal{X}}^\circ$ and all $B \subset \tilde{\mathcal{X}}^\circ$, $P_1(\mathbf{x}, B) = \tilde{P}_1(\mathbf{x}, B)$. Therefore,

$$\mathbb{E}[f(\mathbf{X}_0)f(\mathbf{X}_k)\mathbb{1}_{A_\varrho}] = p\mathbb{E}[f(\tilde{\mathbf{X}}_0)f(\tilde{\mathbf{X}}_k)] - p\mathbb{E}[f(\tilde{\mathbf{X}}_0)f(\tilde{\mathbf{X}}_k)\mathbb{1}_{\tilde{A}_\varrho^c}],$$

implying that

$$\mathbb{C}\text{ov}[f(\mathbf{X}_0), f(\mathbf{X}_k)] = p\mathbb{C}\text{ov}[f(\tilde{\mathbf{X}}_0), f(\tilde{\mathbf{X}}_k)] + p(\tilde{\pi}f)^2 - p\mathbb{E}[f(\tilde{\mathbf{X}}_0)f(\tilde{\mathbf{X}}_k)\mathbb{1}_{\tilde{A}_\varrho^c}] + \mathbb{E}[f(\mathbf{X}_0)f(\mathbf{X}_k)\mathbb{1}_{A_\varrho^c}].$$

We are thus able to conclude the proof with

$$\begin{aligned} \text{var}(f, P_1) &= 1 + 2 \sum_{k=1}^{\infty} \mathbb{C}\text{ov}[f(\mathbf{X}_0), f(\mathbf{X}_k)] \\ &= p\mathbb{V}\text{ar}[f(\tilde{\mathbf{X}}_0)] + 2p \sum_{k=1}^{\varrho-1} \mathbb{C}\text{ov}[f(\tilde{\mathbf{X}}_0), f(\tilde{\mathbf{X}}_k)] + (2\varrho-1)p(\tilde{\pi}f)^2 + \pi(f^2\mathbb{1}_{\tilde{\mathcal{X}}^c}) \\ &\quad + 2 \sum_{k=1}^{\varrho-1} \left[\mathbb{E}[f(\mathbf{X}_0)f(\mathbf{X}_k)\mathbb{1}_{A_\varrho^c}] - p\mathbb{E}[f(\tilde{\mathbf{X}}_0)f(\tilde{\mathbf{X}}_k)\mathbb{1}_{\tilde{A}_\varrho^c}] \right] + 2 \sum_{k=\varrho}^{\infty} \mathbb{C}\text{ov}[f(\mathbf{X}_0), f(\mathbf{X}_k)] \\ &= p\text{var}(f, \tilde{P}_1) + (2\varrho-1)p(\tilde{\pi}f)^2 + \pi(f^2\mathbb{1}_{\tilde{\mathcal{X}}^c}) \\ &\quad + 2 \sum_{k=1}^{\varrho-1} \left[\mathbb{E}[f(\mathbf{X}_0)f(\mathbf{X}_k)\mathbb{1}_{A_\varrho^c}] - p\mathbb{E}[f(\tilde{\mathbf{X}}_0)f(\tilde{\mathbf{X}}_k)\mathbb{1}_{\tilde{A}_\varrho^c}] \right] + 2 \sum_{k=\varrho}^{\infty} \left[\mathbb{E}[f(\mathbf{X}_0)f(\mathbf{X}_k)] - p\mathbb{C}\text{ov}[f(\tilde{\mathbf{X}}_0), f(\tilde{\mathbf{X}}_k)] \right]. \end{aligned}$$

■

Lemma 4. Assume that there exists $0 < \omega \leq 1$ such that $P_1(\mathbf{x}, \mathbf{y}) \geq \omega P_2(\mathbf{x}, \mathbf{y})$, for all $(\mathbf{x}, \mathbf{y}) \in \tilde{\mathcal{X}}_n^2$ with $\mathbf{x} \neq \mathbf{y}$. For any $f \in \mathcal{L}_{0,1}^2(\pi)$ and $\varrho \in \mathbb{N}$,

$$\text{var}(f, P_1) \leq \frac{\text{var}(f, P_2)}{\omega} + \frac{1-\omega}{\omega} + \Delta_\varrho(f)$$

with

$$\begin{aligned} \Delta_\varrho(f) &= 2 \sum_{k=1}^{\varrho-1} \left\{ \mathbb{E}[f(\mathbf{X}_0)f(\mathbf{X}_k)\mathbb{1}_{A_\varrho^c}] - \frac{1}{\omega} \mathbb{E}[f(\mathbf{Y}_0)f(\mathbf{Y}_k)\mathbb{1}_{B_\varrho^c}] + \frac{p}{\omega} \mathbb{E}[f(\tilde{\mathbf{Y}}_0)f(\tilde{\mathbf{Y}}_k)\mathbb{1}_{\tilde{B}_\varrho^c}] - p\mathbb{E}[f(\tilde{\mathbf{X}}_0)f(\tilde{\mathbf{X}}_k)\mathbb{1}_{\tilde{A}_\varrho^c}] \right\} \\ &\quad + 2 \sum_{k \geq \varrho} \left\{ \mathbb{E}[f(\mathbf{X}_0)f(\mathbf{X}_k)] - \frac{1}{\omega} \mathbb{E}[f(\mathbf{Y}_0)f(\mathbf{Y}_k)] + \frac{p}{\omega} \mathbb{C}\text{ov}[f(\tilde{\mathbf{Y}}_0), f(\tilde{\mathbf{Y}}_k)] - p\mathbb{C}\text{ov}[f(\tilde{\mathbf{X}}_0), f(\tilde{\mathbf{X}}_k)] \right\}. \end{aligned}$$

Note that $P_1(\mathbf{x}, \mathbf{y}) \geq \omega P_2(\mathbf{x}, \mathbf{y})$, for all $(\mathbf{x}, \mathbf{y}) \in \tilde{\mathcal{X}}_n^2$ with $\mathbf{x} \neq \mathbf{y}$, is equivalent to $\tilde{P}_1(\mathbf{x}, \mathbf{y}) \geq \omega \tilde{P}_2(\mathbf{x}, \mathbf{y})$, for all $(\mathbf{x}, \mathbf{y}) \in \tilde{\mathcal{X}}_n^2$ with $\mathbf{x} \neq \mathbf{y}$.

Proof. We first apply Lemma 3 and obtain:

$$\begin{aligned} \text{var}(f, P_1) &= p\text{var}(f, \tilde{P}_1) + \pi(f^2\mathbb{1}_{\tilde{\mathcal{X}}^c}) + p(2\varrho-1)(\tilde{\pi}f)^2 \\ &\quad + 2 \sum_{k=1}^{\varrho-1} \left\{ \mathbb{E}[f(\mathbf{X}_0)f(\mathbf{X}_k)\mathbb{1}_{A_\varrho^c}] - p\mathbb{E}[f(\tilde{\mathbf{X}}_0)f(\tilde{\mathbf{X}}_k)\mathbb{1}_{\tilde{A}_\varrho^c}] \right\} \end{aligned}$$

$$+ 2 \sum_{k \geq \varrho} \left\{ \mathbb{E}[f(\mathbf{X}_0)f(\mathbf{X}_k)] - p \mathbb{C}\text{ov}[f(\tilde{\mathbf{X}}_0), f(\tilde{\mathbf{X}}_k)] \right\}.$$

We now apply Lemma 33 of [Andrieu *et al.* \(2018b\)](#) and obtain:

$$\begin{aligned} \text{var}(f, P_1) &\leq \frac{p}{\omega} \text{var}(f, \tilde{P}_2) + \frac{p(1-\omega)}{\omega} + \pi(f^2 \mathbb{1}_{\tilde{\mathcal{X}}^c}) + p(2\varrho-1)(\tilde{\pi}f)^2 \\ &\quad + 2 \sum_{k=1}^{\varrho-1} \left\{ \mathbb{E}[f(\mathbf{X}_0)f(\mathbf{X}_k)] \mathbb{1}_{A_\varrho^c} - p \mathbb{E}[f(\tilde{\mathbf{X}}_0)f(\tilde{\mathbf{X}}_k)] \mathbb{1}_{\tilde{A}_\varrho^c} \right\} \\ &\quad + 2 \sum_{k \geq \varrho} \left\{ \mathbb{E}[f(\mathbf{X}_0)f(\mathbf{X}_k)] - p \mathbb{C}\text{ov}[f(\tilde{\mathbf{X}}_0), f(\tilde{\mathbf{X}}_k)] \right\}. \end{aligned}$$

Applying again [Lemma 3](#) yields the result after using that $0 < p \leq 1$ and

$$\left(1 - \frac{1}{\omega}\right) \left[\pi(f^2 \mathbb{1}_{\tilde{\mathcal{X}}^c}) + p(2\varrho-1)(\tilde{\pi}f)^2 \right] \leq 0.$$

■

In the next lemma, we establish an upper bound for $\Delta_\varrho(f)$. We will use that the Markov kernel P_i operates a contraction on $\mathcal{L}_{0,1}^2(\pi)$ in the sense that for all $f \in \mathcal{L}_{0,1}^2(\pi)$ and all $k \in \mathbb{N}$,

$$\|P_i^k f\|_\pi \leq (1 - \lambda_i)^k, \quad i = 1, 2. \quad (19)$$

Indeed, by definition of λ_i , the right spectral gap of P_i (see (1)), we have that for any $f \in \mathcal{L}_{0,1}^2(\pi)$, $\|P_i f\|_\pi \leq (1 - \lambda_i)$. Then, using that $P_i^k f = P_i P_i^{k-1} f$ and the fact that, by stationarity, $P_i^{k-1} f / \|P_i^{k-1} f\|_\pi \in \mathcal{L}_{0,1}^2(\pi)$, we have

$$\|P_i P_i^{k-1} f\|_\pi = \left\| P_i \frac{1}{\|P_i^{k-1} f\|_\pi} P_i^{k-1} f \right\|_\pi \|P_i^{k-1} f\|_\pi \leq (1 - \lambda_i) \|P_i^{k-1} f\|_\pi,$$

and (19) is obtained by induction. The analogous inequality holds for \tilde{P}_i .

Lemma 5. *For any $\delta > 0$, $\varrho \in \mathbb{N}$ and $f \in \mathcal{L}_{0,1}^2(\pi)$, we have*

$$\Delta_\varrho(f) \leq \frac{8}{\omega p} \left(\varrho^2 \|f\|_{\pi,2+\delta}^2 \left[1 - \pi(\tilde{\mathcal{X}}^\circ) \right]^{\delta/(2+\delta)} + \frac{\exp(-\varrho\lambda)}{\lambda} \right).$$

Proof. First, note that for any $\delta > 0$, using Hölder's inequality,

$$|\mathbb{E}[f(\mathbf{X}_0)f(\mathbf{X}_k)]| \leq \mathbb{E}[|f(\mathbf{X}_0)f(\mathbf{X}_k)| \mathbb{1}_{A_\varrho^c}] \leq \left[\mathbb{E}[|f(\mathbf{X}_0)f(\mathbf{X}_k)|^{1+\delta/2}] \right]^{2/2+\delta} \mathbb{P}(A_\varrho^c)^{\delta/2+\delta}.$$

Moreover, using Cauchy–Schwarz inequality,

$$\mathbb{E}[|f(\mathbf{X}_0)f(\mathbf{X}_k)|^{1+\delta/2}] \leq \left(\mathbb{E}[|f(\mathbf{X}_0)|^{2+\delta}] \right)^{1/2} \left(\mathbb{E}[|f(\mathbf{X}_k)|^{2+\delta}] \right)^{1/2} = \mathbb{E}[|f(\mathbf{X}_0)|^{2+\delta}].$$

Also,

$$\mathbb{P}(A_\varrho^c) = \mathbb{P}\left(\bigcup_{k=1}^{\varrho-1} \mathbf{X}_k \in \partial\tilde{\mathcal{X}} \cup \tilde{\mathcal{X}}^c\right) \leq \sum_{k=1}^{\varrho-1} \mathbb{P}(\mathbf{X}_k \in \partial\tilde{\mathcal{X}} \cup \tilde{\mathcal{X}}^c) \leq \varrho \pi(\partial\tilde{\mathcal{X}} \cup \tilde{\mathcal{X}}^c) = \varrho(1 - \pi(\tilde{\mathcal{X}}^\circ)).$$

Combining these results yields

$$|\mathbb{E}[f(\mathbf{X}_0)f(\mathbf{X}_k)\mathbb{1}_{A_\varrho^c}]| \leq \|f\|_{\pi,2+\delta}^2 [\varrho(1-\pi(\tilde{\mathcal{X}}^\circ))]^{\delta/(2+\delta)} \leq \frac{\|f\|_{\pi,2+\delta}^2}{\omega p} \varrho(1-\pi(\tilde{\mathcal{X}}^\circ))^{\delta/(2+\delta)},$$

using that $0 < \delta/(2+\delta) \leq 1$ and $0 < \omega, p \leq 1$. Similarly, for any $\delta > 0$,

$$|\mathbb{E}[f(\tilde{\mathbf{X}}_0)f(\tilde{\mathbf{X}}_k)\mathbb{1}_{\tilde{A}_\varrho^c}]| \leq \|f\|_{\tilde{\pi},2+\delta}^2 [\tilde{\pi}(\partial\tilde{\mathcal{X}})]^{\delta/(2+\delta)} \leq \frac{\|f\|_{\pi,2+\delta}^2}{\omega p^2} \varrho(1-\pi(\tilde{\mathcal{X}}^\circ))^{\delta/(2+\delta)},$$

using that

$$p\|f\|_{\tilde{\pi},2+\delta}^2 = \left[\sum_{\mathbf{x} \in \tilde{\mathcal{X}}} f(\mathbf{x})^{2+\delta} \pi(\mathbf{x}) \right]^{2/2+\delta} \leq \|f\|_{\pi,2+\delta}^2$$

and the definition of $\tilde{\pi}$.

Similar bounds also hold for $|\mathbb{E}[f(\mathbf{Y}_0)f(\mathbf{Y}_k)\mathbb{1}_{B_\varrho^c}]|$ and $|\mathbb{E}[f(\tilde{\mathbf{Y}}_0)f(\tilde{\mathbf{Y}}_k)\mathbb{1}_{\tilde{B}_\varrho^c}]|$. Therefore,

$$\begin{aligned} 2 \left| \sum_{k=1}^{\varrho-1} \left\{ \mathbb{E}[f(\mathbf{X}_0)f(\mathbf{X}_k)\mathbb{1}_{A_\varrho^c}] - \frac{1}{\omega} \mathbb{E}[f(\mathbf{Y}_0)f(\mathbf{Y}_k)\mathbb{1}_{B_\varrho^c}] + \frac{p}{\omega} \mathbb{E}[f(\tilde{\mathbf{Y}}_0)f(\tilde{\mathbf{Y}}_k)\mathbb{1}_{\tilde{B}_\varrho^c}] - p \mathbb{E}[f(\tilde{\mathbf{X}}_0)f(\tilde{\mathbf{X}}_k)\mathbb{1}_{\tilde{A}_\varrho^c}] \right\} \right| \\ \leq \frac{8}{\omega p} \varrho^2 \|f\|_{\pi,2+\delta}^2 (1-\pi(\tilde{\mathcal{X}}^\circ))^{\delta/(2+\delta)}. \end{aligned}$$

We now bound the second sum in $\Delta_\varrho(f)$. Using Cauchy–Schwarz inequality and (19),

$$|\mathbb{E}[f(\mathbf{X}_0)f(\mathbf{X}_k)]| \leq \|f\|_{\pi,2} \|P_1^k f\|_{\pi,2} \leq (1-\lambda_1)^k \leq (1-\underline{\lambda})^k \leq \frac{1}{\omega} (1-\underline{\lambda})^k.$$

Similarly,

$$\begin{aligned} |\mathbb{Cov}[f(\tilde{\mathbf{X}}_0), f(\tilde{\mathbf{X}}_k)]| &\leq \|f - \tilde{\pi}f\|_{\tilde{\pi},2} \|\tilde{P}_1^k (f - \tilde{\pi}f)\|_{\tilde{\pi},2} = \|f - \tilde{\pi}f\|_{\tilde{\pi},2}^2 \left\| \tilde{P}_1^k \frac{(f - \tilde{\pi}f)}{\|f - \tilde{\pi}f\|_{\tilde{\pi},2}} \right\|_{\tilde{\pi},2} \\ &\leq \mathbb{V}\text{ar}[f(\tilde{\mathbf{X}}_0)] (1-\tilde{\lambda}_1)^k \leq \frac{1}{\omega p} (1-\underline{\lambda})^k, \end{aligned}$$

using that $\mathbb{V}\text{ar}[f(\tilde{\mathbf{X}}_0)] \leq 1/p$.

Similar bounds also hold for $|\mathbb{E}[f(\mathbf{Y}_0)f(\mathbf{Y}_k)]|$ and $|\mathbb{Cov}[f(\tilde{\mathbf{Y}}_0), f(\tilde{\mathbf{Y}}_k)]|$. Therefore,

$$\begin{aligned} 2 \left| \sum_{k \geq \varrho} \left\{ \mathbb{E}[f(\mathbf{X}_0)f(\mathbf{X}_k)] - \frac{1}{\omega} \mathbb{E}[f(\mathbf{Y}_0)f(\mathbf{Y}_k)] + \frac{p}{\omega} \mathbb{C}\text{ov}[f(\tilde{\mathbf{Y}}_0), f(\tilde{\mathbf{Y}}_k)] - p \mathbb{C}\text{ov}[f(\tilde{\mathbf{X}}_0), f(\tilde{\mathbf{X}}_k)] \right\} \right| \\ \leq \frac{8}{\omega} \sum_{k \geq \varrho} (1-\underline{\lambda})^k = \frac{8}{\omega} (1-\underline{\lambda})^\varrho \frac{1}{\underline{\lambda}} \leq \frac{8}{\omega p} \frac{\exp(-\varrho \underline{\lambda})}{\underline{\lambda}}, \end{aligned}$$

using that $1-x \leq \exp(-x)$. ■

We now turn to the proofs of Theorems 2 and 3. These theorems are stated and proved under the asymptotic framework presented in Section 2. In the proofs, it will thus be important to highlight a dependence on n of the target distribution, state-space, and so on.

Proof of Theorem 2. We first apply Lemmas 4 and 5:

$$\begin{aligned} \text{var}(f_n, P_{1,n}) &\leq \frac{1}{\omega(n)} \text{var}(f_n, P_{2,n}) + \frac{1 - \omega(n)}{\omega(n)} \\ &\quad + \frac{8}{\omega(n)p(n)} \left(\varrho(n)^2 \|f_n\|_{\pi_n, 2+\delta}^2 \left[1 - \pi_n(\tilde{\mathcal{X}}_n^\circ)\right]^{\delta/(2+\delta)} + \frac{\exp(-\varrho(n)\underline{\lambda}(n))}{\underline{\lambda}(n)} \right). \end{aligned}$$

Let $\bar{\omega} > \epsilon > 0$. Consider that $n > n^*$, a positive integer which will be defined in relation to other positive integers. Under Assumption 1, we know that there exists n_1^* such that for any $n > n_1^*$,

$$\begin{aligned} \text{var}(f_n, P_{1,n}) &\leq \frac{1}{\bar{\omega} - \epsilon} \text{var}(f_n, P_{2,n}) + \frac{1 - \bar{\omega}}{\bar{\omega}} + \frac{\epsilon}{3} \\ &\quad + \frac{8}{\bar{\omega} - \epsilon} \left(\varrho(n)^2 \|f_n\|_{\pi_n, 2+\delta}^2 \left[1 - \pi_n(\tilde{\mathcal{X}}_n^\circ)\right]^{\delta/(2+\delta)} + \frac{\exp(-\varrho(n)\underline{\lambda}(n))}{\underline{\lambda}(n)} \right). \end{aligned}$$

Take $n^* \geq n_1^*$.

Now, we set $\varrho(n) = \lfloor 1/(1 - \pi_n(\tilde{\mathcal{X}}_n^\circ))^{(\bar{\delta}-\gamma)/2} \rfloor$, where $\lfloor \cdot \rfloor$ is the floor function and $\bar{\delta} := \delta/(2 + \delta)$, and note that, by Assumption 1 and given that $\bar{\delta} > \gamma > 0$, $\varrho(n) \rightarrow \infty$. By assumption, we know that there exists n_2^* such that for any $n > n_2^*$,

$$\|f_n\|_{\pi_n, 2+\delta} \varrho(n)^2 (1 - \pi_n(\tilde{\mathcal{X}}_n^\circ))^{\bar{\delta}} \leq \|f_n\|_{\pi_n, 2+\delta} (1 - \pi_n(\tilde{\mathcal{X}}_n^\circ))^\gamma \leq \frac{\bar{\omega} - \epsilon}{24} \epsilon.$$

Take $n^* \geq n_2^*$.

Given that $\underline{\lambda}(n)$ is bounded away from zero by assumption, we know that there exists n_3^* such that for any $n > n_3^*$,

$$\frac{\exp(-\varrho(n)\underline{\lambda}(n))}{\underline{\lambda}(n)} \leq \frac{\bar{\omega} - \epsilon}{24} \epsilon.$$

Take $n^* \geq n_3^*$. This concludes the proof. ■

Proof of Theorem 3. We follow a similar approach than for the proof of Theorem 2. Let $\bar{\omega} > \epsilon > 0$. Consider that $n > n^*$. Under Assumption 1 and using Lemmas 4 and 5, we know that there exists n_1^* such that for any $n > n_1^*$,

$$\begin{aligned} \text{var}(f_n, P_{1,n}) &\leq \frac{1}{\bar{\omega} - \epsilon} \text{var}(f_n, P_{2,n}) + \frac{1 - \bar{\omega}}{\bar{\omega}} + \frac{\epsilon}{3} \\ &\quad + \frac{8}{\bar{\omega} - \epsilon} \left(\varrho(n)^2 \|f_n\|_{\pi_n, 2+\delta}^2 \left[1 - \pi_n(\tilde{\mathcal{X}}_n^\circ)\right]^{\delta/(2+\delta)} + \frac{\exp(-\varrho(n)\underline{\lambda}(n))}{\underline{\lambda}(n)} \right). \end{aligned}$$

Take $n^* \geq n_1^*$.

As previously, we set $\varrho(n) = \lfloor 1/(1 - \pi_n(\tilde{\mathcal{X}}_n^\circ))^{(\bar{\delta}-\gamma)/2} \rfloor$, (again with $\bar{\delta} > \gamma > 0$) which implies that there exists n_2^* such that for any $n > n_2^*$,

$$\|f_n\|_{\pi_n, 2+\delta} \varrho(n)^2 (1 - \pi_n(\tilde{\mathcal{X}}_n^\circ))^{\bar{\delta}} \leq \|f_n\|_{\pi_n, 2+\delta} (1 - p(n))^\gamma \leq \frac{\bar{\omega} - \epsilon}{24} \epsilon.$$

Take $n^* \geq n_2^*$.

We consider that $\underline{\lambda}(n) \rightarrow 0$; otherwise, we are in the same situation as the previous proof and it has been shown that the result holds. We write

$$\frac{\exp\{-\varrho(n)\underline{\lambda}(n)\}}{\underline{\lambda}(n)} = \exp\left\{-\varrho(n)\underline{\lambda}(n)\left(1 + \frac{\log \underline{\lambda}(n)}{\varrho(n)\underline{\lambda}(n)}\right)\right\} = \exp\left\{-\varrho(n)\underline{\lambda}(n)\left(1 + \frac{[\log \underline{\lambda}(n)]\underline{\lambda}(n)^{1/2}}{\varrho(n)\underline{\lambda}(n)^{3/2}}\right)\right\}.$$

Clearly, $[\log \underline{\lambda}(n)]\underline{\lambda}(n)^{1/2}$ vanishes. Now we establish that $\varrho(n)\underline{\lambda}(n)^{3/2} \rightarrow \infty$ which implies that $\varrho(n)\underline{\lambda}(n) \rightarrow \infty$. By (4),

$$\frac{1 - \pi_n(\tilde{\mathcal{X}}_n^\circ)}{\underline{\lambda}(n)^{3/(\bar{\delta}-\gamma)}} \rightarrow 0,$$

which is equivalent to

$$\frac{(1 - \pi_n(\tilde{\mathcal{X}}_n^\circ))^{(\bar{\delta}-\gamma)/2}}{\underline{\lambda}(n)^{3/2}} \rightarrow 0,$$

which allows to conclude that $\varrho(n)\underline{\lambda}(n)^{3/2} \rightarrow \infty$. Therefore, there exists n_3^* such that for any $n > n_3^*$,

$$\frac{\exp\{-\varrho(n)\underline{\lambda}(n)\}}{\underline{\lambda}(n)} \leq \frac{\bar{\omega} - \epsilon}{24}\epsilon.$$

Take $n^* \geq n_3^*$. This concludes the proof. ■

Proof of Proposition 1. It suffices to prove that the probability to reach the state (\mathbf{y}, ν') in one step is equal to the probability of this state under the target:

$$\sum_{\mathbf{x}, \nu} \pi(\mathbf{x}) (1/2) P((\mathbf{x}, \nu), (\mathbf{y}, \nu')) = \pi(\mathbf{y}) (1/2).$$

where P is the transition kernel.

The probability to reach the state (\mathbf{y}, ν') from some (\mathbf{x}, ν) is given by:

$$\begin{aligned} P((\mathbf{x}, \nu), (\mathbf{y}, \nu')) &= T_\nu(\mathbf{x}, \mathcal{X}) Q_{\mathbf{x}, \nu}(\mathbf{y}) \mathbb{1}(\nu = \nu') \\ &\quad + \mathbb{1}(\nu = -\nu', \mathbf{x} = \mathbf{y}) [(\rho_\nu(\mathbf{x}) + T_\nu(\mathbf{x}, \mathcal{X})) - T_\nu(\mathbf{x}, \mathcal{X})] \\ &\quad + \mathbb{1}(\nu = \nu', \mathbf{x} = \mathbf{y}) [1 - \rho_\nu(\mathbf{x}) - T_\nu(\mathbf{x}, \mathcal{X})] \\ &= q_{\mathbf{x}, \nu}(\mathbf{y}) \alpha_\nu(\mathbf{x}, \mathbf{y}) \mathbb{1}(\nu = \nu') \\ &\quad + \mathbb{1}(\nu = -\nu', \mathbf{x} = \mathbf{y}) \rho_\nu(\mathbf{x}) \\ &\quad + \mathbb{1}(\nu = \nu', \mathbf{x} = \mathbf{y}) [1 - \rho_\nu(\mathbf{x}) - T_\nu(\mathbf{x}, \mathcal{X})]. \end{aligned}$$

We have that

$$\begin{aligned} \pi(\mathbf{x}) (1/2) P((\mathbf{x}, \nu), (\mathbf{y}, \nu')) &= (1/2) \pi(\mathbf{y}) q_{\mathbf{y}, -\nu'}(\mathbf{x}) \alpha_{-\nu'}(\mathbf{y}, \mathbf{x}) \mathbb{1}(-\nu' = -\nu) \\ &\quad + (1/2) \pi(\mathbf{y}) \mathbb{1}(-\nu' = \nu, \mathbf{y} = \mathbf{x}) \rho_{-\nu'}(\mathbf{y}) \\ &\quad + (1/2) \pi(\mathbf{y}) \mathbb{1}(-\nu' = -\nu, \mathbf{y} = \mathbf{x}) [1 - \rho_{-\nu'}(\mathbf{y}) - T_{-\nu'}(\mathbf{y}, \mathcal{X})] \\ &= (1/2) \pi(\mathbf{y}) T_{-\nu'}(\mathbf{y}, \mathcal{X}) Q_{\mathbf{y}, -\nu'}(\mathbf{x}) \mathbb{1}(-\nu' = -\nu) \\ &\quad + (1/2) \pi(\mathbf{y}) \mathbb{1}(-\nu' = \nu, \mathbf{y} = \mathbf{x}) [(\rho_{-\nu'}(\mathbf{y}) + T_{-\nu'}(\mathbf{y}, \mathcal{X})) - T_{-\nu'}(\mathbf{y}, \mathcal{X})] \\ &\quad + (1/2) \pi(\mathbf{y}) \mathbb{1}(-\nu' = -\nu, \mathbf{y} = \mathbf{x}) [1 - \rho_{-\nu'}(\mathbf{y}) - T_{-\nu'}(\mathbf{y}, \mathcal{X})], \end{aligned}$$

where we used the definition of α for the first term and that $\rho_\nu(\mathbf{x}) - \rho_{-\nu}(\mathbf{x}) = T_{-\nu}(\mathbf{x}, \mathcal{X}) - T_\nu(\mathbf{x}, \mathcal{X})$ for the third term. Notice the sum on the right-hand side (RHS) is equal to the probability to reach some $(\mathbf{x}, -\nu)$, starting from $(\mathbf{y}, -\nu')$: $(1/2) \pi(\mathbf{y}) P((\mathbf{y}, -\nu'), (\mathbf{x}, -\nu))$.

Therefore,

$$\begin{aligned} \sum_{\mathbf{x}, \nu} \pi(\mathbf{x}) (1/2) P((\mathbf{x}, \nu), (\mathbf{y}, \nu')) &= \sum_{\mathbf{x}, \nu} (1/2) \pi(\mathbf{y}) P((\mathbf{y}, -\nu'), (\mathbf{x}, -\nu)) \\ &= (1/2) \pi(\mathbf{y}), \end{aligned}$$

which concludes the proof. \blacksquare

We now present a lemma that will be useful in the next proofs. We define $\bar{\pi} := \pi \otimes \mathcal{U}\{-1, +1\}$ and note that in the following we can assume without loss of generality that $\bar{\pi}f = 0$.

Lemma 6. *Assume that \mathcal{X} is finite. Then, for any function $f : \mathcal{X} \times \{-1, +1\} \rightarrow \mathbb{R}$,*

$$\lim_{\lambda \rightarrow 1} \sum_{k>0} \lambda^k \langle f, P_\rho^k f \rangle_{\bar{\pi}} = \sum_{k>0} \langle f, P_\rho^k f \rangle_{\bar{\pi}}. \quad (20)$$

Proof. Let us define the sequence of functions $S_N : \lambda \mapsto \sum_{0 < k \leq N} \lambda^k \langle f, P_\rho^k f \rangle$ defined for $\lambda \in [0, 1)$ and its limit $S(\lambda) = \sum_{k>0} \lambda^k \langle f, P_\rho^k f \rangle_{\bar{\pi}}$ (the dependence of S_N and S on f and P_ρ is implicit). We now show that the partial sum S_N converges uniformly to S on $[0, 1)$, and given that for each $N \in \mathbb{N}$, the function $\lambda \mapsto \lambda^N \langle f, P_\rho^N f \rangle_{\bar{\pi}}$ admits a limit when $\lambda \rightarrow 1$, we have that S admits a limit when $\lambda \rightarrow 1$, given by

$$\lim_{\lambda \rightarrow 1} S(\lambda) = S(1) = \sum_{k>0} \langle f, P_\rho^k f \rangle,$$

which is (20).

First, note that

$$\sup_{\lambda \in [0, 1)} |S_N(\lambda) - S(\lambda)| = \sup_{\lambda \in [0, 1)} \left| \sum_{k>N} \lambda^k \langle f, P_\rho^k f \rangle_{\bar{\pi}} \right| \leq \sup_{\lambda \in [0, 1)} \sum_{k>N} \lambda^k |\langle f, P_\rho^k f \rangle_{\bar{\pi}}| = \sum_{k>N} |\langle f, P_\rho^k f \rangle_{\bar{\pi}}|.$$

Thus, to prove that $\sup_{\lambda \in [0, 1)} |S_N(\lambda) - S(\lambda)| \rightarrow 0$, it is sufficient to prove that the series $\sum_{k>0} |\langle f, P_\rho^k f \rangle_{\bar{\pi}}|$ converges.

By bilinearity of the inner product and by linearity of the iterated operators P_ρ, P_ρ^2, \dots , it can be checked that for any linear mapping ϕ

$$\sum_{k=1}^{\infty} \left| \langle f, P_\rho^k f \rangle_{\bar{\pi}} \right| < \infty \Leftrightarrow \sum_{k=1}^{\infty} \left| \langle \phi(f), P_\rho^k \phi(f) \rangle_{\bar{\pi}} \right| < \infty. \quad (21)$$

Given that \mathcal{X} is finite, any function $f : \mathcal{X} \times \{-1, +1\} \rightarrow \mathbb{R}$ is such that $\sup |f| < \infty$. As a consequence, we may use $\phi(f) := f / \sup |f|$ (recall that $\bar{\pi}f = 0$). In the following we denote by $\mathcal{L}_{0,1}^{2,*}(\bar{\pi})$ the subset of $\mathcal{L}^2(\bar{\pi})$ such that

$$\mathcal{L}_{0,1}^{2,*}(\bar{\pi}) := \left\{ f \in \mathcal{L}^2(\bar{\pi}) : \bar{\pi}f = 0, \sup |f| \leq 1 \right\}.$$

By (21), we only need to check that the series $\sum_{k>0} |\langle f, P_\rho^k f \rangle|$ converges for any $f \in \mathcal{L}_{0,1}^{2,*}(\bar{\pi})$. Given that \mathcal{X} is finite, P_ρ is uniformly ergodic and there exist constants $\gamma \in (0, 1)$ and $C \in (0, \infty)$ such that for any $t \in \mathbb{N}$,

$$\sup_{(\mathbf{x}, \nu) \in \mathcal{X} \times \{-1, +1\}} \|\delta_{\mathbf{x}, \nu} P_\rho^t - \bar{\pi}\|_{\text{tv}} \leq C\gamma^t, \quad (22)$$

where for any signed measure μ , $\|\mu\|_{\text{tv}}$ denotes its total variation. Denoting a state of the extended state-space by $\bar{\mathbf{x}} := (\mathbf{x}, \nu) \in \mathcal{X} \times \{-1, +1\}$, we have that, for any $f \in \mathcal{L}_{0,1}^{2,*}(\bar{\pi})$,

$$\begin{aligned} |\langle f, P_\rho^k f \rangle_{\bar{\pi}}| &= \left| \sum_{\bar{\mathbf{x}}} f(\bar{\mathbf{x}}) \bar{\pi}(\bar{\mathbf{x}}) \sum_{\bar{\mathbf{y}}} f(\bar{\mathbf{y}}) P_\rho^k(\bar{\mathbf{x}}, \bar{\mathbf{y}}) \right| \leq \sum_{\bar{\mathbf{x}}} |f(\bar{\mathbf{x}})| \bar{\pi}(\bar{\mathbf{x}}) \left| \sum_{\bar{\mathbf{y}}} f(\bar{\mathbf{y}}) P_\rho^k(\bar{\mathbf{x}}, \bar{\mathbf{y}}) \right| \\ &= \sum_{\bar{\mathbf{x}}} |f(\bar{\mathbf{x}})| \bar{\pi}(\bar{\mathbf{x}}) \left| \sum_{\bar{\mathbf{y}}} f(\bar{\mathbf{y}}) P_\rho^k(\bar{\mathbf{x}}, \bar{\mathbf{y}}) - \bar{\pi} f \right| \\ &\leq \sum_{\bar{\mathbf{x}}} |f(\bar{\mathbf{x}})| \bar{\pi}(\bar{\mathbf{x}}) \sup_{f \in \mathcal{L}_{0,1}^{2,*}(\bar{\pi})} \left| \sum_{\bar{\mathbf{y}}} f(\bar{\mathbf{y}}) P_\rho^k(\bar{\mathbf{x}}, \bar{\mathbf{y}}) - \bar{\pi} f \right| \\ &\leq \sum_{\bar{\mathbf{x}}} |f(\bar{\mathbf{x}})| \bar{\pi}(\bar{\mathbf{x}}) 2 \|\delta_{\mathbf{x}, \nu} P_\rho^k - \bar{\pi}\|_{\text{tv}} \\ &\leq C \gamma^k, \end{aligned}$$

using Jensen's inequality, that $\bar{\pi} f = 0$, that $\|\mu\|_{\text{tv}} = (1/2) \sup_{|g| \leq 1} |\mu g|$ (see, e.g., Proposition 3 in [Roberts and Rosenthal \(2004\)](#)) and thus (22), and finally that $|f| \leq 1$.

Therefore,

$$\sum_{k>0} |\langle f, P_\rho^k f \rangle_{\bar{\pi}}| \leq C \sum_{k>0} \gamma^k < \infty.$$

As a consequence, S_n converges uniformly to S on $[0, 1)$ which concludes the proof. \blacksquare

Proof of Corollary 1. The results of Theorem 6 in [Andrieu and Livingstone \(2021\)](#) holds in our framework, implying that

$$\text{var}_\lambda(f, P_{\rho^*}) \leq \text{var}_\lambda(f, P_\rho) \leq \text{var}_\lambda(f, P_\rho^w),$$

where $\text{var}_\lambda(f, P_\rho) := \mathbb{V}\text{ar}[f(\mathbf{X}, \nu)] + 2 \sum_{k>0} \lambda^k \langle f, P_\rho^k f \rangle_{\bar{\pi}}$ with $\lambda \in [0, 1]$. [Lemma 6](#) allows to conclude. \blacksquare

Proof of Corollary 2. The proof is an application of Theorem 7 in [Andrieu and Livingstone \(2021\)](#) which will allow to establish that

$$\text{var}_\lambda(f_n, P_\rho) \leq \text{var}_\lambda(f_n, P_{\text{MH}}).$$

We will thus be able to conclude using [Lemma 6](#).

In order to apply Theorem 7 in [Andrieu and Livingstone \(2021\)](#), we must verify that

$$q_{\mathbf{x}}(\mathbf{y}) \alpha(\mathbf{x}, \mathbf{y}) = (1/2) q_{\mathbf{x},+1}(\mathbf{y}) \alpha_{+1}(\mathbf{x}, \mathbf{y}) + (1/2) q_{\mathbf{x},-1}(\mathbf{y}) \alpha_{-1}(\mathbf{x}, \mathbf{y}),$$

for all \mathbf{x} and \mathbf{y} . This is straightforward to verify under the assumptions of [Corollary 2](#):

$$\begin{aligned} (1/2) q_{\mathbf{x},+1}(\mathbf{y}) \alpha_{+1}(\mathbf{x}, \mathbf{y}) + (1/2) q_{\mathbf{x},-1}(\mathbf{y}) \alpha_{-1}(\mathbf{x}, \mathbf{y}) \\ &= \frac{1}{2} \frac{1}{(|\mathbf{N}(\mathbf{x})|/2)} \left(1 \wedge \frac{\pi(\mathbf{y})}{\pi(\mathbf{x})} \right) \mathbb{1}_{\mathbf{y} \in \mathbf{N}_{+1}(\mathbf{x})} + \frac{1}{2} \frac{1}{(|\mathbf{N}(\mathbf{x})|/2)} \left(1 \wedge \frac{\pi(\mathbf{y})}{\pi(\mathbf{x})} \right) \mathbb{1}_{\mathbf{y} \in \mathbf{N}_{-1}(\mathbf{x})} \\ &= \frac{1}{|\mathbf{N}(\mathbf{x})|} \left(1 \wedge \frac{\pi(\mathbf{y})}{\pi(\mathbf{x})} \right) (\mathbb{1}_{\mathbf{y} \in \mathbf{N}_{+1}(\mathbf{x})} + \mathbb{1}_{\mathbf{y} \in \mathbf{N}_{-1}(\mathbf{x})}) = q_{\mathbf{x}}(\mathbf{y}) \alpha(\mathbf{x}, \mathbf{y}). \end{aligned} \quad \blacksquare$$

Proof of Lemma 1. Let $(\mathbf{x}, \mathbf{y}) \in \tilde{\mathcal{X}}_n^2$, $\mathbf{x} \neq \mathbf{y}$, $\mathbf{y} \in \mathbf{N}_v(\mathbf{x})$. Since $\mathbf{x} \in \tilde{\mathcal{X}}_n$, we have $2n_v(\mathbf{x}) \in [n - 2\beta(n), n + 2\beta(n)]$ and thus

$$P_{\text{rev},n}(\mathbf{x}, \mathbf{y}) = \frac{1}{2n_v(\mathbf{x})} \left(1 \wedge \frac{\pi_n(\mathbf{y})}{\pi_n(\mathbf{x})} \frac{n_v(\mathbf{x})}{n_{-v}(\mathbf{y})} \right) \geq \left(1 + \frac{\beta(n)}{n/2} \right)^{-1} \frac{1}{n} \left(1 \wedge \frac{\pi_n(\mathbf{y})}{\pi_n(\mathbf{x})} \frac{n_v(\mathbf{x})}{n_{-v}(\mathbf{y})} \right).$$

Noting that

$$\frac{n_v(\mathbf{x})}{n_{-v}(\mathbf{y})} \geq \max \left\{ 0, \left(1 - \frac{\beta(n)}{n/2} \right) \left(1 + \frac{\beta(n)}{n/2} \right)^{-1} \right\},$$

and that for any $a > 0$ and $b \in (0, 1)$, we have $1 \wedge ab \geq b(1 \wedge a)$ and thus

$$P_{\text{rev},n}(\mathbf{x}, \mathbf{y}) \geq \frac{1}{n} \left(1 \wedge \frac{\pi_n(\mathbf{y})}{\pi_n(\mathbf{x})} \right) \left(1 + \frac{\beta(n)}{n/2} \right)^{-1} \max \left\{ 0, \left(1 - \frac{\beta(n)}{n/2} \right) \left(1 + \frac{\beta(n)}{n/2} \right)^{-1} \right\}.$$

This completes the proof since $\beta(n) = o(n)$ implies that for a large enough n , $1 - \beta(n)/(n/2) > 0$ and that $P_{\text{MH},n}(\mathbf{x}, \mathbf{y}) = (1/n)(1 \wedge \pi_n(\mathbf{y})/\pi_n(\mathbf{x}))$. \blacksquare

Proof of Corollary 3. Analogous to that of Corollary 2. \blacksquare

Proof of Lemma 2. Let $\mathbf{x} \in \tilde{\mathcal{X}}_n$ and $\mathbf{y} \in \mathbf{N}_v(\mathbf{x})$, then

$$P_{\text{rev},n}(\mathbf{x}, \mathbf{y}) = q_{\mathbf{x}}(\mathbf{y}) \frac{c_n(\mathbf{x})}{2c_{n,v}(\mathbf{x})} \left(1 \wedge \frac{c_n(\mathbf{x})}{c_n(\mathbf{y})} \varphi_n(\mathbf{x}, \mathbf{y}) \right), \quad \varphi_n(\mathbf{x}, \mathbf{y}) := \frac{c_{n,v}(\mathbf{x})/c_n(\mathbf{x})}{c_{n,v}(\mathbf{y})/c_n(\mathbf{y})}.$$

For any $\mathbf{x} \in \tilde{\mathcal{X}}_n$, $c_{n,v}(\mathbf{x})/c_n(\mathbf{x}) \in [1/2 - \beta(n)/c_n(\mathbf{x}), 1/2 + \beta(n)/c_n(\mathbf{x})]$ so that

$$\varphi_n(\mathbf{x}, \mathbf{y}) \geq \max \left\{ \frac{c_n(\mathbf{x}) - 2\beta(n)}{c_n(\mathbf{x}) + 2\beta(n)c_n(\mathbf{x})/c_n(\mathbf{y})}, 0 \right\} \geq \max \left\{ \frac{1 - 2\beta(n)/c_n(\mathbf{x})}{1 + 2\tau_n\beta(n)/c_n(\mathbf{x})}, 0 \right\}.$$

As in the proof of Lemma 1,

$$P_{\text{rev},n}(\mathbf{x}, \mathbf{y}) \geq q_{\mathbf{x}}(\mathbf{y}) \left(1 \wedge \frac{c_n(\mathbf{x})}{c_n(\mathbf{y})} \right) \left(1 + \frac{\beta(n)}{c_n(\mathbf{x})/2} \right)^{-1} \max \left\{ \frac{1 - 2\beta(n)/c_n(\mathbf{x})}{1 + 2\tau_n\beta(n)/c_n(\mathbf{x})}, 0 \right\}.$$

By assumption $c_n(\mathbf{x}) \geq \inf\{c_n(\mathbf{x}) : \mathbf{x} \in \tilde{\mathcal{X}}_n\} \geq nm$ and we thus have that $\beta(n)/c_n(\mathbf{x}) \rightarrow 0$ since $\beta(n) = o(n)$. Thus for n sufficiently large,

$$\frac{1 - 2\beta(n)/nm}{1 + 2\tau_n\beta(n)/nm} \in (0, 1)$$

so that

$$P_{\text{rev},n}(\mathbf{x}, \mathbf{y}) \geq P_{\text{MH},n}(\mathbf{x}, \mathbf{y}) \left(1 + \frac{\beta(n)}{nm/2} \right)^{-1} \left(\frac{1 - 2\beta(n)/nm}{1 + 2\tau_n\beta(n)/nm} \right).$$

Proof of Proposition 2. It suffices to prove that the probability to reach the state $\mathbf{y}, \theta'_y \in A, v'$ in one step is equal to the probability of this state under the target:

$$\sum_{\mathbf{x}, v} \int \pi(\mathbf{x}, \theta_{\mathbf{x}}) \times (1/2) \left(\int_A P((\mathbf{x}, \theta_{\mathbf{x}}, v), (\mathbf{y}, d\theta'_y, v')) \right) d\theta_{\mathbf{x}} = \int_A \pi(\mathbf{y}, \theta'_y) \times (1/2) d\theta'_y, \quad (23)$$

where P is the transition kernel. Note that we abuse notation here by denoting the integration variable θ'_y on the left-hand side (LHS) given that we in fact use a vector of auxiliary variables $\mathbf{u}_{x \rightarrow y}$ to generate the proposal when switching models, which do not necessarily have the same dimension as θ'_y .

We consider two distinct events: a model switch is proposed, that we denote S , and a parameter update is proposed (therefore denoted S^c). We know that the probabilities of these events are $1 - \tau$ and τ , respectively. We rewrite the LHS of (23) as

$$\begin{aligned} & \sum_{\mathbf{x}, \nu} \int \pi(\mathbf{x}, \theta_{\mathbf{x}}) \times (1/2) \left(\int_A P((\mathbf{x}, \theta_{\mathbf{x}}, \nu), (\mathbf{y}, d\theta'_y, \nu')) \right) d\theta_{\mathbf{x}} \\ &= \sum_{\mathbf{x}, \nu} (1 - \tau) \int \pi(\mathbf{x}, \theta_{\mathbf{x}}) \times (1/2) \left(\int_A P((\mathbf{x}, \theta_{\mathbf{x}}, \nu), (\mathbf{y}, d\theta'_y, \nu') | S) \right) d\theta_{\mathbf{x}} \\ &+ \sum_{\mathbf{x}, \nu} \tau \int \pi(\mathbf{x}, \theta_{\mathbf{x}}) \times (1/2) \left(\int_A P((\mathbf{x}, \theta_{\mathbf{x}}, \nu), (\mathbf{y}, d\theta'_y, \nu') | S^c) \right) d\theta_{\mathbf{x}}. \end{aligned} \quad (24)$$

We analyse the two terms separately. We know that

$$P((\mathbf{x}, \theta_{\mathbf{x}}, \nu), (\mathbf{y}, d\theta'_y, \nu') | S^c) = \delta_{(\mathbf{x}, \nu)}(\mathbf{y}, \nu') P_{S^c}(\theta_{\mathbf{x}}, d\theta'_y),$$

where P_{S^c} is the transition kernel associated with the method used to update the parameters. Therefore, the second term on the RHS of (24) is equal to

$$\begin{aligned} & \tau \sum_{\mathbf{x}, \nu} \int \pi(\mathbf{x}, \theta_{\mathbf{x}}) \times (1/2) \left(\int_A P((\mathbf{x}, \theta_{\mathbf{x}}, \nu), (\mathbf{y}, d\theta'_y, \nu') | S^c) \right) d\theta_{\mathbf{x}} \\ &= \tau \times \pi(\mathbf{y}) \times (1/2) \int \pi(\theta_y | \mathbf{y}) \left(\int_A P_{S^c}(\theta_y, d\theta'_y) \right) d\theta_y. \end{aligned}$$

We also know that P_{S^c} leaves the conditional distribution $\pi(\cdot | \mathbf{y})$ invariant, implying that

$$\begin{aligned} & \tau \times \pi(\mathbf{y}) \times (1/2) \int \pi(\theta_y | \mathbf{y}) \left(\int_A P_{S^c}(\theta_y, d\theta'_y) \right) d\theta_y \\ &= \tau \times \pi(\mathbf{y}) \times (1/2) \int_A \pi(\theta'_y | \mathbf{y}) d\theta'_y = \tau \int_A \pi(\mathbf{y}, \theta'_y) \times (1/2) d\theta'_y. \end{aligned} \quad (25)$$

For the model switching case (the first term on the RHS of (24)), we use the fact that there is a connection between $P((\mathbf{x}, \theta_{\mathbf{x}}, \nu), (\mathbf{y}, \theta'_y, \nu') | S)$ and the kernel associated to a specific RJ. Consider that in this RJ, $q_x(\mathbf{y}) = (1/2)q_{x,-1}(\mathbf{y}) + (1/2)q_{x,+1}(\mathbf{y})$ for all \mathbf{x} and $\mathbf{y} \in \mathbf{N}(\mathbf{x})$ and that all other proposal distributions in RJ are the same as in [Algorithm 3](#) during model switches. In this case, $\alpha_{\text{RJ}} = \alpha_{\text{NRJ}}$ and it is considered that to go from \mathbf{x} to \mathbf{y} , $q_{x,\nu}$ is chosen (this happens with probability 1/2) and, in the reverse move, $q_{y,-\nu}$ is chosen (which also happens with probability 1/2).

We now analyse each term of the first sum in (24),

$$\sum_{\mathbf{x}, \nu} (1 - \tau) \int \pi(\mathbf{x}, \theta_{\mathbf{x}}) \times (1/2) \left(\int_A P((\mathbf{x}, \theta_{\mathbf{x}}, \nu), (\mathbf{y}, d\theta'_y, \nu') | S) \right) d\theta_{\mathbf{x}}.$$

First, consider that $\mathbf{y} \in \mathbf{N}_\nu(\mathbf{x})$, i.e. the case of an accepted model switch, thus model \mathbf{y} is reached from model $\mathbf{x} \neq \mathbf{y}$, coming from direction ν (with $\nu = \nu'$ because the move is accepted). Given the

reversibility of RJ, the probability to go from model \mathbf{x} with parameters in B to model $\mathbf{y} \neq \mathbf{x}$ with parameters in A is

$$\int_B \pi(\mathbf{x}, \boldsymbol{\theta}_{\mathbf{x}}) \left(\int_A P_{\text{RJ}}((\mathbf{x}, \boldsymbol{\theta}_{\mathbf{x}}), (\mathbf{y}, d\boldsymbol{\theta}'_{\mathbf{y}})) \right) d\boldsymbol{\theta}_{\mathbf{x}} = \int_A \pi(\mathbf{y}, \boldsymbol{\theta}'_{\mathbf{y}}) \left(\int_B P_{\text{RJ}}((\mathbf{y}, \boldsymbol{\theta}'_{\mathbf{y}}), (\mathbf{x}, d\boldsymbol{\theta}_{\mathbf{x}})) \right) d\boldsymbol{\theta}'_{\mathbf{y}}, \quad (26)$$

where P_{RJ} is the transition kernel of the RJ. Note that

$$P_{\text{RJ}}((\mathbf{x}, \boldsymbol{\theta}_{\mathbf{x}}), (\mathbf{y}, d\boldsymbol{\theta}'_{\mathbf{y}})) = (1/2)(1 - \tau) P((\mathbf{x}, \boldsymbol{\theta}_{\mathbf{x}}, \nu'), (\mathbf{y}, d\boldsymbol{\theta}'_{\mathbf{y}}, \nu') | S),$$

given that the difference between both kernels is that in RJ, it is randomly decided to use $q_{\mathbf{x}, \mathbf{y}}$; there is thus an additional probability factor of 1/2. Analogously, we have that $P_{\text{RJ}}((\mathbf{y}, \boldsymbol{\theta}'_{\mathbf{y}}), (\mathbf{x}, d\boldsymbol{\theta}_{\mathbf{x}})) = (1/2)(1 - \tau) P((\mathbf{y}, \boldsymbol{\theta}'_{\mathbf{y}}, -\nu'), (\mathbf{x}, d\boldsymbol{\theta}_{\mathbf{x}}, -\nu') | S)$. Using this and taking B equals the whole parameter (and auxiliary) space in (26), we have

$$\begin{aligned} & (1 - \tau) \int \pi(\mathbf{x}, \boldsymbol{\theta}_{\mathbf{x}}) \times (1/2) \left(\int_A P((\mathbf{x}, \boldsymbol{\theta}_{\mathbf{x}}, \nu'), (\mathbf{y}, d\boldsymbol{\theta}'_{\mathbf{y}}, \nu') | S) \right) d\boldsymbol{\theta}_{\mathbf{x}} \\ &= (1 - \tau) \int_A \pi(\mathbf{y}, \boldsymbol{\theta}'_{\mathbf{y}}) \times (1/2) \left(\int P((\mathbf{y}, \boldsymbol{\theta}'_{\mathbf{y}}, -\nu'), (\mathbf{x}, d\boldsymbol{\theta}_{\mathbf{x}}, -\nu') | S) \right) d\boldsymbol{\theta}'_{\mathbf{y}}. \end{aligned} \quad (27)$$

Now, consider that $\mathbf{y} = \mathbf{x}$, i.e. a rejected model switch so model \mathbf{y} is reached from model \mathbf{y} and the direction is such that $-\nu = \nu'$. The probability of the transition is

$$(1 - \tau) \int_A \pi(\mathbf{y}, \boldsymbol{\theta}'_{\mathbf{y}}) \times (1/2) \left(1 - \sum_{\mathbf{x} \in \mathbf{N}_{-\nu'}(\mathbf{y})} \int P((\mathbf{y}, \boldsymbol{\theta}'_{\mathbf{y}}, -\nu'), (\mathbf{x}, d\boldsymbol{\theta}_{\mathbf{x}}, -\nu') | S) \right) d\boldsymbol{\theta}'_{\mathbf{y}}.$$

So, the total probability of reaching $\mathbf{y}, \boldsymbol{\theta}'_{\mathbf{y}} \in A, \nu'$ through a model switch is (recalling (24)):

$$\begin{aligned} & \sum_{\mathbf{x}, \nu} (1 - \tau) \int \pi(\mathbf{x}, \boldsymbol{\theta}_{\mathbf{x}}) \times (1/2) \left(\int_A P((\mathbf{x}, \boldsymbol{\theta}_{\mathbf{x}}, \nu), (\mathbf{y}, d\boldsymbol{\theta}'_{\mathbf{y}}, \nu') | S) \right) d\boldsymbol{\theta}_{\mathbf{x}} \\ &= \sum_{\mathbf{x}: \mathbf{y} \in \mathbf{N}_{\nu'}(\mathbf{x})} (1 - \tau) \int \pi(\mathbf{x}, \boldsymbol{\theta}_{\mathbf{x}}) \times (1/2) \left(\int_A P((\mathbf{x}, \boldsymbol{\theta}_{\mathbf{x}}, \nu'), (\mathbf{y}, d\boldsymbol{\theta}'_{\mathbf{y}}, \nu') | S) \right) d\boldsymbol{\theta}_{\mathbf{x}} \\ & \quad + (1 - \tau) \int_A \pi(\mathbf{y}, \boldsymbol{\theta}'_{\mathbf{y}}) \times (1/2) \left(1 - \sum_{\mathbf{x} \in \mathbf{N}_{-\nu'}(\mathbf{y})} \int P((\mathbf{y}, \boldsymbol{\theta}'_{\mathbf{y}}, -\nu'), (\mathbf{x}, d\boldsymbol{\theta}_{\mathbf{x}}, -\nu') | S) \right) d\boldsymbol{\theta}'_{\mathbf{y}} \\ &= \sum_{\mathbf{x} \in \mathbf{N}_{-\nu'}(\mathbf{y})} (1 - \tau) \int_A \pi(\mathbf{y}, \boldsymbol{\theta}'_{\mathbf{y}}) \times (1/2) \left(\int P((\mathbf{y}, \boldsymbol{\theta}'_{\mathbf{y}}, -\nu'), (\mathbf{x}, d\boldsymbol{\theta}_{\mathbf{x}}, -\nu') | S) \right) d\boldsymbol{\theta}'_{\mathbf{y}} \\ & \quad + (1 - \tau) \int_A \pi(\mathbf{y}, \boldsymbol{\theta}'_{\mathbf{y}}) \times (1/2) \left(1 - \sum_{\mathbf{x} \in \mathbf{N}_{-\nu'}(\mathbf{y})} \int P((\mathbf{y}, \boldsymbol{\theta}'_{\mathbf{y}}, -\nu'), (\mathbf{x}, d\boldsymbol{\theta}_{\mathbf{x}}, -\nu') | S) \right) d\boldsymbol{\theta}'_{\mathbf{y}} \\ &= (1 - \tau) \int_A \pi(\mathbf{y}, \boldsymbol{\theta}'_{\mathbf{y}}) \times (1/2) d\boldsymbol{\theta}'_{\mathbf{y}}, \end{aligned}$$

using (27) and that if \mathbf{x} allows to reach \mathbf{y} using the direction ν' , then $\mathbf{x} \in \mathbf{N}_{-\nu'}(\mathbf{y})$. Combining this result with (25) allows to conclude the proof. \blacksquare

B Supplementary material

We present in [Example 1](#) a model such that (11) is satisfied. We next present in [Example 2](#) a sequence $\{\pi_n\}$ that allows to define a control subset as in (18) and to verify the assumptions of [Theorem 3](#).

Example 1. Let π_n be such that

$$\pi_n \left\{ 1 < i < j < n : \inf_{i \leq k \leq j} x_k = 1, \sup_{k \notin \{i, \dots, j\}} x_k = -1 \right\} = 1. \quad (28)$$

By construction, a random variable $\mathbf{X} \sim \pi_n$ consists of a series of (at least one) -1 component(s) followed by a series of (at least two) $+1$ component(s) and then a series of (at least one) -1 component(s), π_n -almost surely. For $i \in \{1, \dots, n\}$, let $R_i : \mathcal{X}_n \rightarrow \mathcal{X}_n$ be the operator that flips the i -th coordinate, formally defined as $R_i(\mathbf{x}) = \mathbf{x} - 2x_i \delta_i$, where δ_i is the Kronecker symbol, i.e. the vector of $\{0, 1\}^n$ that has 1 at entry i and 0 elsewhere. For $\mathbf{x} \in \mathcal{X}_n$ such that $\{i, j\}$ are as in (28), define $\mathbf{N}(\mathbf{x})$ as $\mathbf{N}(\mathbf{x}) = \{R_{i-1}(\mathbf{x}), R_i(\mathbf{x}), R_j(\mathbf{x}), R_{j+1}(\mathbf{x})\}$. By definition, the neighbourhood of $\mathbf{x} \in \mathcal{X}_n$ is made of states obtained by extending or shortening the series of $+1$ components of \mathbf{x}_n . To split $\mathbf{N}(\mathbf{x})$ into two directional neighbourhoods, the partial ordering on \mathcal{X} is defined through the set

$$\mathcal{R} = \left\{ (\mathbf{x}, \mathbf{y}) \in \mathcal{X}^2 : \inf_{1 \leq i \leq n} (y_i - x_i) \geq 0 \right\}.$$

Given this partial ordering, $\mathbf{N}(\mathbf{x})$ is split into $\mathbf{N}_{+1}(\mathbf{x}) = \{R_{i-1}(\mathbf{x}), R_{j+1}(\mathbf{x})\}$ and $\mathbf{N}_{-1}(\mathbf{x}) = \{R_i(\mathbf{x}), R_j(\mathbf{x})\}$, where $\{i, j\}$ are as in (28). Clearly for any π_n which satisfies (28), we have for π_n -almost all $\mathbf{x} \in \mathcal{X}_n$, $|\mathbf{N}_{+1}(\mathbf{x})| = |\mathbf{N}_{-1}(\mathbf{x})| = 2 = |\mathbf{N}(\mathbf{x})|/2$ and we are in the context of [Corollary 2](#). A specific distribution π_n which verifies (28) is defined as follows: let $I := \inf\{i : \mathbf{x}_i = 1\}$ and $L := \sum_{k=1}^n \mathbf{1}_{\mathbf{x}_k=1}$ follow a truncated geometric distribution with parameters $\lambda_1 \in (0, 1)$ and $\lambda_2 \in (0, 1)$ respectively such that $\pi_n\{1 < I < n-1 \cap 1 < L < n-2 \cap L+I < n\} = 1$. Since everything is tractable in this example, asymptotic variances $\text{var}(f, P)$ can be calculated exactly for a given Markov kernel P and a test function f . The right panel of [Figure 5](#) shows the ratio of asymptotic variances $\text{var}(f, P_{\text{MH},n})/\text{var}(f, P_{\rho,n})$ for three different functions f . Here, the simplest switching rate function was used $\rho \equiv \rho_v^w$, i.e. $\rho_v(\mathbf{x}) = 1 - T_v(\mathbf{x}, \mathcal{X}_n)$. As anticipated by [Corollary 2](#), these ratios are always larger than one. However, this experiment shows that they can indeed be much larger than one and increase with n , hence justifying the lifted approach. Intuitively, the mild variations of π_n over neighbouring states (see left panel of [Figure 5](#)) explain why the lifted Markov chain outperforms significantly Metropolis-Hastings in this example: the persistent nature of the lifted chain increases (or decreases) consistently the length of the $+1$ series until an unlikely rejection occurs (since $a_v(\mathbf{x}, \mathbf{y}) \approx 1$, $\mathbf{y} \in \mathbf{N}_v(\mathbf{x})$) or that the boundary of the support is reached.

Example 2. Let $\mathcal{X}_n = \{-1, +1\}^n$. In this example, in addition to the state space dimension, $n \in \mathbb{N}$ also characterizes the geometrical features of π_n : as $n \rightarrow \infty$ more and more probability mass is put on a structure that can be seen as a path \mathfrak{P}_n within \mathcal{X}_n defined as

$$\mathfrak{P}_n := \left\{ \mathbf{x} \in \mathcal{X}_n : \sup_{i \leq j} x_i = -1, \inf_{i > j} x_i = +1, \text{ for some } j \in \{1, \dots, n-1\} \right\} \cup \{-1\}^n \cup \{+1\}^n.$$

The states belonging to the path are denoted $\{\mathbf{x}_i\}_{i=1}^{n+1}$ such that $\{\mathbf{x}_1 < \mathbf{x}_2 < \dots < \mathbf{x}_{n+1}\}$. Therefore, $\mathbf{x}_1 = \{-1\}^n$, $\mathbf{x}_2 = \{-1, \dots, -1, +1\}$, $\mathbf{x}_3 = \{-1, \dots, -1, +1, +1\}$ and so on. Moreover, we define the subset $\mathfrak{P}_n^\circ = \mathfrak{P}_n \setminus \{-1\}^n \cup \{+1\}^n$. In order to set up a context that resemble applications, the natural neighborhood structure defined as $\mathbf{N}(\mathbf{x}) = \{\mathbf{y} \in \mathcal{X}_n : \sum_{i=1}^n |x_i - y_i| = 1\}$ is slightly modified as follows:

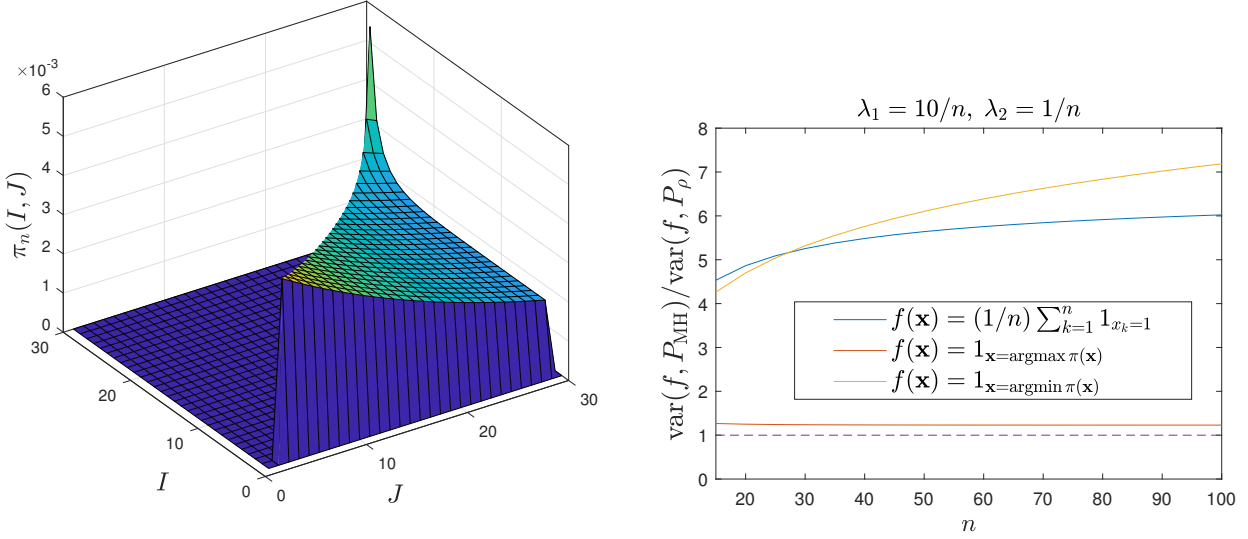


Figure 5. (Example 1) Left: illustration of the distribution when $(I, J = I + L)$ with $n = 30$, $\lambda_1 = 1/3$ and $\lambda_2 = 1/30$. Right: ratio of the asymptotic variances $\text{var}(f, P_{\text{MH},n})/\text{var}(f, P_{\rho,n})$ for three different functions f . As established in Corollary 2, we always have $\text{var}(f, P_{\text{MH},n})/\text{var}(f, P_{\rho,n}) \geq 1$ and for some functions, in addition of being several times larger than 1, that ratio increases significantly with n .

- if $\mathbf{x} \notin \mathfrak{P}_n$, $\tilde{\mathbf{N}}(\mathbf{x}) = \mathbf{N}(\mathbf{x}) \setminus \mathfrak{P}_n^\circ$ and if $\mathbf{x} \in \mathfrak{P}_n^\circ$, $\tilde{\mathbf{N}}(\mathbf{x}) = \mathbf{N}(\mathbf{x}) \cap \mathfrak{P}_n^\circ$,
- if $\mathbf{x} \in \{-1\}^n \cup \{+1\}^n$, $\tilde{\mathbf{N}}(\mathbf{x}) = \mathbf{N}(\mathbf{x}) \cup \{-\mathbf{x}\}$.

The first modification is designed so as to account that in many applications, the part of the state space on which π_n concentrates has a certain depth (it is not possible to exit this subset in a one-step transition for the vast majority of states in that subset), such as in the Ising model of Section 5.1. The second modification provides the state space with a torus-like feature, as described in Section 3.2, since the extreme states \mathbf{x}_1 and \mathbf{x}_n are neighbors. As explained in Section 3.2, this neighborhood structure may be split into $\tilde{\mathbf{N}}_+(\mathbf{x}) = \{\mathbf{y} \in \tilde{\mathbf{N}}(\mathbf{x}) : \mathbf{x} < \mathbf{y}\}$ and $\tilde{\mathbf{N}}_-(\mathbf{x}) = \{\mathbf{y} \in \tilde{\mathbf{N}}(\mathbf{x}) : \mathbf{y} < \mathbf{x}\}$. The neighborhood structure $\tilde{\mathbf{N}}$ induces the following mapping on $\mathcal{X}_n \times \mathcal{X}_n$

$$d_n(\mathbf{x}, \mathbf{y}) = \inf\{i \in \mathbb{N} : \exists \{\mathbf{z}_1, \dots, \mathbf{z}_{i-1}\} \in \mathcal{X}_n^{i-1} \text{ such that} \bigcup_{v \in \{-1, +1\}} \{\mathbf{z}_1 \in \tilde{\mathbf{N}}_v(\mathbf{x})\} \cap_{k=1}^{i-2} \mathbf{z}_k \in \tilde{\mathbf{N}}_v(\mathbf{z}_{k+1}) \cap \{\mathbf{z}_{i-1} \in \tilde{\mathbf{N}}_v(\mathbf{y})\}\},$$

which defines a distance on \mathcal{X}_n . This distance is the smallest number of transitions in the same direction required to go from \mathbf{x} to \mathbf{y} , meaning that $\{\mathbf{x} > \mathbf{z}_1 > \dots > \mathbf{z}_{d_n(\mathbf{x}, \mathbf{y})-1} > \mathbf{y}\}$ or $\{\mathbf{x} < \mathbf{z}_1 < \dots < \mathbf{z}_{d_n(\mathbf{x}, \mathbf{y})-1} < \mathbf{y}\}$. In the following, this distance is used to measure the distance from an arbitrary state

- to the center of the path,

$$\mathbf{x} \in \mathcal{X}_n, \quad \mathbf{d}_n(\mathbf{x}) = d_n(\mathbf{x}, \mathbf{x}_{n/2+1}) \mathbb{1}_{\{n \text{ is even}\}} + (d_n(\mathbf{x}, \mathbf{x}_{(n+1)/2}) \wedge d_n(\mathbf{x}, \mathbf{x}_{(n+3)/2})) \mathbb{1}_{\{n \text{ is odd}\}},$$

- to the path

$$\mathbf{x} \in \mathcal{X}_n, \quad \mathbf{d}_n(\mathbf{x}) = [d_n(\mathbf{x}, \{-1\}^n) \wedge d_n(\mathbf{x}, \{+1\}^n)] \mathbb{1}_{\{\mathbf{x} \notin \mathfrak{P}_n\}}.$$

This allows to define the distribution π_n , parameterized by $a \in (2/3, 1)$, as

$$\mathbf{x} \in \mathcal{X}_n, \quad \pi_n(\mathbf{x}) \propto \left(\frac{1}{3}\right)^{n\mathbf{d}_n(\mathbf{x})} a^{\mathbf{d}_n(\mathbf{x})}. \quad (29)$$

Intuitively, the mode of π_n is at the centre of the path, the mass decays geometrically along the path and beyond the path, the mass is further shrunk in the tails.

Consider the problem of sampling from π_n of [Example 2](#) using the locally-balanced version of either the lifted or the Metropolis-Hastings algorithms. We show how a careful application of [Theorem 3](#) shows that, provided that n is sufficiently large, the lifted Markov chain is more efficient than the Metropolis-Hastings one for, at least, a certain function of interest, namely $f_n(\mathbf{x}) = \sum_{i=1}^n x_i/n$.

We first show that \mathfrak{P}_n can be used as a control subset, thus setting $\tilde{\mathcal{X}}_n = \mathfrak{P}_n$. By construction, the interior and boundary of $\tilde{\mathcal{X}}_n$ are defined as

$$\tilde{\mathcal{X}}_n^\circ = \mathfrak{P}_n \setminus \{\mathbf{x}_1 \cup \mathbf{x}_{n+1}\}, \quad \partial\tilde{\mathcal{X}}_n = \mathbf{x}_1 \cup \mathbf{x}_{n+1}.$$

When $n \rightarrow \infty$, π_n concentrates on \mathfrak{P}_n exponentially fast. In particular, it can be checked that for all $r < 1/2$,

$$\lim_{n \rightarrow \infty} \left(\frac{1}{a^r}\right)^n (1 - \pi_n(\tilde{\mathcal{X}}_n^\circ)) = 0. \quad (30)$$

Indeed, considering that n is odd (a similar derivation holds if n is even), denoting by $\bar{\pi}_n$ the unnormalized probability, we note that since $0 < \bar{\pi}_n(\mathcal{X}_n \setminus \mathfrak{P}_n) \leq 2^n a^{(n+1)/2} / 3^n$ and $\bar{\pi}_n(\mathfrak{P}_n) = 2(1 + a + \dots + a^{(n-1)/2})$

$$1 - \pi_n(\tilde{\mathcal{X}}_n^\circ) = \frac{\bar{\pi}_n(\mathcal{X}_n \setminus \mathfrak{P}_n) + \bar{\pi}_n(\partial\tilde{\mathcal{X}}_n)}{\bar{\pi}_n(\mathcal{X}_n \setminus \mathfrak{P}_n) + \bar{\pi}_n(\mathfrak{P}_n)} \leq \frac{2^n a^{(n+1)/2} / 3^n + 2a^{(n-1)/2}}{2(1 - a^{(n+1)/2}) / (1 - a)} \leq \left(a^{1/2}\right)^n \frac{(1 - a)}{\sqrt{a}(1 - a^{n/2})}.$$

Recall that the locally-balanced function g used in the locally-balanced proposal presented at [Section 4.2](#) is such that $g(x) = x/(1 + x)$ and note that, by direct calculation, we obtain that for each $(\mathbf{x}, \mathbf{y}) \in \mathfrak{P}_n$, with $\mathbf{x} \neq \mathbf{y}$ and any $n \in \mathbb{N}$,

$$\frac{P_{\text{rev.},n}(\mathbf{x}, \mathbf{y})}{P_{\text{MH},n}(\mathbf{x}, \mathbf{y})} \in \left\{ \frac{1+a}{2}, \frac{a/2}{1+a\kappa_n} \left(\frac{1}{2} + \frac{3}{2a} + \kappa_n \right), \frac{1}{2} + \frac{1}{1+a} (1 + \kappa_n/a) \right\}, \quad \kappa_n = (n-1)a/(a+3^n).$$

It can be checked that for n sufficiently large (in fact for those n satisfying $n3^{-n} \leq (1-a)/(2a^3)$), we have

$$P_{\text{rev.},n}(\mathbf{x}, \mathbf{y}) \geq \frac{1+a}{2} P_{\text{MH},n}(\mathbf{x}, \mathbf{y}), \quad (\mathbf{x}, \mathbf{y}) \in \tilde{\mathcal{X}}_n^2, \quad \mathbf{x} \neq \mathbf{y}. \quad (31)$$

Equation (31) shows that [Assumption 1](#) of [Theorem 3](#) holds with $\omega(n) = (1+a)/2$, for all $n \in \mathbb{N}$.

Based on numerical results carried out on a computer (see Figure 6), the spectral gap of $P_{\text{rev.},n}$, $\tilde{P}_{\text{rev.},n}$, $P_{\text{MH},n}$ and $\tilde{P}_{\text{MH},n}$ are surmised to vanish at a quadratic rate, that is $\underline{\lambda}(n) \sim \lambda/n^2$. Notice that the result for $\tilde{P}_{\text{MH},n}$ is in line with some well known results in [Diaconis et al. \(2000\)](#) on polynomially mixing Markov chains, see also [Diaconis \(2013\)](#). Assuming that this result holds, we have that for any $\delta > 0$ and $\gamma < \bar{\delta} = \delta/(2+\delta)$, $1 - \pi_n(\tilde{\mathcal{X}}_n^\circ) = o(\underline{\lambda}(n)^{3/(\bar{\delta}-\gamma)})$, that is the assumption (4) of [Theorem 3](#) holds for any choice of $\delta > 0$ and $\gamma < \bar{\delta}$.

Consider the function $f_n(\mathbf{x}) = (1/n) \sum_{i=1}^n x_i$. One can check that, because f_n is odd and the mass function π_n is even, $\pi_n f_n = 0$. Moreover, noting that $\|f_n\|_{\pi_n, 2} > 0$ and $\|f_n\|_{\pi_n, 2} \neq 1$, f_n needs to be normalized to remain in the framework of [Theorem 3](#). We thus seek to compare $\text{var}(P_{\text{MH},n}, \bar{f}_n)$ and its

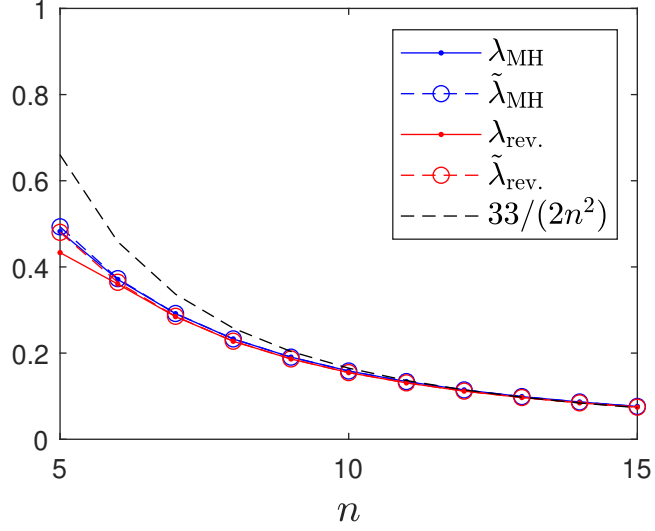


Figure 6. Illustration of the spectral gap of $P_{\text{MH},n}$, $P_{\text{rev},n}$ and their restricted version obtained from a calculation carried out on a computer for $n \in \{5, 15\}$. Beyond the dimension $n = 15$, calculation of the transition matrices failed.

lifted counterpart $\text{var}(P_{\rho,n}, \bar{f}_n)$. The last check to apply [Theorem 3](#) is that $\|\bar{f}_n\|_{\pi_n,2+\delta}$ does not grow too fast relatively to $1/(1 - \pi_n(\tilde{\mathbf{X}}^\circ))$. We note that because $|f_n| \in [0, 1]$,

$$\|\bar{f}_n\|_{\pi_n,2+\delta} \leq \frac{1}{\|f_n\|_{\pi_n,2}}. \quad (32)$$

We conclude using the following rough, but not too rough, lower bound on $\|f_n\|_{\pi_n,2}$. Consider n even, then

$$\|f_n\|_{\pi_n,2+\delta}^2 \geq \sum_{\mathbf{x} \in \tilde{\mathbf{X}}} f_n(\mathbf{x})^2 \pi_n(\mathbf{x}) = \frac{8}{n^2 Z_n} W_n, \quad W_n := \sum_{k=1}^{n/2} k^2 a^k,$$

where Z_n is the normalizing constant in the definition of π_n given at Eq. (29). We have that for any $\nu > 0$,

$$\frac{1}{n^{1+\nu}} \|\bar{f}_n\|_{\pi_n,2+\delta} \leq \frac{1}{n^{1+\nu} \|f_n\|_{\pi_n,2}} \leq \frac{1}{n^\nu} \frac{1}{2\sqrt{2}} \left[\frac{Z_n}{W_n} \right]^{1/2}.$$

A similar derivation holds whenever n is odd. Now, noting that

$$Z_n \geq 2 \left[1 + a + a^2 + \cdots + a^{n/2} \right] = 2 \frac{1 - a^{n/2+1}}{1 - a} \sim 2 \frac{1}{1 - a},$$

and that the series W_n converges to $a(a+1)/(1-a)^3$, we have that $\|\bar{f}_n\|_{\pi_n,2+\delta} = o(n^{1+\nu})$. Together with (30) show that $\{\bar{f}_n\}$ verifies (3) of [Theorem 3](#). Therefore, for any $\epsilon > 0$, we have for a sufficiently large n that, using $\bar{\omega} = (1+a)/2$ (see Eq. (31))

$$\text{var}(\bar{f}_n, P_{\text{rev},n}) \leq \frac{1}{(a+1)/2 - \epsilon/2} \text{var}(\bar{f}_n, P_{\text{MH},n}) + \frac{1-a}{1+a} + \epsilon/2.$$

For instance, taking $\epsilon = 1 - a$, for n sufficiently large,

$$\text{var}(\bar{f}_n, P_{\rho,n}) \leq \frac{1}{a} \text{var}(\bar{f}_n, P_{\text{MH},n}) + \frac{3}{2}(1-a). \quad (33)$$

It is remarkable that such a result can be obtained since, for *all* $n \in \mathbb{N}$, it does not hold that $P_{\text{rev},n}(\mathbf{x}, \mathbf{y}) - P_{\text{MH},n}(\mathbf{x}, \mathbf{y}) \geq 0$ for all $(\mathbf{x}, \mathbf{y}) \in \mathcal{X}^2$, $\mathbf{x} \neq \mathbf{y}$. Hence, $P_{\text{rev},n}$ does not dominate $P_{\text{MH},n}$ in the usual Peskun sense and the result of [Andrieu and Livingstone \(2021\)](#) does not allow to compare $\text{var}(\bar{f}_n, P_{\rho,n})$ and $\text{var}(\bar{f}_n, P_{\text{MH},n})$. Indeed, one can check that taking $\mathbf{z} \in \partial\tilde{\mathcal{X}}$ and $\mathbf{x} \notin \tilde{\mathcal{X}}$ such that $\mathbf{z} \in \mathbf{N}_\nu(\mathbf{x})$, we have that

$$P_{\text{MH},n}(\mathbf{z}, \mathbf{x}) = \frac{g(3^n/a)}{1/2 + g(1/a) + (n-a)g(a/3^n)}, \quad P_{\text{rev},n}(\mathbf{z}, \mathbf{x}) = 1/2,$$

and, for all $n \in \mathbb{N}$,

$$\frac{P_{\text{MH},n}(\mathbf{z}, \mathbf{x})}{P_{\text{rev},n}(\mathbf{z}, \mathbf{x})} \geq \frac{(1+a)3^n}{1+n+3^n} > 1.$$

This means that, if, hypothetically, one were able to establish a quantitative Peskun ordering between $P_{\text{rev},n}$ and $P_{\text{MH},n}$, they would obtain something like $P_{\text{rev},n}(\mathbf{x}, \mathbf{y}) \geq \omega(n)P_{\text{MH},n}(\mathbf{x}, \mathbf{y})$ for each $(\mathbf{x}, \mathbf{y}) \in \mathcal{X}^2$ with $\omega(n) \leq (3^{-n} + n3^{-n} + 1)/(1+a)$ which decreases with n to $1/(1+a)$. Assuming the best case scenario with $\omega(n) = 1/(1+a)$, the comparison between the lifted and MH asymptotic variances would then be

$$\text{var}(\bar{f}_n, P_\rho) \leq (1+a)\text{var}(\bar{f}_n, P_{\text{MH},n}) + a, \quad \text{for all } n \in \mathbb{N}. \quad (34)$$

Taking the constant a arbitrarily close to one, one can compare (for a large enough n) the difference in tightness offered by the two bounds of Eqs. (33) and (34). Thus, not only the weaker Peskun ordering introduced in this paper allows one to establish an ordering with greater ease, but the asymptotic variances inequality can also be much tighter.